



High-strength steel: ultimate material or expensive alternative?

Feasibility and optimization of using high-strength structural steel in offshore topsides

Offshore engineering
Wout Dekkers

High-strength steel: ultimate material or expensive alternative?

Feasibility and optimization of using
high-strength structural steel in offshore
topsides

by

Wout Dekkers

to obtain the degree of Master of Science:
Offshore & Dredging Engineering at the
Delft University of Technology,
to be defended publicly on the 26th of January 2024.

Student number: 4928377
Project duration: February, 2023 – January, 2024
Thesis committee: Ir. A. van der Stap, TU Delft/Shell, chairman
Ir. J. Hoving, TU Delft, supervisor
Dr. T. Tankova, TU Delft, supervisor
H. Driessen, Enersea, supervisor
G. Kaashoek, HSM Offshore Energy, supervisor

Cover: Borselle alpha offshore high voltage substation by HSM Offshore Energy, from <https://hsmoffshoreenergy.com/project/borssele-alpha-ohvs/>

An electronic version of this thesis is available at <http://repository.tudelft.nl/>.

Preface

In front of you lies my master's thesis: *"High-strength steel: the ultimate material or expensive alternative?"* This thesis was written at HSM Offshore Energy in collaboration with Enersea and aimed to show the potential of utilizing high-strength steels on topsides. The objective of the companies was to investigate the feasibility of utilizing high-strength steel on offshore topsides and to see if the use of high-strength steel could make them more appealing to potential clients in the future and to compete better in the ever-changing offshore market.

During my master's program in Offshore and Dredging Engineering, I didn't have many courses in structural engineering. However, while working on my thesis from February to December 2023, I had the opportunity to explore the world of structural engineering and steel design. Ever since I was a young boy, I have been fascinated with steel structures and the offshore industry, and I thoroughly enjoyed diving into this topic for my thesis. My grandfather, who used to work for HSM Offshore Energy for a major part of his life, played a significant role in my admiration for this industry. He shared many of his past projects and experiences with me, and it has been an amazing experience to follow in his footsteps during my graduation period by writing this thesis at HSM Offshore Energy. Although I cannot share my experiences with him due to COVID-19, I am confident that he would have been proud and overly enthusiastic to hear about my work. Therefore, I want to express my gratitude to HSM for giving me this opportunity and to my colleagues who supported me throughout this research. I have gained valuable knowledge about high-strength steel and steel structures in general, and I want to extend my thanks to Enersea for providing me with the theoretical background and to Hans Driessen for his support and expertise during the many brainstorming sessions. Finally, I would like to thank my thesis committee, consisting of Jeroen Hoving, Andre van der Stap, and Trayana Tankova, for seeing the potential of this research and for their guidance and thoughts about my project. I have learned a lot throughout this journey and am excited about the possibilities that lie ahead.

I hope that my insights on high-strength steel on offshore topsides will be helpful to offshore engineers and anyone interested in the subject. It is my sincere wish that this thesis will inspire you to recognize the potential of high-strength steel in topsides and that the screening tool constructed in this research can be expanded into a more accurate tool in the future to quickly estimate the expected weight and cost reductions for every engineer. I hope you find this thesis informative and enjoyable to read.

*Wout Dekkers
Schiedam, January 2024*

Summary

Steel is a widely used material in construction because of its availability, high strength-to-weight ratio, and recyclability. However, steel manufacturing consumes a lot of energy, and there is an increasing demand for more environmentally friendly building materials. Consequently, high-strength steel is becoming more popular as it reduces the mass of a structure, requiring less material and easier fabrication, transport, and welding, leading to a lower carbon footprint. Although high-strength steel has been available for many years, its use in offshore topsides is limited due to stability and deflection issues. Recent research, mostly based on the use of steel structures in buildings, suggests that high-strength steel can significantly reduce costs, weight, and carbon emissions. It is uncertain whether the same benefits can be expected for offshore topsides. Additionally, engineers need an easy-to-use screening tool in the early design stage to implement high-strength steel in their designs when the exact loadings are still unknown.

This research aims to assess the feasibility of utilizing high-strength structural steel in offshore topsides, and investigates how the use of high-strength steel can be optimized in topside design. First, the situations where the use of high-strength steel can be advantageous in topsides are analysed and the components that typically makeup topsides, including their sizes, lengths, and weights, are listed. Subsequently, these insights are applied to compare the feasibility of using high-strength steel to topside structural components for seven different topsides. It is concluded that specifically beams, columns, and bracings are worth further investigation in the context of this research.

To evaluate the beams, columns and bracings, situations from an existing topside were assessed to see if high-strength steel is beneficial. It was concluded that high-strength steel is advantageous for beams, especially for deck beams and main beams, while for deck stringers and cantilever beams, it depends on the situation. For columns, it was concluded that high-strength steel shows significant potential within the typical slenderness range of columns and bracings, but the extent of the benefits depends on the slenderness value of the columns and bracings.

Two different screening tools were constructed to assess the feasibility of high-strength steel within an entire topside. For beams, this method mainly relies on determining the ULS/SLS-ratio to find the transition point of a beam from strength governing towards deflection governing. For columns and bracings, the method assumed only axial loading and used a loop in which the diameter of a high-strength steel column was reduced until the same buckling resistance was found. It was concluded that the length of a particular beam can tell an engineer if it is worth further investigating the potential of high-strength steel, while columns showed potential in all cases. The methods were tested with a case study in which an entire topside was assessed for its feasibility of utilizing high-strength steel beams and columns. Only hot-rolled primary and secondary beams combined with the columns and bracings were considered for this topside. When S460M steel was used for strength-governing beams and seamless tubulars, in combination with S690Q steel for welded tubular columns, the highest benefits were found and a maximum steel weight reduction of 15% was found for the considered components. At the same time, the material costs were reduced by 10%, the welding costs by 13% and the embodied carbon savings equalled 14%. When comparing these results with the total topside steel weight, 5% of the topside steel weight was reduced by using a combination of S460 and S690 steels. It was concluded that high-strength steel is feasible for offshore topsides and is more environmentally friendly and cost-effective, providing a promising alternative to conventional steels within certain components on offshore topsides.

This research presents a screening tool that is simple to use and assesses the feasibility of high-strength steel. Other engineers can easily extend this tool. As more detailed calculations are included in the screening tool, it is expected that additional cost reductions and embodied carbon savings can be found. Furthermore, including additional steel components in the assessment, such as plate girders, may result in finding much higher total weight reductions.

Contents

Preface	i
Summary	ii
List of Figures	iv
List of Tables	vi
Nomenclature	viii
1 Introduction	1
1.1 Motivation	1
1.2 Companies perspective	1
1.3 Problem definition	2
1.4 Research scope and aim	3
1.5 Research methodology	4
1.6 Report outline	4
2 High-strength steel: state-of-the-art	5
2.1 Production processes	5
2.2 Mechanical properties	6
2.3 Engineering considerations	8
2.3.1 Static beam resistance	8
2.3.2 Static column resistance	11
2.3.3 Weldability	13
2.3.4 Fatigue	15
2.3.5 Corrosion	15
2.3.6 Fire resistance	15
2.4 Costs and environmental impact	15
2.4.1 Costs of high-strength steels	15
2.4.2 Environmental considerations for high-strength steel	17
2.4.3 Offshore considerations for high-strength steel	19
2.5 Conclusion of the literature review	19
3 Assessment of structural components in topsides	21
3.1 Design of offshore topsides - key figures & structural components	21
3.2 Comparative research with existing topsides	26
3.3 Conclusion regarding topside structural components	30
4 Feasibility of high-strength steel in topside beams, columns and bracings	31
4.1 High-strength steel beams	31
4.1.1 Introduction to high-strength steel beams	31
4.1.2 High-strength steel deck stringers	37
4.1.3 High-strength steel deck beams	44
4.1.4 High-strength steel main beams	48
4.1.5 High-strength steel cantilever beams	52
4.2 High-strength steel circular hollow columns & bracings	53
4.3 Conclusion of high-strength components in topsides	55
5 Methodology to assess the feasibility of high-strength steel in topsides	56
5.1 Screening tool for beams in a deck	56
5.2 Screening tool for columns and bracings	58
5.3 Methodology for preliminary design	59

6	Case study: feasibility of high-strength steel in topsides	61
6.1	Case introduction and assumptions	61
6.2	Case study: high-strength steel beams	63
6.3	Case study: high-strength steel columns & bracings	65
6.4	Conclusions of high-strength steel in a case topside	66
7	Conclusions & recommendations	67
7.1	Conclusions	67
7.2	Limitations	68
7.3	Recommendations for the industry	69
7.4	Recommendations for further research	70
	References	71
A	Additional information about the offshore industry	75
A.1	Short history and future perspective of the offshore industry	75
A.2	Type of offshore platforms and North Sea perspective	77
B	Deck stringer calculations	80
C	Deck beam calculations	86
D	Extra tables	90

List of Figures

1.1	Costs, weights and welding comparison between different steel grades [8]	2
1.2	Typical weight flowchart for offshore platforms	3
2.1	Historical development of rolled steel products [17]	5
2.2	Schematic simplification of steelmaking processes [18]	6
2.3	Stress-strain curves for different steel grades [21]	7
2.4	Brittle fracture and ductile failure [26]	7
2.5	Charpy V-temperature transition curves for different steels [27]	8
2.6	Cross section behaviour in bending according to Eurocode 3	9
2.7	Selection of flexural buckling curve [20]	11
2.8	Representation of the buckling curves for different steel grades [5]	12
2.9	Example of hybrid compressive member [34]	13
2.10	Preheat temperature vs. plate thickness for different normalized and TMCP steels [36]	13
2.11	Dimensioning of tension bars with different steel grades and corresponding butt welds [37]	14
2.12	Economic efficiency of heavy plates, if only the material price is taken into account (2011) [37]	16
2.13	Examples of different structural shapes [41]	17
2.14	Cumulative energy demand (CED) for heavy plates made of various steel grades [37]	18
2.15	Relation of CED, GWP and AP of heavy plates for various steel grades compared with S235J2 [37]	18
2.16	Required weight savings in [%] compared with S235J2 [37]	18
3.1	Modular and integrated topside examples	22
3.2	Truss type and portal-frame type topside	22
3.3	Structural components of an offshore platform	23
3.4	Different decks on offshore platforms (naming according to HSM)	23
3.5	Truss type and portal-frame type topside	25
3.6	Examples of a diamond plate connection	25
3.7	Example of a circular hollow section connection	25
3.8	Topside weight [t] vs. Floor area between deck legs [m ²]	27
3.9	Topside steel weight per floor area between deck legs [kg/m ²]	27
3.10	Typical deck layout (Main beams in blue, deck beams in orange and deck stringers in dotted yellow)	28
3.11	Weight percentage of different structural components for different topsides	29
3.12	Extended Sankey diagram of weight [tonnes] based on Borkum Riffgrund	30
4.1	Ultimate limit state vs. serviceability limit state for an IPE240	33
4.2	The influence of the load ratio on the ULS/SLS-ratio for an IPE240	34
4.3	The influence of different yield stresses on the ULS/SLS-ratio for an IPE240	35
4.4	The influence of different IPE's on the ULS/SLS-ratio	35
4.5	The influence of different type of cross-sections on the ULS/SLS-ratio	36
4.6	The influence of different type of supports on the ULS/SLS-ratio	37
4.7	The ULS/SLS-ratio for all typical IPE deck stringers (different supports)	38
4.8	Example part of a deck for deck stringer assessment	38
4.9	RFEM simplified model of example deck	39
4.10	Moment diagram of middle deck stringers modelled in RFEM	39
4.11	Deflection diagram of middle deck stringers modelled in RFEM	40
4.12	Sniped connections modelled as T-profile connected to the IPE240	40
4.13	Example of deck stringers in a lay-down area	41

4.14	Different typical deck beams (different supports, distributed load)	44
4.15	Example situation of a deck beam	45
4.16	Effect of point loads on the ULS/SLS-ratio	46
4.17	RFEM model of example deck beam	46
4.18	Moment diagram of deck beam modelled in RFEM	47
4.19	Deflection diagram of deck beam modelled in RFEM	47
4.20	Different typical main beams (different supports, distributed load)	49
4.21	The effect of the lateral torsional buckling resistance	49
4.22	Example typical deck layout	50
4.23	RFEM model of deck with heavy equipment	50
4.24	RFEM model of deck with heavy equipment	51
4.25	Different typical cantilever beams with different loadings	52
4.26	Buckling resistance $[N/m^2]$ vs. non-dimensional slenderness for hot-formed tubulars	53
4.27	Buckling resistance $[N/m^2]$ vs. non-dimensional slenderness for welded cold-formed tubulars	54
4.28	Example column of high-strength steel	54
5.1	Visualization of the introduced methodology to assess the potential of high-strength steel beams in topside decks	57
5.2	Visualization of the introduced methodology to assess the potential of high-strength steel columns and bracings	59
6.1	Considered topside for the case study	61
6.2	Steel scope of the considered topside	62
6.3	Type of assumed supports: simply supported: circled with yellow - fixed: circled with red	64
A.1	Offshore piers and on-lake platforms	75
A.2	Kerr-McGee's Kermac Rig No.16 is considered to be the world's first offshore platform, located 10 miles from the shore [48].	76
A.3	The world's biggest oil disaster: Piper Alpha [53]	76
A.4	Classification of offshore structures	77
A.5	Fixed structures (1,2,10), compliant tower (3), TLP (4,5), SPAR (6), Semisubmersible (7,8), FPSO (9)	78
A.6	Waterdepth of southern North Sea vs. bottom-founded and floating platform distribution in the North Sea	79

List of Tables

2.1	Minimal required yield strength at room temperature of normalized and thermomechanical rolled weldable fine grain structural steels (EN10025-4 [24] and EN10025-3 [25]) . . .	7
2.2	Available structural steel plates according to EN10025-2,3,4 and 6	16
2.3	Price differences for different high-strength steel grades	16
2.4	Price for different steel grades for H- and I-shape sections	17
3.1	General information about the assessed topsides	26
3.2	Generalized ranges of structural components from topside assessment and literature study	29
4.1	Effect of different snipe lengths on deck stringers	41
4.2	Possible replacement of beams with S460 (IPE) - simply supported and distributed load	43
4.3	Possible replacement of beams with S460 (IPE) - 3-span continuous beam and distributed load	43
4.4	Possible HEA S460 replacement - simply supported and distributed load	44
4.5	Possible HEA S460 replacement - continuous beam (3-span) assumption	44
4.6	Possible replacement of beams with S460 (HEB) - simply supported and distributed load	48
5.1	Maximum length for IPEs (S355) to be strength-governing	60
6.1	Values used to estimate welding cost reduction for columns	63
6.2	Weight reductions caused by using S460 steel in topside beams (all beams assumed to be simply-supported)	63
6.3	Weight reductions caused by using S460 steel in topside beams (different support assumptions)	64
6.4	Weight and cost reduction for using S460M or S690Q for welded cold-formed tubular (axial loaded)	65
6.5	Weight and cost reduction for using S460M or S690Q for hot-formed tubulars (axial loaded)	65
6.6	Total weight and cost reduction for using S460M or S690Q for axial loaded columns and bracings	66
D.1	Possible replacement of beams with S460 (HEB) - simply supported and distributed load	90
D.2	Possible replacement of beams with S460 (HEB) - fixed assumption (point load)	90
D.3	Possible replacement of beams with S460 (HEB) - fixed assumption (distributed load) .	91
D.4	Possible replacement of beams with S460 (HEA) - simply supported and distributed load	91
D.5	Possible replacement of beams with S460 (HEA) - continuous beam (3-span) assumption	91
D.6	Possible replacement of beams with S460 (IPE)	92
D.7	Possible replacement of beams with S460 (IPE) - continuous beam (3-span) assumption	92
D.8	Maximum length for HEBs to be strength governing.	92
D.9	Maximum length for HEAs to be strength governing.	93

Nomenclature

Abbreviations

Abbreviation	Definition
HSS	High-strength steel
ULS	Ultimate Limit State
SLS	Serviceability Limit State
N	Normalized steel
TM or TMCP	Thermomechanical rolled steel
QT	Quenched and Tempered steel
CE	Carbon Equivalent
HAZ	Heat Affected Zone
CED	Cumulative energy demand
GWP	Global warming potential
AP	acidification potential
BoSD	Basis of Structural Design
MSL	Mean Sea Level
U.C.	Unity check
TUW	Welded tubular
TUS	Seamless tubular

Symbols

Symbol	Definition	Unit
T	Temperature	[°C]
$M_{c,Rd}$	Bending moment resistance	[Nm]
M_{Ed}	Design bending moment	[Nm]
$W_{pl/el}$	Plastic or elastic section modulus	[m ³]
f_y	Yield stress	[Pa]
V_{Ed}	Design shear force	[N]
A_w	Area of the web	[m ²]
A_f	Area of the flange	[m ²]
N_{Ed}	Design axial force	[N]
$N_{c,Rd}$	Design resistance for compression	[N]
$N_{b,Rd}$	Design resistance for buckling	[N]
A	Cross-sectional area	[m ²]
E	Youngs modulus	[Pa]
I	Area moment of inertia	[m ⁴]
L	Length	[m]
N_{cr}	Euler's critical load	[N]
D	Diameter	[m]
t	Thickness	[m]
q	Unfactored distributed load	[N/m]
q_{uls}	factored distributed load for ULS	[N/m]
q_{sls}	factored distributed load for SLS	[N/m]
G	Permanent distributed load	[N/m]
Q	Permanent distributed load	[N/m]

Symbol	Definition	Unit
z	Distance from neutral axis to extreme fibre	[m]
σ_y	Yield stress	[Pa]
γ_{M0}	Partial safety factor	[-]
δ	Deflection	[m]
δ_{max}	Maximum allowable deflection	[m]
τ_{Ed}	design shear stress value	[Pa]
$\sigma_{von-mises}$	Von-mises stress	[Pa]
χ	Buckling reduction factor	[-]
α	Factor corresponding buckling curve	[-]
$\bar{\lambda}$	non-dimensional slenderness coefficient	[-]
λ	load ratio	[-]

1

Introduction

1.1. Motivation

Over the past few decades, significant progress has been made in developing various steel grades worldwide. As of 2022, the steel industry can produce nearly 3500 different steel grades, which can be used in various engineering applications that require specific material properties [1]. Due to its ability to be fully recycled, its availability, and its high strength-to-weight ratio, steel remains one of the most commonly used building materials today. However, the manufacturing of steel is very energy-intensive. According to the European Union, by the annual global production of approximately 180 million tons of crude steel [2], the steel industry is responsible for 7% of the global CO₂ emissions [3]. Therefore, the demand for more environmentally friendly building materials is increasing.

Consequently, high-strength steels are becoming increasingly popular in the construction industry. Using high-strength steel reduces a structure's mass, requiring less material, easier fabrication, lighter transport equipment and less welding volume. This leads to a lower carbon footprint in a structure's construction and recycling phases, making the project more climate-friendly [4]. Additionally, high-strength steel could reduce overall project costs as less material is required while also allowing for smaller weld lengths. Nonetheless, despite being used for years in the automotive industry and other industries where weight reduction is crucial in combination with an applied tensile force, such as in the legs of offshore drilling rigs and bridge cables, high-strength steels are not yet widely used in the construction industry. The main reason is that the increased strength leads to smaller cross-sections, which result in more susceptibility to stability and deflection issues for the beams and columns [5].

Nevertheless, the European-funded research project "*Stronger steels in the built environment*" (STROBE) recently concluded that designing steel structures with high-strength steel up to 700MPa can be beneficial within the building industry [6]. The study analyzed the performance of multiple high-strength steel members for the ultimate and serviceability limit states and concluded that some current Eurocode 3 rules regarding high-strength steels are conservative. Amendments were made, which will be included in the next version of Eurocode 3. According to STROBE, designing structures with high-strength steel can lead to cost savings between 5 and 14%, weight reduction of 49%, and embodied carbon savings up to 45%. These results demonstrate that high-strength steel has great potential for use in buildings.

1.2. Companies perspective

This research is being carried out for two companies located in Schiedam that operate in the offshore industry - HSM Offshore Energy and Enersea. HSM Offshore Energy is an integrated solution provider for multi-disciplinary offshore projects and has been building offshore structures for over 60 years. Enersea, on the other hand, is an offshore engineering company that provides consultancy, production system design and structural design. Together, they have developed a scalable range of offshore green hydrogen platforms that are ready to be built. Both companies believe that innovation is vital for the challenging offshore industry and are investigating ways to build more environmentally friendly and cost-effective offshore structures. The majority of their offshore projects are located in the southern

North Sea and consist of bottom-founded jacket platforms. These bottom-founded jacket platforms can weigh several thousand tons and cost millions of Euros to manufacture. As wages are high in Europe, construction companies in Europe need to find smart ways to reduce costs to compete with foreign companies. Additionally, European governments require energy projects to have smaller carbon footprints, which means the offshore industry needs to continuously seek innovative solutions. This research demonstrates the companies' dedication to investigating new possibilities. Their objective for this research is to evaluate if high-strength steel could be an option for their offshore platforms and to determine if high-strength steel could make the construction of offshore platforms more environmentally friendly and cost-effective. In this way, they can increase their appeal to potential clients to choose for European fabrication and engineering of quality.

1.3. Problem definition

High-strength steel has proven feasible and cost-efficient in many specific construction applications where a tensile force is applied. Typically, high-strength steels are defined as having a yield strength between $460MPa$ and $690MPa$ [5]. Figure 1.1 illustrates the differences in weight and costs between conventional and high-strength steels for a steel component loaded with an axial tensile force only. The figure demonstrates that despite the higher yield stresses being more expensive, a component designed with high-strength steel may still be cheaper due to the significant weight reduction. Additionally, using high-strength steel results in decreased welding costs and cross-sectional areas, but it should be noted that for S700 steel, pre-welding heating must be performed to a greater extent, increasing these costs [7]. In the case of only a tensile force, only strength is essential, and as the yield stress increases, the cross-section can be reduced, causing a reduction in weight. However, most structural components within an offshore platform do not only experience a tensile force but must also be checked for stability and deflections. In these cases, a reduction in cross-section makes a member more slender and causes less resilience against stability, plasticity, deflection and dynamic problems. Therefore, increasing the yield strength will not automatically result in an improved design, and the application of high-strength steel should be analysed carefully.

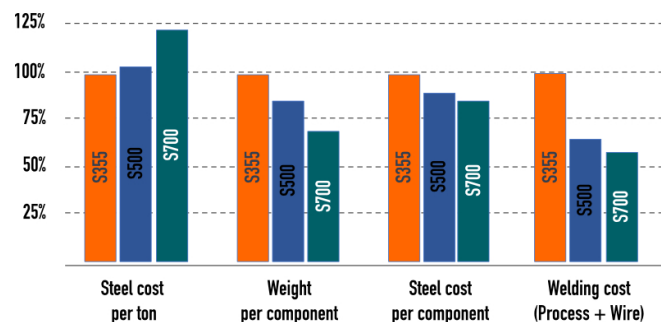


Figure 1.1: Costs, weights and welding comparison between different steel grades [8]

The results of STROBE [6] show that even when these problems arise, huge benefits can still be found when using high-strength steel. The research of STROBE focussed on beam-like cross-sections, and they concluded that some structural components within a building could be beneficially replaced with high-strength steel, such as heavily loaded columns, long-span roof trusses (when not limited by deflection), transfer beams and beams with large web openings. The STROBE research only focussed on beam-like cross-sections such as standard H-beams, I-beams or plate girders. For plate girders, previous research already proved that they could economically replace fabricated S355 plate girders [9], but that this is restricted by web buckling, partly caused by conservative design rules for plate girders [10]. However, offshore structures consist of not only beam-like structural components but also many tubular components. Tubular components allow for lighter structures with better buckling resistance due to the increase in the radius of gyration [11]. Despite these types of members being more expensive, the cost increment is tackled by the reduction in weight on the topsides. High-strength steel tubular columns have also proven beneficial for very stocky columns where buckling is not governing [12], despite that the current design rules also showed to be too conservative [13][14]. These conclusions show that

using high-strength steel in steel structures has real potential. Nonetheless, these studies primarily focused on case studies in buildings rather than how much could be won for typical offshore platform components. For offshore engineers, it is unclear if they can expect the same benefits offshore.

Furthermore, offshore platforms are designed to accommodate specific equipment, which determines the size and length of the beams. The process of structural engineering for topsides is heavily based on experience, with comparable designs often used as a starting point. The selection of members is not a standard process and varies from engineer to engineer depending on their background experience [15]. This means that conceptual offshore structures are initially designed by selecting standard cross-sections and lengths based on experience before knowing the loading on a member. To assess whether high-strength steel is suitable for such a design approach, a method is required to determine its feasibility based only on the cross-section and length of a member without knowing the exact loading on a member. Such a method has not been found in previous literature.

1.4. Research scope and aim

This research aims to investigate whether using high-strength structural steel in offshore platforms is feasible, even without knowing the exact loading. Typically, fatigue, dynamics, and corrosion limit the diameter of the substructure's structural components, which means that it's not expected that there will be significant benefits on offshore substructures. Therefore, this research will only focus on the steel scope of the topside. The purpose of this report is to provide engineers with a comprehensive overview of the potential advantages of using high-strength steel on offshore topsides. The research answers the following research question:

Is it feasible to use high-strength structural steel in offshore topsides, and how can the use of high-strength structural steel in topside design be optimised?

Figure 1.2a shows an example topside built by HSM Offshore Energy. Standard weight ratios can approximate the weight distribution, and this distribution is shown in a Sankey diagram in figure 1.2b. As this research only focuses on the structural steel scope of a topside, it can be seen in the Sankey diagram that this research focuses on weight reduction for 1,250t, or 24%, of the total platform weight. Assuming the maximum weight reduction percentage concluded by STROBE would result in a weight reduction of approximately 600 tonnes, a total topside weight reduction of 11%. Though it is a significant amount, it is not expected, as many steel components can not be replaced with high-strength steel due to deflection limitations.

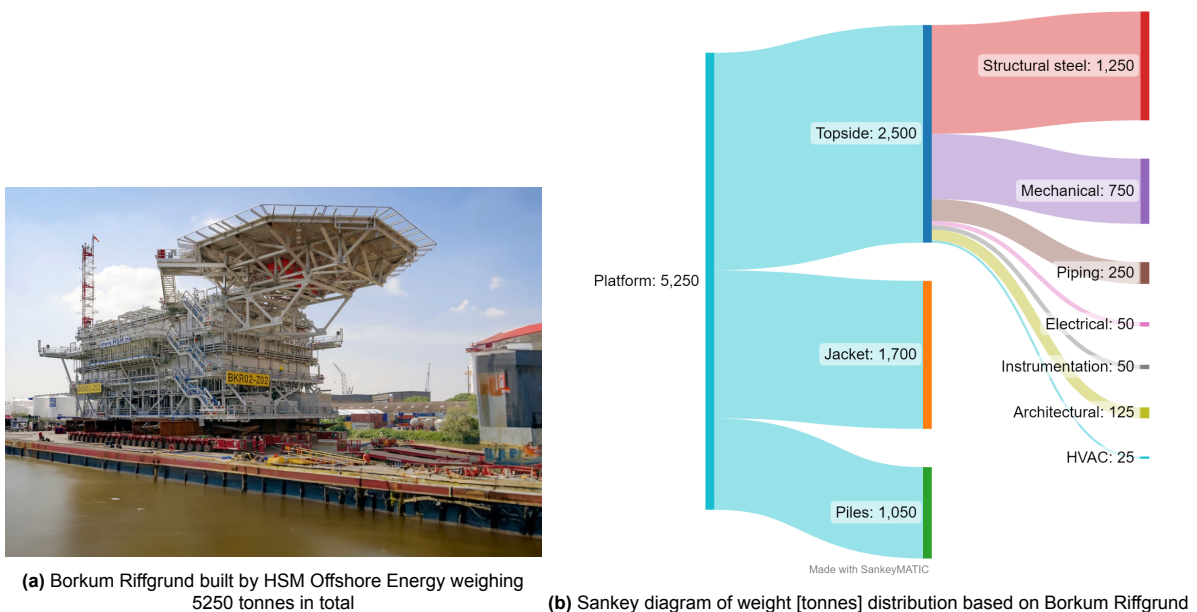


Figure 1.2: Typical weight flowchart for offshore platforms

Several sub-questions arise from this: Where and when exactly is high-strength steel beneficial? What are typical members, spans and cross-sections within the design of topsides? How can something be concluded without knowing the exact loading on structural components? And what will be the effect of the overall topside weight, costs and embodied carbon savings?

1.5. Research methodology

In order to answer the main research question and its sub-questions, various research methods are needed. Firstly, a desk study is required to evaluate the situations where high-strength steel can be advantageous or disadvantageous for structural components. Also, the desk study is necessary to analyze the previous research done in this area. Additionally, the desk study is essential to investigate which structural components are commonly used in topsides and what the sizes and lengths of these components are. Secondly, since the sizes and lengths of structural components can vary significantly, a comparison study is required to compare the existing literature with the observations from the platforms previously built at HSM. The observations are conducted with different 3D models from platforms built on HSM and their weight reports. From this comparison, the different ranges of sizes, lengths, and amounts of components can be concluded. Once the typical ranges are identified, a screening tool will be constructed to assess the feasibility of using high-strength steel without knowing the exact loads. To achieve this, a load ratio defined by [16] will be introduced, and small case studies in the form of finite element analysis or numerical calculations will be used to test the assumptions. The program used for the finite element analyses is RFEM6, and Python is used for the numerical calculations. Combining the constructed method with the typical ranges can determine whether high-strength steel is beneficial for the typical ranges of topside structural components. Lastly, to test the method on a total topside, a case study will be performed for an existing topside to investigate the effect of utilizing high-strength steel in an entire topside and to see what the effects are on the total weight, costs and carbon savings.

Nevertheless, this research will have some limitations. The numerous steel components present in a topside make it challenging to make generalizations about all the components. Therefore, only the most commonly found components can be assessed, while specific structural components, such as a crane pedestal, are not included in this research. At the same time, the possibility remains that these can also be replaced with high-strength steel. Thus, the results can probably be less beneficial than when all components are considered. Moreover, as generalization is required, comparisons with existing topside examples are assumed to be designed for their full capacity, which is, in reality, seldom the case. Furthermore, it is worth noting that details such as connections will change when high-strength steel is used. However, this research only provides generalized conclusions, and no detailed calculations are performed for these connections. Lastly, it is important to take into consideration other factors such as transportation, installation, and jacket design when using high-strength steel, which can affect the cost and weight reduction. These factors are only included as discussion points within the scope of this research.

1.6. Report outline

This report is organized into several chapters, each with a specific focus. In Chapter 2, the current state of the art of high-strength steel will be discussed, and this chapter will cover the research that has already been done on high-strength steel, its benefits, and the disadvantages that should be considered by performing a literature review. Chapter 3 will discuss typical topside components. Firstly, by diving into the literature for key figures, and secondly, by assessing multiple existing topsides built at HSM Offshore Energy. This chapter will conclude by discussing which structural components are worth further research and will provide typical sizes for these components on topsides. Chapter 4 will focus on the individual structural components and will explain how to assess the feasibility of high-strength steel without knowing the exact loads. Chapter 5 will then explain how a generalized screening tool can be used to assess an entire topside for its feasibility of utilizing high-strength steel, and Chapter 6 will use this methodology to perform a case study to evaluate a topside for the feasibility of high-strength steel. Finally, Chapter 7 will discuss the assumptions and results of this research and provide a conclusion by answering the research question.

2

High-strength steel: state-of-the-art

This chapter presents a literature review on the current state-of-the-art of high-strength steel. Section 2.1 explains the methods used to produce high-strength steel and highlights recent research on new developments. Section 2.2 provides a brief discussion and summary of the most important mechanical properties of steel and their effects. Section 2.3 elaborates on the considerations that should be considered when designing structures with high-strength steel and summarizes the latest research on using high-strength steel in structures. Section 2.4 discusses the availability, current costs and environmental impact of high-strength steel. Finally, section 2.5 summarizes the most important conclusions from the literature review.

2.1. Production processes

High-strength steel has been widely used in the offshore industry for several decades. Pipelines, the legs of a jack-up, submarines, etc., are all good examples of specific applications that make use of high-strength steel. Nonetheless, high-strength steel is not yet often used in topside structural steel. Offshore structures typically require steels with high yield strength, good toughness and ductility properties, and good weldability. Thanks to modern fabrication processes, high-strength steel can be developed with these required properties. By adding alloy elements to steel and using heat treatment processes, nearly 3500 different types of steel can be manufactured, each with their specific material properties. [1]. Nowadays, weldable high-strength steel is available in three different conditions based on their heat treatment process: normalized rolled (N), thermomechanical rolled (M) and quenched and tempered (Q&T) [5]. Figure 2.1 shows the historical development of these heat treatment processes and the corresponding steel grades manufactured with these heat treatment processes. As can be seen from the figure, high-strength steels are already available up to 1200MPa , but welding these very high-strength steels ($700+\text{MPa}$) requires complicated welding procedures, which drastically increases the fabrication costs [17]. Therefore, this research focuses only on steel grades up to S690.

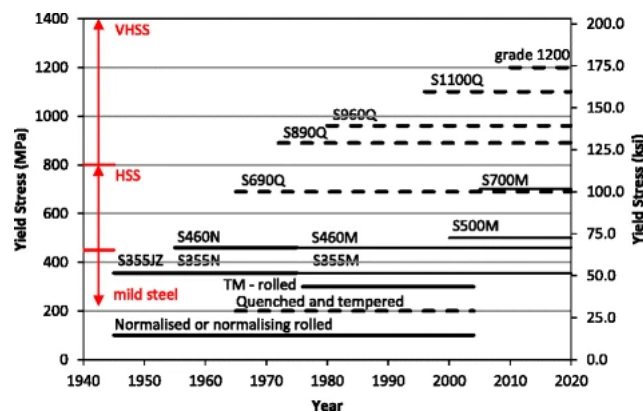


Figure 2.1: Historical development of rolled steel products [17]

Figure 2.2 shows the principles of the different post-heating processes. The oldest process is the normalized rolling process, which involves hot rolling the steel at temperatures between 900°C and 1200°C and then cooling it with air. This process produces steels with moderate yield strength and toughness requirements, and a maximum yield stress of 460MPa can typically be achieved [18]. Nonetheless, the increase in strength is achieved through higher alloy percentages, which negatively affects the weldability for higher yield stresses [19].

It is also possible to manufacture steels up to S500 using thermomechanical rolling (TM or TMCP). This process involves controlled hot rolling followed by controlled cooling, which results in a fine-grained microstructure. The fine-grained microstructure increases toughness and yield stress. Additionally, other alloying elements such as vanadium and niobium can be added to the steel to further increase its strength. Using the TMCP process, steel tends to have lower alloy contents, which greatly improves weldability [20]. Furthermore, preheating thicker plates can be reduced significantly due to these low alloying contents [19].

Finally, quenched and tempered steels have the ability to achieve the highest possible yield stress. In today's market, commercially available quenched and tempered steels can have a yield stress of up to 1100MPa . This heat treatment process aims to produce a microstructure which mainly consists of martensite. To prevent the formation of softer microstructures, the steel is instantly cooled from 900 degrees to less than 300 degrees within just a few seconds [19]. If the steel is only cooled, the material would be very strong, but also very brittle. To regain toughness, the steel is heated again but at a lower temperature and then cooled at a slower rate. Although these quenched and tempered steels are very strong, they are more challenging to weld due to their higher carbon and other alloying element contents [20].

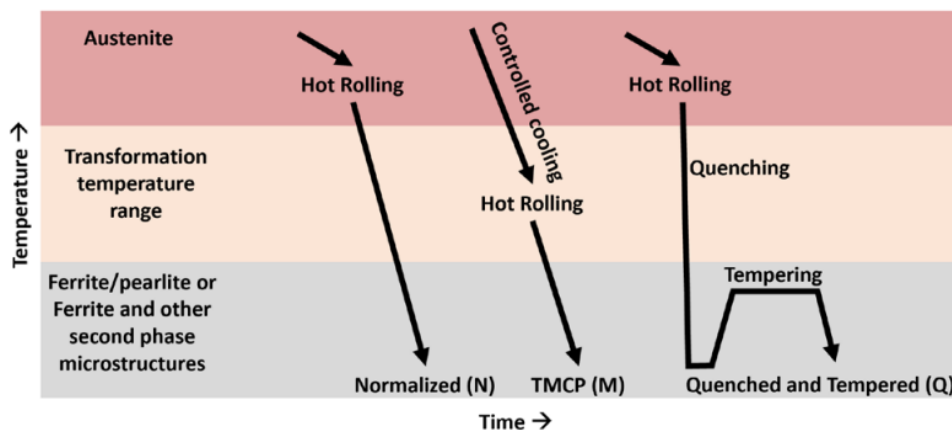


Figure 2.2: Schematic simplification of steelmaking processes [18]

2.2. Mechanical properties

The combination of the chemical composition of steel and the applied heat treatment process results in different stress-strain characteristics for steels with varying strength. Figure 2.3 compares the stress-strain curves of conventional S235 and S355 steel with those of high-strength steels like S460 and S690. The stress-strain curves can be divided into three stages. The first stage is a linear slope defined by the Young's modulus in the elastic range up to the yield stress. The second stage is a plastic region where strain hardening occurs up to the ultimate tensile stress. Finally, in the third stage, necking occurs until the material ultimately fractures. Although these curves have been used for many years for structural steels and realistic models to represent these curves have been constructed over the years, most experimental data is obtained from test data from structural steels up to 460MPa . Test data for higher strength steels is relatively limited [21], but recent research performed by Coelho et al. [22] and Wang et al. [23] aimed to fill this gap in the literature.

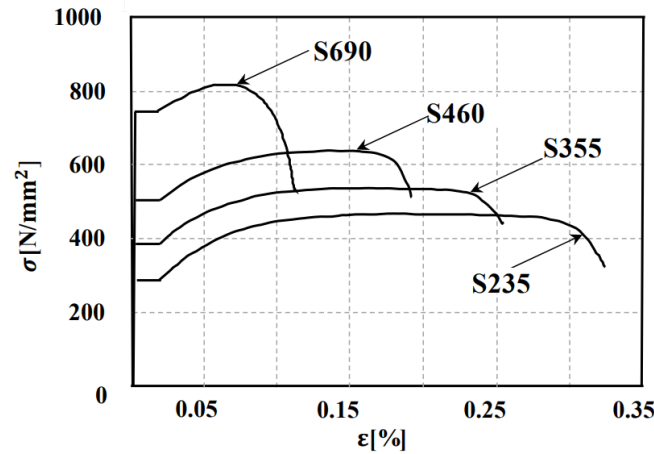


Figure 2.3: Stress-strain curves for different steel grades [21]

The regulations prescribe minimal required yield strengths for different steel grades, but it is important to note that the required yield strength reduces with thickness caused by the increase in needed alloying elements. Table 2.1 illustrates how the minimum required yield strength decreases with an increase in thickness for normalized and thermomechanically rolled steels. This reduction is essential to maintain the weldability of the steel [6].

Table 2.1: Minimal required yield strength at room temperature of normalized and thermomechanical rolled weldable fine grain structural steels (EN10025-4 [24] and EN10025-3 [25])

Steel grade	Minimum required yield strength [MPa]							
	≤16	>16 ≤40	>40 ≤63	>63 ≤80	>80 ≤100	>100 ≤150(N)/120(M)	>150 ≤200	>200 ≤250
S355N	355	345	335	325	315	295	285	275
S355M	355	345	335	325	370	365	-	-
S460N	460	440	430	410	400	380	370	-
S460M	460	440	430	410	400	385	-	-

From figure 2.3, it is clear that higher-strength steels have a lower ductility as the straining length where the fracture occurs decreases. Ductility is important for steel structures to take into account unexpected plastic strains. According to the method used by the Eurocodes, structures are designed for ductile failure modes shown in figure 2.4 [26]. As brittle fracture is not allowed to happen in any circumstance, certain ductility requirements for materials are essential. These are, therefore, typically included in the material properties requirements. Despite the fact that high-strength steels show lower ductility, the structural design of structures with high-strength steel is not significantly affected according to STROBE [6].

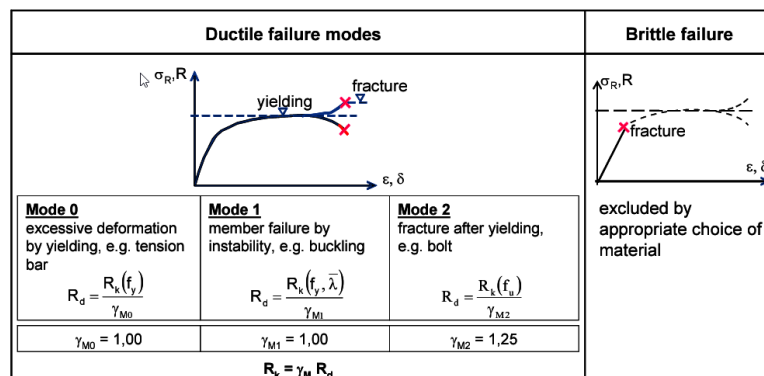


Figure 2.4: Brittle fracture and ductile failure [26]

Nevertheless, the stress-strain curves are affected by temperature and at low temperatures, the material can fail abruptly before reaching the yield stress due to brittle fracture. This is an important consideration for the offshore industry, which operates in very cold water. Fracture toughness is a measure of a material's resistance to crack propagation and is used to describe its ability to withstand brittle fracture at specific temperatures. Figure 2.5 illustrates the variation in typical Charpy-V impact energy with temperature for different steels. The graph demonstrates that thermomechanically rolled S460 steel has superior fracture toughness properties compared to non-alloy S355 steel. For quenched and tempered steels, the fracture toughness is somewhat lower than conventional S355 steel, but it improves at lower temperatures.

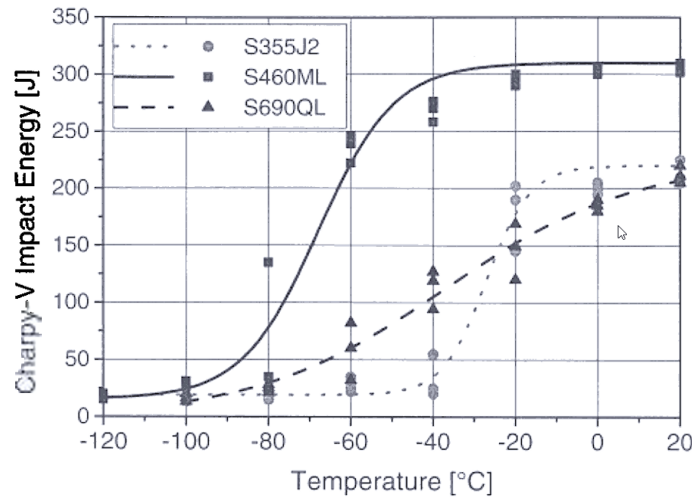


Figure 2.5: Charpy V-temperature transition curves for different steels [27]

As previously discussed, the properties of the material can be modified by adding specific alloys to the steel and tweaking the production process. To guarantee safe usage, regulations like the Eurocodes require material certificates that determine the minimum values of typical material properties. Engineers then use steel that has the necessary properties for their projects. The advantage of these minimum values is that they guarantee weldability and safety, allowing high-strength steels to be used safely in steel structures. In conclusion, steel with higher strength can be produced with the required toughness and ductility requirements. Although ductility is less compared to that of mild-strength steels, it usually does not limit the design of high-strength steel structures. The biggest disadvantage of high-strength steel is that it may lead to deflection issues, as the Young's modulus does not increase with a higher yield stress.

2.3. Engineering considerations

This section summarises essential factors to consider when using high-strength steel in steel structure designs. First, the design rules according to Eurocode 3 for beams and columns are discussed in paragraphs 2.3.1 and 2.3.2, respectively. These paragraphs also cover related literature and recent findings, highlighting the differences between conventional steel and high-strength steel. Additionally, the welding of high-strength steel is discussed and compared with conventional steel in paragraph 2.3.3. Furthermore, short discussions of high-strength steel fatigue, corrosion and fire resistance are discussed in paragraphs 2.3.4, 2.3.5 and 2.3.6, respectively.

2.3.1. Static beam resistance

Statically loaded beams are normally checked for two different limit states: the ultimate limit state and the serviceability limit state. These limit states verify if a structure can resist internal failure or instability phenomena (ULS) and that it performs properly throughout its lifetime by not experiencing too much deflection (SLS). Typically the check for the ULS consists of a rotational capacity via a cross-section classification, a shear force check and a bending moment resistance check.

To check if statically loaded beams have enough rotation capacity, the Eurocodes have defined four different cross-section classes, which are shown in figure 2.6. Class 1 cross-sections have a high rotation capacity, while local buckling will only occur after huge plastic deformations. These type of cross-sections can form plastic hinges without reduction of the beam's resistance and plastic analyses can be used to calculate the bending moment resistance. Class 2 cross-sections can also develop plastic moment resistance, but cannot form plastic hinges due to limited rotation capacity, while local buckling will occur much sooner. Class 3 cross-sections will experience local buckling before they can develop plastic moment resistance. For this cross-section class the elastic analysis should be used. Finally, cross-section in class 4 do not have enough resistance and local buckling will occur before even the yield stress is reached. This last cross-section class is therefore usually not allowed in structural applications.

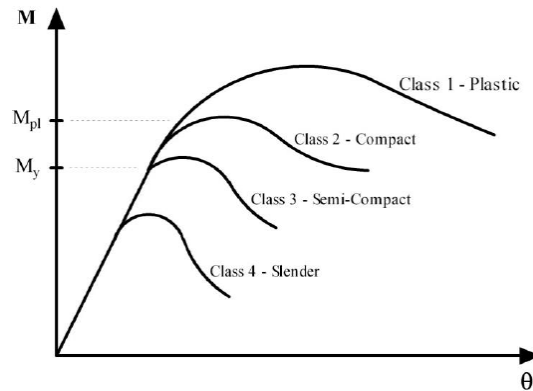


Figure 2.6: Cross section behaviour in bending according to Eurocode 3

For higher-strength steels, the susceptibility to local buckling is higher [5]. To determine a cross-section's ability to resist local buckling, Eurocode 3 uses a factor ϵ , which can be calculated with equation 2.1. However, this factor can only be calculated for steel grades up to S460, while the current design standards prohibit plastic design for high-strength steels greater than S460. Nonetheless, recent research proved that plastic design is also feasible for high-strength steel beams [28]. Another study [29] suggests changes to the current cross-section classification limits for high-strength steel beams. The study concludes that the class 1 limits for the flanges should be changed from 9ϵ to 8ϵ , and the web limits should be changed from 72ϵ to 60ϵ , as insufficient rotation capacities occurred with the conventional limits for class 1. The limits for other classifications are sufficient for beams with high-strength steel and can be extended for use up to S700 steel. These new limitations will soon be implemented into the newest version of Eurocode 3 [6], making plastic analysis possible for high-strength steel beams.

$$\epsilon = \sqrt{\frac{235}{f_y}} \quad (2.1)$$

According to Eurocode 3, laterally restrained beams can be assessed by the cross-sectional resistance and deflection check only. If shear forces are assumed to be neglectable, and that a beam is only subjected to uniaxially bending, the design bending resistance ($M_{c,Rd}$) of the cross-section can be determined by equation 2.2 or 2.3 depending on the cross-section classification.

$$M_{c,Rd} = \frac{W_{pl,min} f_y}{\gamma_{M0}} \quad (2.2)$$

$$M_{c,Rd} = \frac{W_{el,min} f_y}{\gamma_{M0}} \quad (2.3)$$

The member needs to satisfy equation 2.4 in order to have sufficient resistance against bending and equation 2.5 to have sufficient resistance against deflections. In equation 2.4, M_{Ed} represents the design value of the bending moment and in equation 2.5, δ represents the deflection, which can be calculated with standard deflection formulas or with finite element analysis.

$$\frac{M_{Ed}}{M_{c,Rd}} \leq 1.0 \quad (2.4)$$

$$\frac{\delta}{\delta_{max}} \leq 1.0 \quad (2.5)$$

Nonetheless, the shear force cannot always be neglected, and the member should be checked against it, which is done with equation 2.6 in the case of an elastic analysis. In this equation, τ_{Ed} is the design value of the local shear stress. The value of τ_{Ed} can be determined for I and H beams with equation 2.7. In this equation, V_{Ed} is the design value of the shear force and A_w and A_f are the area of the web and flange, respectively.

$$\frac{\tau_{Ed}}{f_y/(\sqrt{3}\gamma_{M0})} \leq 1.0 \quad (2.6)$$

$$\tau_{Ed} = \frac{V_{Ed}}{A_w}, \quad \text{if } \frac{A_f}{A_w} \geq 0.6 \quad (2.7)$$

The interaction between bending and the shear force is an important factor to check. If the elastic analysis is used, a criterion for a state of plane stress from Von Mises is used. The equation for the elastic analysis is shown in equation 2.8.

$$\sigma_{von-mises} = \sqrt{\sigma^2 + 3\tau^2} \leq \frac{f_y}{\gamma_{M0}} \quad (2.8)$$

When the plastic analysis is used, and shear and bending are both occurring, the bending resistance should be reduced to allow for the presence of the shear force. Usually, this is not very significant for low values of the shear force, and therefore, the bending resistance should only be reduced when $V_{Ed} > 0.5V_{pl,Rd}$. The plastic shear resistance, $V_{pl,Rd}$, can be calculated with equation 2.9 and, when necessary, the reduced design moment resistance is obtained from equation 2.10 for I or H sections, in which $\rho = (2V_{Ed}/V_{pl,Rd} - 1)^2$.

$$V_{pl,Rd} = \frac{A_v(f_y/\sqrt{3})}{\gamma_{M0}} \quad (2.9)$$

$$M_{y,V,Rd} = \left(W_{pl,y} - \frac{\rho A_w^2}{4t_w} \right) \frac{f_y}{\gamma_{M0}} \quad (2.10)$$

If beams would be laterally unrestrained, the bending moment resistance can be determined with equation 2.11. Recent research proved that these current design rules for lateral torsional buckling of beams are conservative for high-strength steels [30]. This is mainly due to the reduction of residual stresses that occur with increasing steel strength. The research has concluded that the existing design rules for lateral torsional buckling have the potential for improvement.

$$M_{cr} = C_1 \frac{\pi^2 EI_z}{(kL)^2} \left\{ \sqrt{\left(\frac{k}{k_w} \right)^2 \frac{I_w}{I_z} + \frac{(kL)^2 GI_t}{\pi^2 EI_z} + (C_2 z_g)^2} - C_2 z_g \right\} \quad (2.11)$$

Hybrid plate girders are another interesting development in the field of high-strength steel. Recent research [31] has shown that by using high-strength steel flanges (460 MPa) and conventional steel webs, the costs can be reduced by up to 17%. Nevertheless, another research [6] claimed a somewhat lesser cost benefit of only 4% for hybrid girders with S460, but 13% cost reductions could be achieved with flanges of S690. Additionally, these S460 and S690 hybrid plate girders have achieved weight savings of 21% and 41%, respectively, along with embodied carbon savings of 19% and 36%.

It is evident that using high-strength steel can be advantageous for designing beams, but deflection becomes a significant issue and affects beam design earlier. Therefore, designing high-strength steel beams requires a careful approach [5]. According to STROBE's research [6], it was found that long-span roof trusses, transfer beams, and beams with large web openings could benefit the most from using high-strength steel, provided they are not limited by deflection.

2.3.2. Static column resistance

If a member is subjected to axial compression, such as a column, the member should be verified according to equation 2.12. In this equation, N_{Ed} is the design value of the axial compression force, and $N_{c,Rd}$ is the design resistance of the cross-section for compression. $N_{c,Rd}$ is determined by Af_y/λ_{M0} for cross-section class 1, 2 and 3. However, members in compression should also be checked against buckling according to equation 2.13, in which $N_{b,Rd}$ is the design buckling resistance. Often, buckling is the governing failure mechanism for steel members under compression.

$$\frac{N_{Ed}}{N_{c,Rd}} \leq 1.0 \quad (2.12)$$

$$\frac{N_{Ed}}{N_{b,Rd}} \leq 1.0 \quad (2.13)$$

The flexural buckling resistance is calculated by equation 2.14, in which χ represents the buckling reduction factor. The buckling reduction factor is calculated with equation 2.15, in which ϕ is a factor which is calculated with equation 2.16 and depends on two variables: α , which corresponds with the associated buckling curves that can be determined from figure 2.7, and the non-dimensional slenderness coefficient $\bar{\lambda}$.

$$N_{b,Rd} = \frac{\chi Af_y}{\gamma_{M1}} \quad (2.14)$$

$$\chi = \frac{1}{\phi + \sqrt{\phi^2 - \bar{\lambda}^2}} \quad (2.15)$$

$$\phi = 0.5[1 + \alpha(\bar{\lambda} - 0.2) + \bar{\lambda}^2] \quad (2.16)$$

Cross-section	Limits	Buckling axis	Buckling curve		
			S275 S355 S420	S460 to S700 inclusive	
Rrolled sections (beams, columns)	$h/b > 1.2$	$t_f \leq 40$ mm	y-y z-z	a b	a_0 $a_0^{(1)}$
		$40 < t_f \leq 100$ mm	y-y z-z	b c	a $a^{(2)}$
	$h/b \leq 1.2$	$t_f \leq 100$ mm	y-y z-z	b c	a $a^{(2)}$
		$t_f > 100$ mm	y-y z-z	d d	c c
Welded I sections	$t_f \leq 40$ mm	y-y z-z	b c	b c	
	$t_f > 40$ mm	y-y z-z	c d	c d	
Hollow sections	hot finished	any	a	a_0	
	cold formed	any	c	c	
Welded box sections	generally (except as below)	any	b	b	
	thick welds: $a > 0.5t_f$ $b/t_f < 30$ $h/t_w < 30$	any	c	c	

¹⁾ In the next version of EN 1993-1-1, curve a_0 is reduced to curve a.

²⁾ In the next version of EN 1993-1-1, curve a is reduced to curve b.

Figure 2.7: Selection of flexural buckling curve [20]

High-strength steel columns can benefit from reduced impact of residual stresses, just as with lateral torsional buckling of beams. According to Eurocode 3, hot-rolled sections can use more beneficial buckling curves. Recent research indicates that welded I-sections can also benefit from this theory. Recommendations were proposed to use more beneficial buckling curves for welded I-sections [32]. For offshore structures, columns are almost always made from circular-hollow sections. The Eurocodes require the use of buckling curve c for steels up to 700MPa for these types of cross-sections, but a

study into the structural performance of cold-formed high-strength steel hollow section columns proved that conservative results were obtained with these current regulations by about 13 to 18% [13]. Another study concluded that the current design rules are conservative with 10% for high-strength steel cold-formed tubular hollow section beam-columns. It states that buckling curve 'a' would be more suitable than the current 'c', leading to higher benefits of using high-strength steel circular columns [33].

The non-dimensional slenderness coefficient can be obtained by using equation 2.17. This coefficient is dependent on the cross-sectional area of the material, its yield stress, and the Euler's critical load (N_{cr}). In order to calculate the Euler's critical load, which is also known as the elastic critical load, equation 2.18 can be used. This equation requires the Young's modulus, area moment of inertia, and effective length of the column.

$$\bar{\lambda} = \sqrt{Af_y/N_{cr}} \quad (2.17)$$

$$N_{cr} = \frac{\pi^2 EI}{L^2} \quad (2.18)$$

When columns are made of high-strength steel, two factors affect their slenderness. Firstly, the reduction in cross-sectional area and area moment of inertia due to the use of less material, and secondly, the increase in yield stress. Figure 2.8 illustrates the effect of using different yield stresses on the total buckling resistance. It's evident that short, stocky columns offer the most significant benefits. The STROBE study examined the use of high-strength steel columns of rolled sections and welded I sections in buildings [6]. The research analyzed two case studies, one of a 10-story building and one of a 20-story building. The study concluded that a reduction of 25% in steel could be achieved for rolled sections and 25% to 48% for fabricated I sections in a 20-story building. The overall costs were somewhat higher if fabricated I sections were made of S460, but reduced when fabricated I sections were made of S690. For rolled sections, the costs were reduced in both cases by approximately 10%. It concluded that the use of high-strength steel becomes more beneficial with increasing building height.

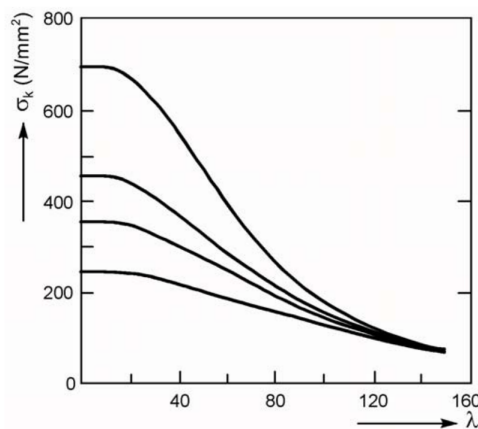


Figure 2.8: Representation of the buckling curves for different steel grades [5]

Nevertheless, rolled and welded I-section columns are typically not utilized in offshore structures, which instead make use of circular hollow sections. Research has also shown that high-strength steel is considerably economically beneficial for columns made of circular tubes [12]. This is particularly true for simple columns, especially those which are stocky, but the benefits decrease with eccentricity. The same research has also investigated the use of columns in frames and concluded that the use of high-strength steel in frames can lead to significant economic benefits. For unbraced frames, deflection becomes the governing factor, which reduces the economic advantage of using high-strength steel. Therefore, the research concluded that there is no benefit in using high-strength steel in sway frames where the ratio of the applied loads, N_{Ed} , to the critical load, N_{cr} , is less than 10.

Recent research has also explored the potential of hybrid columns that combine different types of steel to improve load-bearing capacity and energy absorption in steel structures [34]. An example of this is shown in figure 2.9, where plates of S355 are welded between tubular hot-rolled S460 or S690 corners. By using these hybrid columns, it is possible to avoid the brittleness that can occur with higher-strength steel. According to research, the load-bearing limit increased by 50% and the columns could absorb 10% more energy for high-strength steel, with even better results seen when using ultra-high strength steel ($700+MPa$). While these types of columns are currently not used in offshore structures, they demonstrate the potential of high-strength steel for future steel structures.

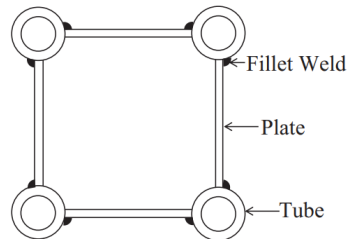


Figure 2.9: Example of hybrid compressive member [34]

2.3.3. Weldability

The current production methods for high-strength steel allow for the creation of steel with both high strength and sufficient toughness, making it highly weldable. However, the welding characteristics may vary slightly depending on the production route and individual characteristics of the high-strength steel grades [20]. Although the same welding operations can be performed for high-strength steels, welding operations should be carried out with greater care by experienced welders as the complexities increase for higher-strength steels. To ensure good welding, defects in both the weld metal and parent metal must be minimized. The ability of a steel to be weldable can be expressed in the carbon equivalent (CE), which can be calculated using equation 2.19 from EN1011-2.

$$CE = C + \frac{Mn}{6} + \frac{Cu + Ni}{15} + \frac{Cr + Mo + V}{5} \quad (2.19)$$

According to Omajene et al. [35], steels with a CE less than 0.4% have excellent weldability properties. Steels with a CE between 0.41% and 0.45% also have good weldability, but it is recommended to use low hydrogen electrodes. Steels with CE between 0.42% and 0.52% have fair weldability, and it is important to control the interpass temperature. Finally, steels with a CE higher than 0.52% have poor weldability, and post-weld heat treatment is necessary. In all cases, preheating is an essential part of the welding procedure to minimize the risk of hydrogen cracking. The need for preheating depends on the plate thickness. Figure 2.10 shows the recommended preheating temperatures for normalized and thermomechanical rolled steels against varying plate thicknesses.

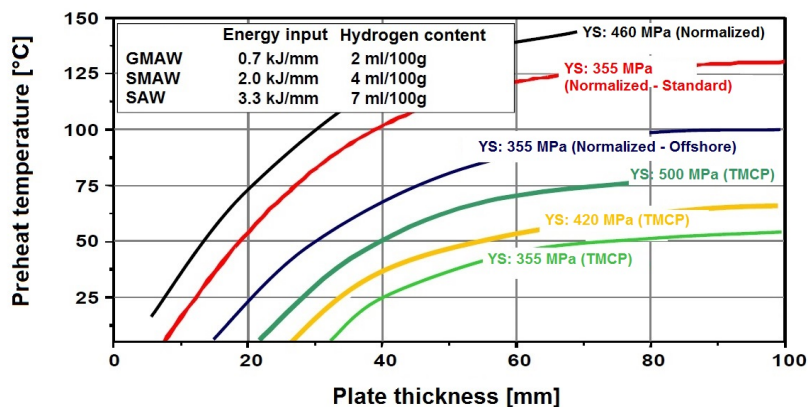


Figure 2.10: Preheat temperature vs. plate thickness for different normalized and TMCP steels [36]

As shown in figure 2.10, the preheating temperature required for conventional normalized S355 offshore steel is higher compared to high-strength S500 thermomechanical rolled steel. As discussed in section 2.1, thermomechanical rolled steel has lower alloy content, which results in a lower CE. Therefore, thermomechanical rolled steel has less chance of experiencing cold cracking, resulting in lower recommended preheating temperatures. Limits on the heat input are still important, while TM steels are susceptible to softening in the heat-affected zone (HAZ) [20]. Quenched and tempered steels are not shown in figure 2.10, but their CE tends to be much higher for thicker plate thicknesses while alloy compositions grow to ensure sufficient hardening in the core. Therefore, the susceptibility to cold-cracking increases, and higher preheat temperatures are required to prevent cold-cracking [19].

If proper welding techniques are applied and the appropriate heat treatments are used, high-strength welds can be reached, and optimal strength, toughness and durability can be achieved for high-strength steel. Nevertheless, preheating is a very time-consuming fabrication step, which increases fabrication costs. According to HSM Offshore Energy [7], extra time of approximately 30% is often required to pre-heat steel. Furthermore, preheating is also desired to be avoided because of job safety, while welders are often in closed or small spaces. Reducing the preheat temperatures results in more desired working conditions, higher efficiency and better end results [19]. As TM steel requires less preheating temperature, economical and working benefits can usually be obtained during fabrication.

Despite quenched and tempered steels requiring a higher preheating temperature for a specific plate thickness, part of this problem can be reduced because of the advantage of high-strength steel; higher-strength can result in smaller and thinner structural components. Therefore, the required preheating temperature will also decrease. Figure 2.11 illustrates the relationship between increased yield strength, required plate thickness, and welding volume for a tensile-loaded plate. The figure shows that if S690 is used, a reduction of approximately 48% in thickness and 68% in welding volume can be achieved. This could potentially lead to a lower required preheating temperature compared to conventional normalized S355 steel. Nonetheless, it is important to note that the example in figure 2.11 is for a tensile-loaded plate. When a high-strength steel component subjected to bending is assessed, a much less thickness reduction can be expected [5].

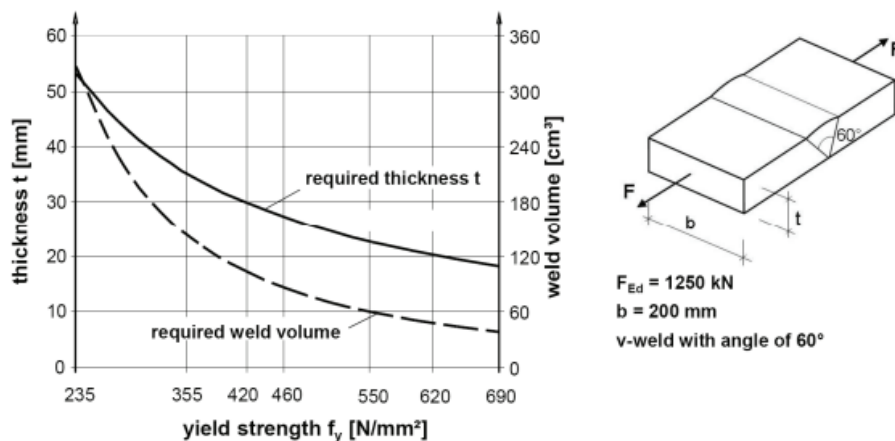


Figure 2.11: Dimensioning of tension bars with different steel grades and corresponding butt welds [37]

Another important factor, according to welding consultant Bodt [38], is the human factor in welding quenched and tempered steels. Practise has shown that projects have failed because of discipline, control, and careful welding practice because humans did not follow proper procedures. Although this can easily be avoided by following proper welding procedures, the risk for these types of failure is much lower for normalized and thermomechanical rolled steels. Therefore, thermomechanical rolled steels are preferred at HSM Offshore.

2.3.4. Fatigue

Structures, where fatigue is governing do typically not benefit from using high-strength steel [39]. Fatigue consists of two different processes: crack initiation and crack propagation. In the case of unwelded steel components, their fatigue life is usually determined by crack initiation. The period of crack initiation generally increases with the tensile strength of the steel [5]. Therefore, high-strength steel would be beneficial for unwelded components to improve their fatigue life. However, for welded structures, things are different as they act more like notched samples. Welded structures are typically governed by crack propagation as they have pre-existing weld features and high tensile residual stresses [20]. Unfortunately, fatigue crack propagation is independent of material strength. Smaller joints created using thinner high-strength steel plates result in higher stress variations, negatively impacting the crack propagation and, thus, the structure's fatigue life. Hence, structures where fatigue is governing require careful analysis when using high-strength steel [5].

Offshore jackets are highly susceptible to fatigue [40], which means that using high-strength members on them is not expected to provide significant benefits. On the other hand, topsides are much less affected by fatigue and high-strength steel could be possibly beneficial, but it is still important to consider fatigue when designing a topside with high-strength steel.

Improving the fatigue resistance of a material can be achieved by designing better welds and reducing local stress concentrations through good geometry. It is essential to follow good welding practices to minimize imperfections in the welds. Additionally, ultrasonic impact treatment has been proven to reduce local residual stresses, which can increase the fatigue properties of the material [5].

2.3.5. Corrosion

When it comes to corrosion, there is no significant difference in the level of protection required for high-strength steel compared to milder steel. The same methods of protection can be used for both, but it is important to note that stress corrosion cracking is more likely to occur when using high-strength steel due to the higher levels of stress in the joint [5]. To reduce the risk of stress corrosion cracking, ultrasonic impact treatment can be used. Additionally, when connecting mild steel with high-strength steel, it is important to check and design for galvanic corrosion, which can have a significant impact on the strength of high-strength steel [5].

2.3.6. Fire resistance

The final engineering consideration that will be discussed in this report is fire resistance. In the event of an accident, a structure should remain capable of resisting its loads. For steels up to 700MPa , fire resistance can be assumed to be the same as for conventional steels [20], but different material properties may occur when high-strength steel structures cool down after reaching temperatures above 500 degrees Celsius. It is important to note that the focus of this report does not include accidental loads and, thus, fire. Therefore, the fire resistance of high-strength steel will be assumed to be sufficient, but it is advised to keep in mind that material properties can change after exposure to fire.

2.4. Costs and environmental impact

This section starts with providing information on the availability and prices of various types of steel in paragraph 2.4.1. Additionally, different methods of producing high-strength steel have varying effects on climate change. Paragraph 2.4.2 explores the impact of climate change on different steel grades based on research performed by Stroetmann [37]. Finally, paragraph 2.4.3 compares the offshore industry with the onshore construction industry in terms of potential cost and embodied carbon savings.

2.4.1. Costs of high-strength steels

High-strength steels are on the market for decennia as the interest in high-strength structural steel is growing rapidly. As an enormous amount of different steels with different properties are available nowadays, a selection of only two high-strength steel grades is chosen for this research: S460 and S690. Topsides are mainly fabricated from two start products directly available after the manufacturing of steel in steel plants: plating and structural shapes. The information within this paragraph is mainly based on information provided by the purchasing department of HSM Offshore Energy.

Various types of structural steel plates with different toughness requirements are available. The maximum available thicknesses of the considered steel grades are shown in Table 2.2 according to EN10025. Figure 2.12 illustrates the differences in prices of different steel grades in 2011 [37]. That year, the price difference between conventional steel of S355 and high-strength steel of S460 and S690 was approximately 3% and 35%, respectively. However, only a weight reduction of 3% and 27% was required to create economic benefits. If only a tensile force is applied on a plate, S460 and S690 are 30% and 95% stronger than S355, respectively. Therefore, these weight reductions are quickly expected when only a tensile force is applied, but this is not often the case for offshore topsides.

Table 2.2: Available structural steel plates according to EN10025-2,3,4 and 6

Steel grade	Steel quality	Steel type	Max. plate thickness [mm]
S355	Non-alloy	J/J2/K2	400
	Normalised	N/NL	250
	Thermomechanical	M/ML	150
S460	Normalised	N/NL	250
	Thermomechanical	M/ML	150
	Q&T	Q/QL/QL1	200
S690	Q&T	Q/QL/QL1	200

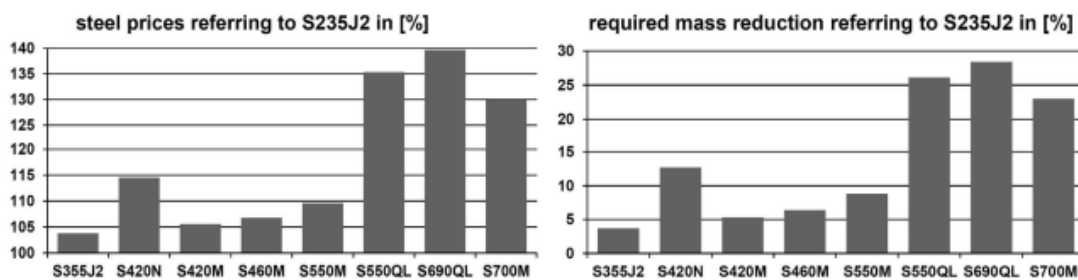


Figure 2.12: Economic efficiency of heavy plates, if only the material price is taken into account (2011) [37]

Nevertheless, several European steel suppliers were asked for prices by HSM Offshore Energy, and it was found that there were differences in prices compared to the ones showed in figure 2.12. It should be noted that steel prices fluctuate daily and that different properties, thicknesses, or lengths can result in different prices. Therefore, multiple prices were assessed, and it was concluded that steel plates of S355N cost around 1000€/ton, while S355M costs 1350€/ton. Many construction companies prefer TM steel due to its better welding properties, while N steel is often used only for specific applications. It is often cheaper to use more expensive S355M steel as it reduces welding time. For high-strength steel, prices increase, and table 2.3 shows the price differences between S460N, S460M, and S690Q compared to S355 steel. It can be seen that this price difference is much lower when compared to S355M.

Table 2.3: Price differences for different high-strength steel grades

Steel grade	Price compared with S355N	Price compared with S355M
S460N	+69%	+24%
S460M	+46%	+7%
S690Q	+63%	+20%

Until now, only price differences caused by material costs and different welding procedures have been highlighted. It is worth noting that tools used to process high-strength steel may experience a slight reduction in their lifetime, which can lead to additional costs. Nevertheless, in most cases, these costs are negligible [20]. The fabrication costs significantly increase only when plates need to be cold-formed

into circular hollow sections [7], which is often required to manufacture columns and bracings for offshore topsides. Bending high-strength steel requires more controlled processing, but for S460, the costs do not significantly increase or are even the same. For S690, on the other hand, the costs increase significantly due to the increase in strength and the decrease in ductility, making it harder to bend the steel plates into the correct form. As a result, higher pressure is required, leading to higher costs [5]. According to HSM Offshore Energy, this rise in manufacturing costs of cold-formed columns and bracings is approximately equal to 150€/ton.

Apart from using plating in its original form or cold-formed columns and bracings, offshore topsides are constructed with various structural shapes. Different standardized structural shapes are available in various sections. Figure 2.13 provides examples of the different structural shapes that are available. Among these shapes, H-shape, I-shape, and circular hollow sections are the most commonly used for topsides [40]. It must be noted that these structural shapes are only widely available as thermomechanically rolled, limiting the strength to S460 steel. S690 will therefore not be considered when assessing structural shapes such as beams.

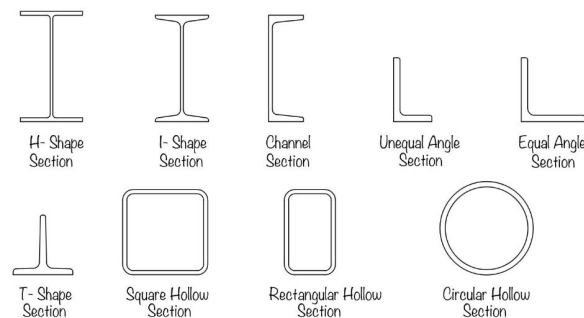


Figure 2.13: Examples of different structural shapes [41]

The cost of structural sections is generally higher than that of plating due to the additional manufacturing processes required to achieve the correct shape and geometry. For circular hollow sections, the price for S355 is approximately 3000€/ton, while the price for S460 steel is 14% higher. The prices for H- and I-shape sections are somewhat lower and can be found in table 2.4.

Table 2.4: Price for different steel grades for H- and I-shape sections

Steel grade	Price [Euro/ton]
S355N	1250
S355M	1200
S460N	1400
S460M	1300

Nowadays, there is an increasing amount of research being conducted on the use of high-strength steel in compliance with regulations such as the Eurocodes. As these codes are updated with the latest findings, high-strength structural steels can be utilized more efficiently. This could lead to a rise in demand for high-strength steel, which in turn could result in lower costs and greater use of high-strength steel in the future.

2.4.2. Environmental considerations for high-strength steel

The demand for high-strength steel is increasing as engineers aim to reduce the weight of structures and lower the total embodied carbon emissions. However, different steel grades are produced using different methods, which means that reducing weight does not necessarily result in embodied carbon savings. Stroetmann [37] conducted research on the environmental impact of high-strength steels. Figure 2.14 illustrates the cumulative energy demand (CED) for different steels, representing the direct and indirect energy required to produce a steel. The figure shows that there is no difference in steels for continuous casting, the pusher furnace, and crude steel, but for high-strength steel, more alloys are required, and it can be seen from the figure that this requires much more energy. Additionally, the

rolling mill and heat treatment require more energy, but less compared to the increase in alloys. In total, higher-strength steel has an increased cumulative energy demand.

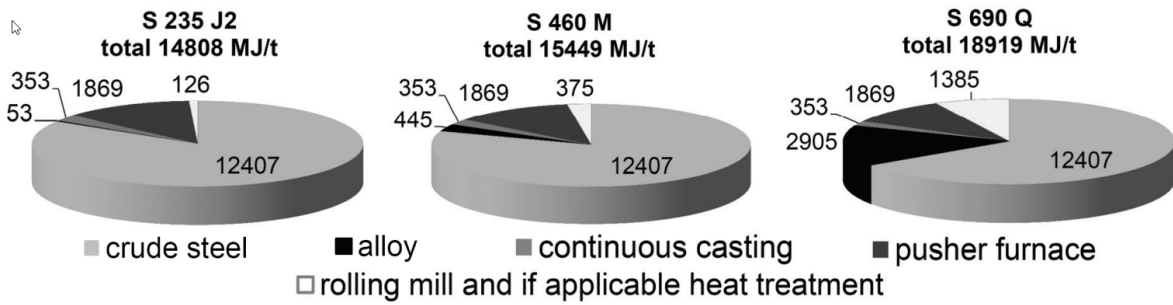


Figure 2.14: Cumulative energy demand (CED) for heavy plates made of various steel grades [37]

Nevertheless, figure 2.14 only showed the cumulative energy demand for S235, S460 and S690. Again, based on Stroetmann [37], figure 2.15 shows the total CED, the global warming potential (GWP) and the acidification potential (AP) of different steel grades. As previously explained, TM steel has a lower carbon equivalent, resulting in less energy required to produce these steels. This can explain the drop in the CED when looking at TM steels. It can be concluded that S460M steel has a lower CED than the conventionally used S355J2 steel, while the GWP and AP are comparable. On the other hand, for S690Q, the carbon equivalent is higher, resulting in higher energy demand and GWP and AP, explaining the rise for Q&T steels. From this figure, it can be concluded that S460M steel has an environmental advantage over S355J2 steel, even without a reduction in mass. However, S690 requires significant weight reduction to achieve such an advantage. Stroetmann [37] further showed this conclusion with figure 2.16 in which the required weight savings in percentage are given compared to S235J2 steel. In general, it concludes that if enough weight savings are achieved, high-strength steel can be beneficially applied to decrease the impact of environmental and climate change.

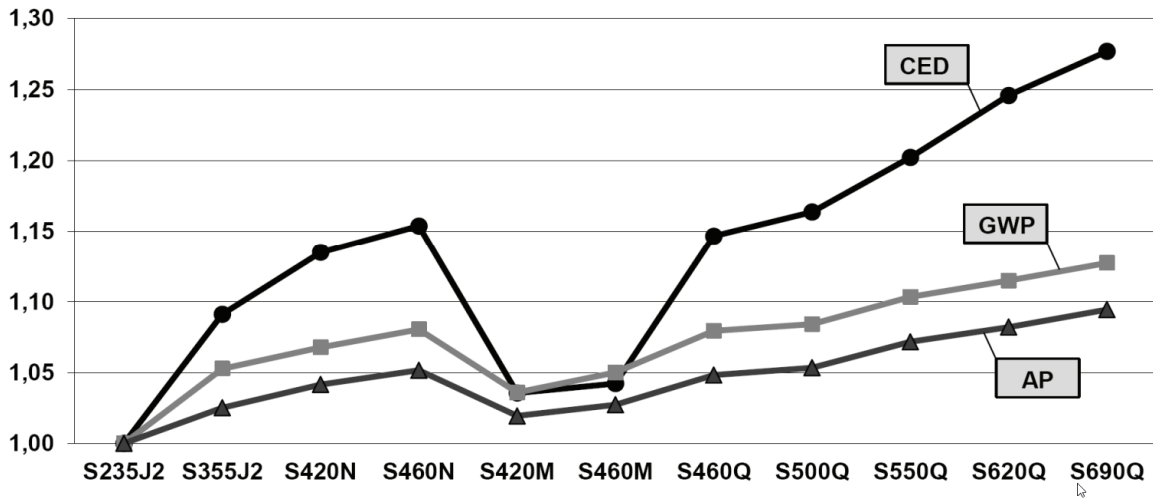


Figure 2.15: Relation of CED, GWP and AP of heavy plates for various steel grades compared with S235J2 [37]

	S355J2	S420N	S460N	S420M	S460M	S460Q	S500Q	S550Q	S620Q	S690Q
heavy plates	6,6	9,3	10,6	3,3	4,1	10,2	11,1	13,4	15,5	17,1
rolled sections	6,7	8,8	9,9	3,4	4,2	10,0	10,7	12,6	14,2	15,6

Figure 2.16: Required weight savings in [%] compared with S235J2 [37]

2.4.3. Offshore considerations for high-strength steel

The literature research, such as STROBE [6] and Stroetmann [37], evaluated the environmental impact of high-strength steel in onshore construction. Offshore structures differ significantly from onshore structures, especially in terms of transportation and installation. Offshore topsides are usually loaded onto a barge and transported to the sea, where a heavy lift ship installs the topside on the previously installed jacket. If high-strength steel is used and the topside's mass is reduced, the transport and lift condition may change. Weight reduction can lead to less transport fuel consumption, and in the case of sufficient weight reduction, even a smaller heavy-lifting ship could be used. This could result in significant cost reduction as heavy-lifting ships are expensive. Additionally, using less fuel and smaller heavy-lift ships would reduce the overall embodied carbon emissions of an offshore project.

Furthermore, reducing the topside's weight by using high-strength steel results in a smaller vertical force on the jacket. It is possible that a reduction in topside mass could improve the natural frequency of the structure, resulting in a jacket with smaller member sizes [40].

2.5. Conclusion of the literature review

In this chapter, an extensive literature study was conducted to explore the current state of high-strength steel. Thanks to modern fabrication processes, there are now 3500 different steels available with strengths up to 1200MPa . High-strength structural steel with excellent weldability is available in three conditions based on their heat treatment process: normalized rolled, thermomechanical rolled, and quenched and tempered. This research focuses on high-strength steels with a yield stress of S460 and S690. It has been concluded that an increase in yield strength typically results in a decrease in ductility and toughness, which makes welding more challenging. However, the main problem with high-strength steel is that the Young's modulus remains the same for increased strength, creating earlier deflection or stability problems.

In recent decades, more research has been conducted into high-strength steel. Multiple studies in high-strength steel beams have concluded that different cross-section classification limits are required for class 1 due to the limited rotation capacity of high-strength steel. Studies have also shown that high-strength steel for beams is most beneficial when beams are short and heavily loaded and not governed by deflection. Short and heavy is a vague definition, and it is not known when precisely a beam on a topside is short, heavily loaded, and not governed by deflection. Moreover, hybrid beams, where webs are made of conventional steel and flanges of high-strength steel, have proved to be advantageous for plate girders, and high benefits can be expected for plate girders. Furthermore, columns have been proven to be beneficially replaced with high-strength steel when they are short and stocky, especially when the columns are braced. As residual stresses have less impact compared to conventional steel, research has concluded that more advantageous buckling curves can be used for high-strength steel than is currently allowed. Also, research has proved that hybrid columns can create much weight reduction, but the welding lengths significantly increase, and it is not expected that these columns will be used on offshore topsides soon. More research is required to determine if columns in topsides are short and stocky and thus feasible for high-strength steel.

Welding is the most important fabrication element for topside fabrication, but the decrease in toughness properties makes it harder to weld. Certain heat treatments such as thermomechanical rolling and quenched and tempering can improve the toughness properties. As TM steels have a lower carbon equivalent, their toughness properties tend to be better than normalized steels, resulting in excellent welding properties. Q&T steels tend to be more difficult to weld, but this can be improved by preheating. Nevertheless, preheating is often not desired, as it increases the fabrication costs and creates a more challenging work environment. Therefore, it is essential to include the rise in price by preheating when comparing S460 and S690. For S460, it can be concluded that this steel does not require extra time or money to weld.

Because of the decreasing sizes by using high-strength steel, fatigue resistance becomes more challenging. If high-strength steel is applied, it is advised to minimize fatigue, design proper connection geometries, and perform post-weld treatment if required. Corrosion and fire resistance do not differ

much from conventional steels.

When it comes to steel plate prices, the conventional 355N steel is the cheapest option. However, due to its excellent welding properties, TM steel is often preferred. If S460M or S690Q steel plates would be used, the material costs for plates would increase by 7% and 20%, respectively. When circular hollow columns are formed from plates, there are no additional fabrication costs for S460M steel, but for S690Q steel, an additional cost of 150€/ton must be included, mainly because of the extra pre-heating time. For standard profiles, the costs are the lowest for TM steel. S355M beams cost around 1200€/ton, while S460M beams cost around 1300€/ton. S690Q beams do not exist.

Different production methods are used for different steel types, and their environmental impact also differs. It can be concluded that TM steel is more environmentally friendly compared to conventional S355J2 steel without much weight reduction. As weight reduction increases, more environmental benefits can be expected for S460M steel. For S690Q steel, the impact on the environment is much higher, especially because of the required alloys in Q&T steel. Nevertheless, if weight reduction is achieved, the environmental impact can still be lower.

Weight reduction for offshore topsides has additional benefits, especially regarding the required transport. As offshore transport requires a lot of fuel, a reduction in weight also reduces the fuel consumption, indirectly contributing to less carbon dioxide emissions. If enough weight reduction can be achieved, even smaller crane ships could be used, which would lead to economic benefits. Moreover, the reduction of topside weight could also lead to a smaller jacket, which again contributes to economic and environmental benefits.

Although there has been considerable research conducted on the use of high-strength steel, there are currently no case studies or methods available that demonstrate the potential for its application in topsides. As a result, the rest of this research aims to assess the feasibility of implementing high-strength steel in offshore topsides.

3

Assessment of structural components in topsides

In the previous chapter, several conclusions were drawn about high-strength steel. To further determine whether high-strength steel is a viable option for topsides, it is necessary to understand the structural components that make up a topside, their typical lengths, sizes, and weight distribution. First, this chapter will begin by examining the literature for standard design rules for topsides in terms of structural design in section 3.1. Additionally, section 3.1 will define specific definitions that are used throughout the remainder of this report. Secondly, section 3.2 will assess various existing topsides for their primary and secondary steel, obtaining weight distributions, typical lengths and structural component sizes while comparing these values with the literature results. Finally, in section 3.3, the conclusions of the literature and topside assessment will be discussed to determine which structural components are worth further research.

3.1. Design of offshore topsides - key figures & structural components

The main purpose of a topside is to provide support for the various functions of a platform, such as oil and gas processes or electricity transformation. The overall design of the topside depends on the size of the necessary equipment, floor area, and number of processes. The industry has a long and remarkable history, which is briefly discussed in Appendix A. Designing topsides requires a lot of experience, and according to HSM Offshore Energy and Enersea, their structural design relies heavily on the experiences gained in the past. Even with advanced computer programs, experience is still crucial, and rules and standards are based on estimations and generalized results. Therefore, past experiences with designing offshore structures are essential for creating new designs. Engineers often use a similar design as a starting point and make adjustments to some members if necessary. Member selection is not a standard process and varies greatly from engineer to engineer, depending on their background experience [15].

Topsides can generally be divided into two types: modular topsides and integrated deck topsides. Modular topsides consist of a module support frame with multiple modules on top of the frame, installed individually. The modular topside type is used when the weight or sizes exceed the maximum available crane capacity and can weigh from 10,000 tons up to 40,000 tons [40]. Figure 3.1a shows the Britannia topside, an example of a modular topside. The topside has multiple modules, and many offshore lifting operations were required to install this topside. Figure 3.1b shows an example of an integrated deck topside, which can weigh up to 10,000 tons [15]. These topsides only require one or a few lifting operations offshore, while they can be lifted entirely or installed with a float-over operation. As integrated topsides are the most abundant type of topsides in the southern North Sea, and while they are fabricated as a single unit, this research will only consider integrated offshore topsides.

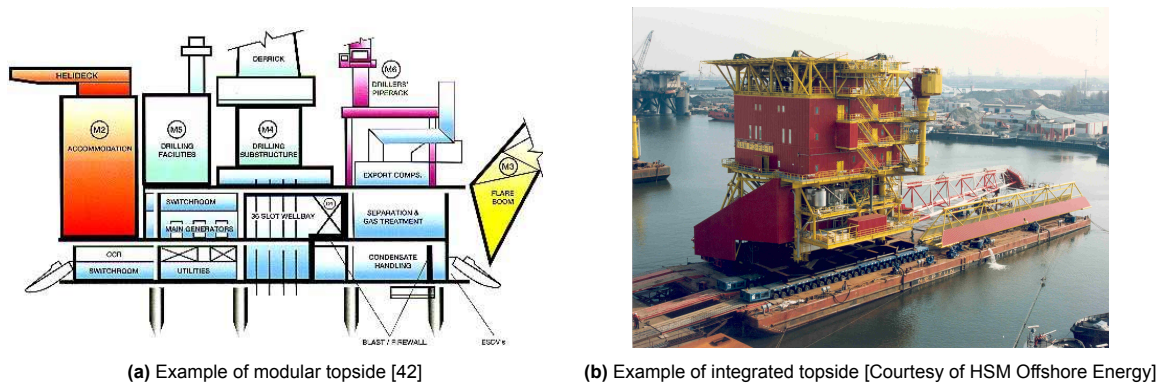


Figure 3.1: Modular and integrated topside examples

There are two structural configurations for integrated deck topsides on jacket-type platforms [15]: a truss-type topside or a portal-frame-type topside. The truss-type topside, shown in figure 3.2a, allows loadings to distribute through the bracings to the main columns. Using truss-type topsides often results in the possibility of creating lighter structures, but the bracings obstruct the platform's layout, so this configuration is not always suitable. In a portal-frame topside, shown in figure 3.2b, no bracings obstruct the layout, and the whole deck area can be used, but this requires heavier beams and an increased topside height. According to HSM Offshore Energy [7], a combination of the two is often used. Heavy plate girder beams are used where bracings are not preferred because of the layout, while bracings are used at the far sides, where no equipment is located.

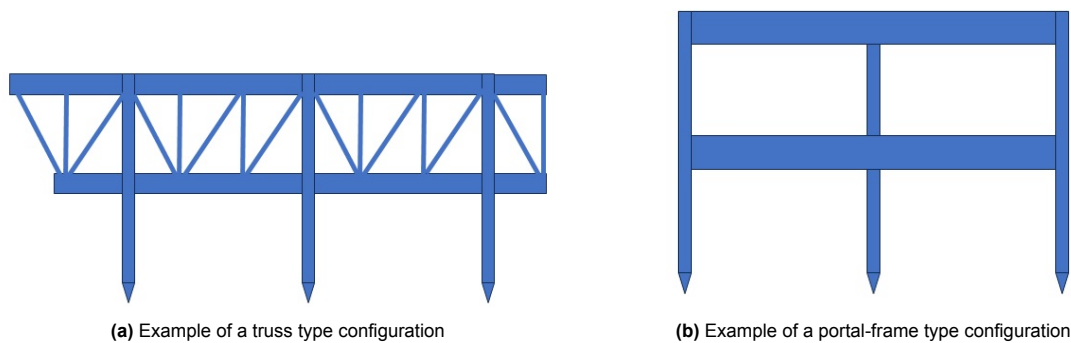


Figure 3.2: Truss type and portal-frame type topside

As preliminary designs of offshore topsides are often created by experience, there are many rules of thumb and typical numbers for topside members. Many of these typical numbers are summarized by the European Steel Design Education Programme (ESDEP) [43]. Although this source is relatively outdated, many of these numbers are still valid and are therefore summarized in this section. According to ESDEP, the steel structure of a topside consists of the following structural components, which are also shown in figure 3.3:

- Deck legs (main columns)
- Primary girders (main beams)
- Deck beams
- Deck stringers
- Floors (plating or grating)
- Bracings and secondary columns

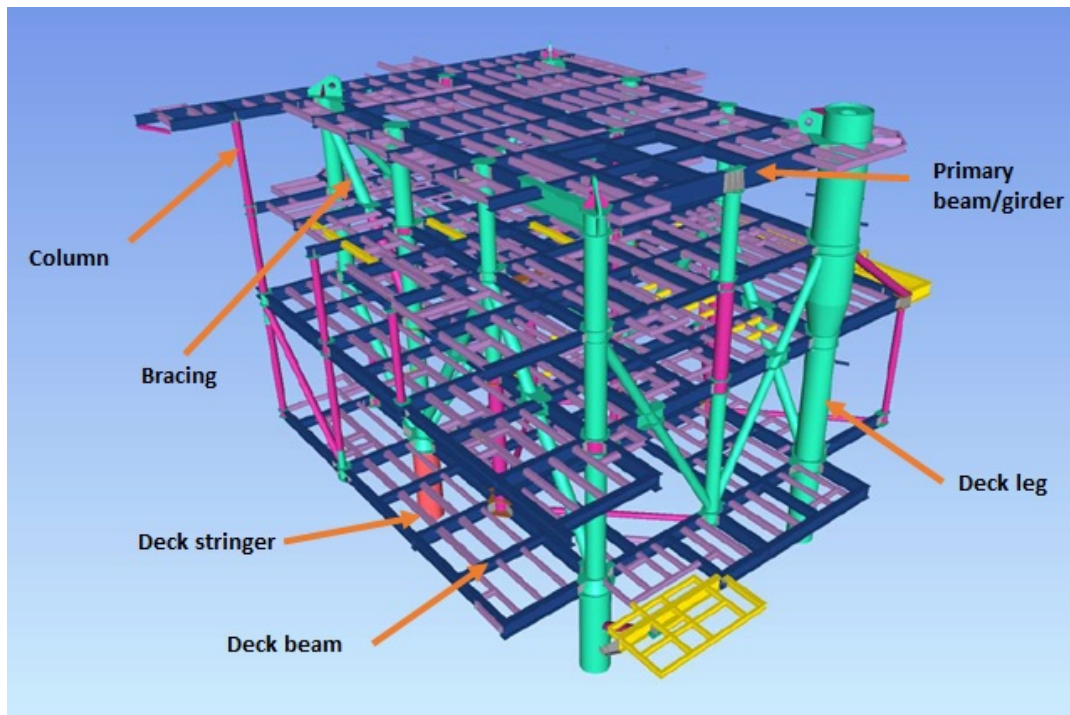


Figure 3.3: Structural components of an offshore platform

Often, a topside consists of multiple decks. There are multiple possible names for the decks, but for High-voltage offshore substations, the following decks are normally considered: cellar deck, main deck, and roof deck. Sometimes, there are smaller decks in between, which are called mezzanine decks. These decks are shown in figure 3.4. As mentioned earlier, the decks' height and area are determined by the functionality of the topside. The intermediate height between the decks on platforms within the North Sea typically differs from approximately 6 to 9 metres. The height of the cellar deck above the mean sea level (MSL) is determined by the maximum elevation of the wave crests, the elevation because of tides and storm sway, and a minimum air gap of 1.5 metres. In the southern North Sea, this distance is typically about 10 metres above MSL [44].

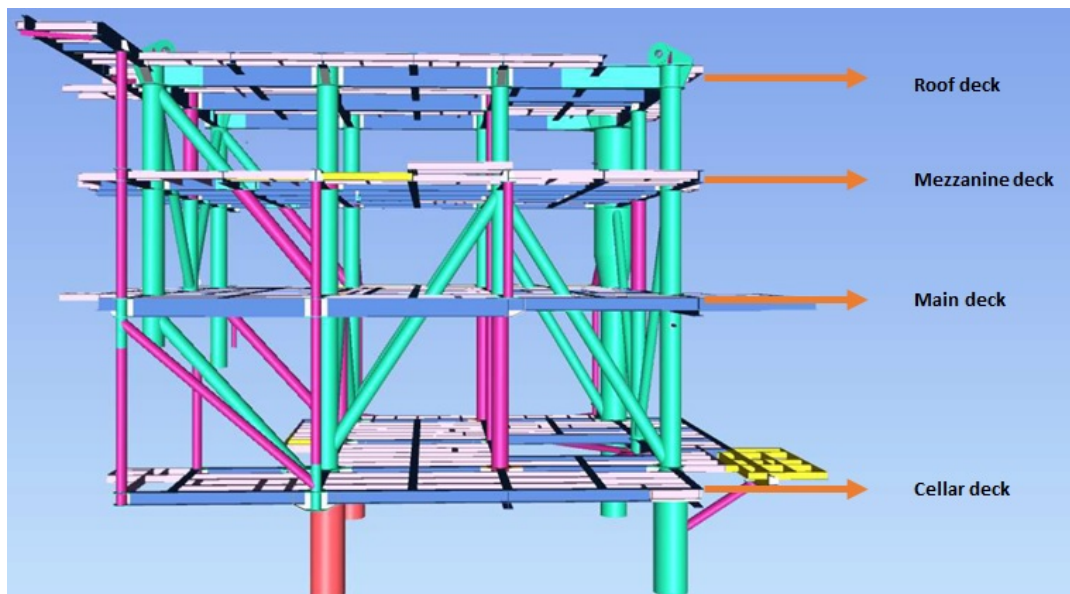


Figure 3.4: Different decks on offshore platforms (naming according to HSM)

Topsides usually consist of circular hollow sections for the columns and bracings. Hollow section columns are usually lighter than structures with beam columns, caused by an increase in the radius of gyration [11]. However, these types of members are more expensive, but this cost increment is tackled by the reduction in weight on the topsides. For a preliminary design of the deck legs, the deck leg diameter can be assumed to be equal to the pile diameter [15]. Using that diameter and the height of the cellar deck, the effective length could be determined from the degree of fixity of the leg into the deck; with this, the thickness of the deck leg could be calculated. Typically, deck legs have a D/t ratio of 35 to 40, according to Reddy and Swamidass [40]. According to Chakrabarti [15], the column spacings of the main deck legs for a four-legged platform in the Gulf of Mexico are typically 12x12 metres, and cantilever beams typically span half the column span. Nonetheless, ESDEP mentions that production platforms on the North Sea often have a column base of 15x15 metres.

The decks are connected to the deck legs and consist mainly of beams. Floor plates usually span around 1 metre, and the thickness can vary from 6 to 10mm. The chosen thickness is often determined by the wheel footprint of the design forklift truck [43]. In general, there are two options for floor plates: steel plates or grating. Steel plates can handle much heavier loads, and fluids will not leak through them, while grating can be used if weight reduction is desired. The deck stringers, which support the flooring, usually have a span of 5 metres, and the member often varies between an IPE ranging from 240 to 270 or an HEA ranging from 240 to 280. H-beams ranging from 800-1000 are often used as deck beams to support the major equipment and deck stringers. These deck beams are connected to the main beams. The height of main beams is typically conventionally chosen and varies from 1000 to 1200mm and are often built of plate-girders, beams made from plates. This is done while standard beam sizes do not pass 1000mm. A span of 12 to 15 metres is typical for the main beams. For a preliminary design, the beam sizes are usually determined by straight beam formulae using the live loads and the weights of the heaviest equipment. An initial deck load can be assumed to vary from 24 to 48kN/m² for the main deck, and for the cellar, roof and mezz deck, initial loading of 14 to 24kN/m² can be assumed [15]. Nevertheless, this is considered to be very high according to Endersea.

All of the structural components located on the topside of offshore structures require well-designed connections. These connections, also known as joints, are typically welded instead of bolted. Although bolting is cheaper, it requires more maintenance as it is susceptible to corrosion and loosening over time. Additionally, welding is stronger than bolting due to the drilled holes required for the bolts, which reduces the material strength. Unlike in the building industry, where bolting is common, welding is preferred for offshore structures as they require very strong connections and are usually installed by one lifting operation. Typical welding connections on offshore topsides can broadly be divided into three different types:

- Welded beam-to-beam connection
- Welded beam-to-circular hollow section column connection
- Circular hollow section welded joints

The welded beam-to-beam connection is usually used in the decks to connect beams to each other. Depending on the desired situation, these connections can be very stiff or flexible. For the connection of stringers to the deck beam, there are generally two options to create a connection: the stack floor concept and the flush floor concept. The stack floor concept is the easiest one to fabricate and is illustrated in figure 3.5a. In this flooring type, a stringer is placed upon the bigger deck beam and directly welded to the deck beam. However, this concept can sometimes create corners that are inaccessible for maintenance, which could eventually increase the costs significantly. Additionally, the total height of the topside will increase when the stack floor concept is applied. Therefore, the flush floor concept connections are preferred at HSM Offshore Energy [7], of which an example is shown in figure 3.5b. These connections level the stringers with the deck beam, and the flooring can be placed directly on both type of beams. It requires some extra prefabrication but is easier to conserve and maintain.

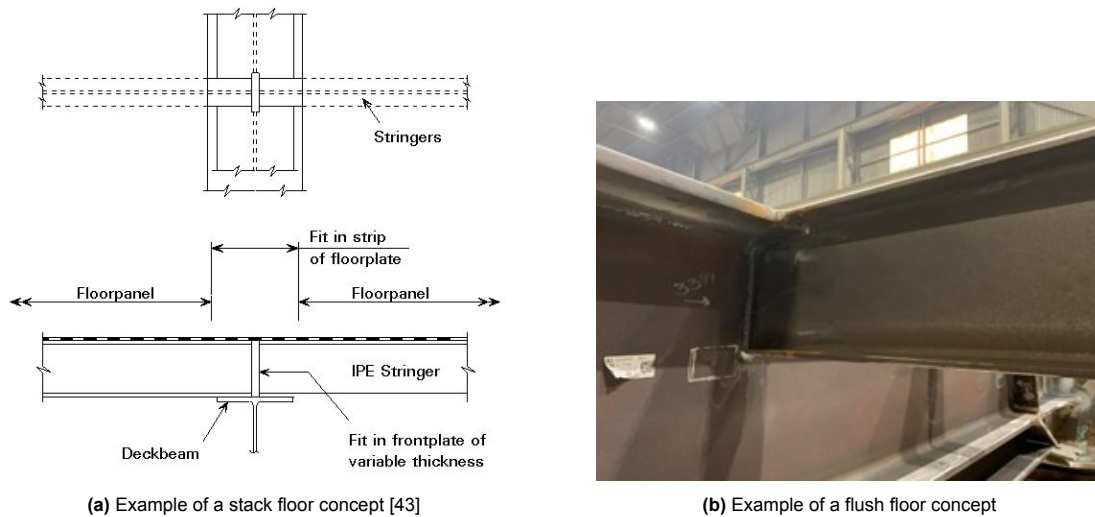


Figure 3.5: Truss type and portal-frame type topside

Offshore topside columns are typically made up of circular-hollow-tubular legs. To connect these columns to the main beams and enable them to withstand shear force and bending moment, diaphragm plates (also known as diamond plates) are used. These plates are welded onto the outer diameter of the columns to connect the beams to the circular columns. The connections are usually very rigid, as demonstrated in figure 3.6.

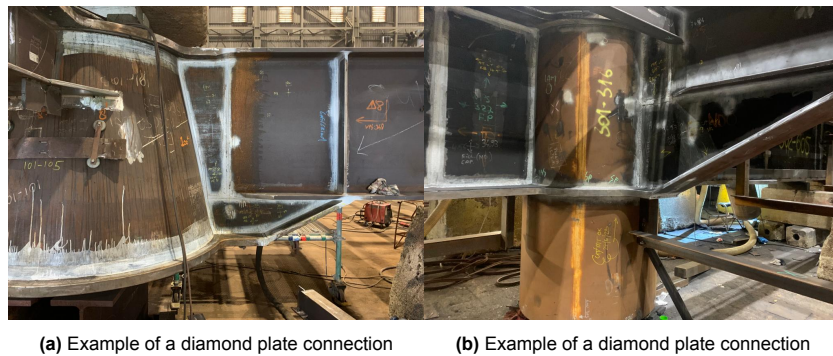


Figure 3.6: Examples of a diamond plate connection

The final connection, which is often applied on offshore structures, is the circular hollow to circular hollow connection. An example of such a connection is shown in 3.7. Essential aspects to check for these joints are plastification of the chord and the punching shear resistance because of the thin-walled cross-sections.



Figure 3.7: Example of a circular hollow section connection

When considering the total weight of a topside, it can be divided into various categories, such as structural steel weight (50%), mechanical or equipment weight (30%), piping weight (10%), and other weights (10%). Weight reduction of topsides can be achieved by four different approaches: functionality, sizing, layout compactness, and structural design. Functionality has the highest impact on weight reduction. Reducing the amount of processes on a topside could drastically decrease the required layout area and, thus, the total weight of the topside. Another option after the functionalities of the topside are evident is to minimize the sizes of the required equipment. Smaller sizes result in less required area and a decrease in total weight, but this is often not possible as the equipment is usually already chosen to be as small as possible. Then, optimizing the topside layout can be applied to reduce weight by minimizing the required area. Proper bracing design, efficient use of space, and little spare spaces can help to optimize the layout. Finally, the last option is to reduce weight through structural design. The structural design can be optimized using different materials, good member sizing, and clever engineering tricks, which is the type of weight reduction that this research focuses on.

According to HSM Offshore Energy [45], the structural scope of the topside typically accounts for about one-sixth of the total topside cost. Decreasing the weight of these structures while maintaining an acceptable design for fabrication, installation, and maintenance could lead to significant economic benefits for the overall project. From this section, it can be concluded that the structural steel scope of topsides mainly consists of five structural components: beams, columns, bracings, plating or grating and extra steel required for connections. Although there are many more steel parts such as pad-eyes, crane pedestals, pipe supports, equipment supports, etc., these parts are usually smaller in number than the aforementioned components, and the size of these parts is often more critical than their strength. Therefore, high-strength steel is not expected to be feasible for these parts, or if feasible, their small amount will contribute little to reducing costs and weight. Hence, these specific parts will not be considered. Nonetheless, it is yet to be known how much the five structural components discussed in this research make up the total topside weight, and further research is required to conclude if it is worth investigating these components further.

3.2. Comparative research with existing topsides

HSM Offshore Energy has a long-standing experience in constructing topsides. Consequently, this research was able to utilize several projects with corresponding weight reports and drawings. Seven topsides, varying in size and functionality, were selected for this study and are shown in table 3.1. All seven topsides were compared for their general dimensions, deck layout, member sizes and weight distribution. The only prerequisite was that the topside should have a jacket-type substructure. It is believed that the deflection becomes more substantial for a topside with a monopile substructure as compared to the topsides mounted on top of a jacket. Additionally, the jacket-type platforms are usually heavier and more commonly used, making them more suitable for assessing the feasibility of high-strength steel.

Table 3.1: General information about the assessed topsides

Topside	Functionality	Overall topside dimensions (LxWxH) [m]	Topside weight [tonnes]	Deck leg layout [m]	Number of deck legs
1	Gas production	40x20x17	2200	18x18	4
2	Wellhead	35x20x20	900	14x14	4
3	High-voltage substation	41x34x25	2400	23x20	4
4	High-voltage substation	40x25x20	2500	17x13	4
5	High-voltage substation	58x32x26	3700	20x14	6
6	High-voltage substation	35x25.5x15	1200	15x13	4
7	Gas production	61.5x34x15	3200	17x17	6

The offshore industry has been around for several decades, and many empirical equations are available to estimate the size of the deck and the topside weight. Most often these equations are usually based on

the amount of gas or oil production, such as given by Reddy [40]. Figure 3.8 displays the seven topside weights versus their floor area. Although the r-squared value of the plot is only 0.53, indicating relatively low accuracy of the trendline, it can be concluded that topside weight increases with an increase in floor area. Based on the data from these seven topsides, an estimate of the topside weight can be calculated using the formula: $Weight = 5 \cdot Area + 650$.

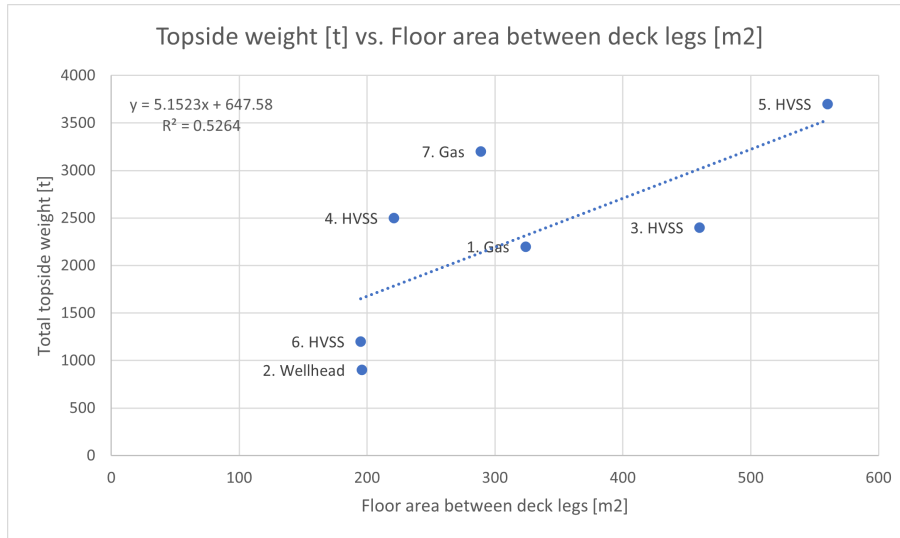


Figure 3.8: Topside weight [t] vs. Floor area between deck legs [m2]

Another way to look at it is by looking at how much steel weight a topside contains per floor area. As discussed in the previous section, 50% of the topside’s weight can be considered to be the steel weight. According to HSM Offshore Energy, a topside’s steel weight can be estimated at $400\text{kg}/\text{m}^2$ per square meter of floor area, regardless of the topside’s size. Figure 3.9 displays the steel weight of the seven topsides divided by their floor areas. The figure indicates that $400\text{kg}/\text{m}^2$ is approximately the mean, but the steel weight per floor area generally decreases as the floor area increases. As smaller floor areas have a higher steel weight and probably shorter beam lengths, high-strength steel could be more advantageous for smaller floor areas, while deflection will be less significant. It must be noted that the trendline’s accuracy is low to conclude that this is always the case.

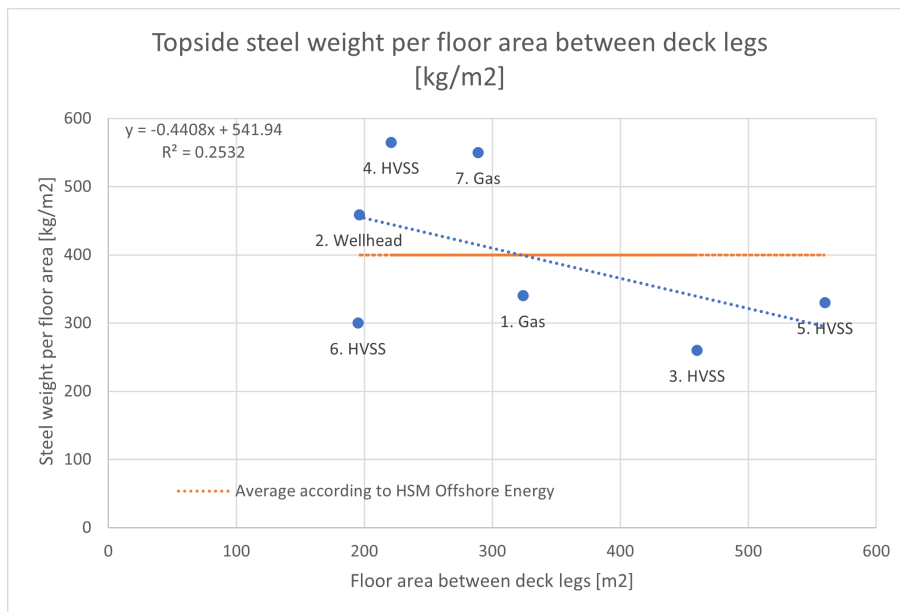


Figure 3.9: Topside steel weight per floor area between deck legs [kg/m2]

It was observed that the deck layouts of the seven topsides were correlated when considering only primary and secondary steel. A typical deck layout constructed by HSM is represented in Figure 3.10. It should be noted that none of the topsides had an exact layout, as shown in the figure. This is because different equipment, areas, functionalities, and requirements require other layouts. Nonetheless, the figure represents that a deck typically consists of main columns (shown in red circles), main/primary beams (shown as blue lines), deck beams (shown as orange lines) and deck stringers (shown in dotted yellow lines).

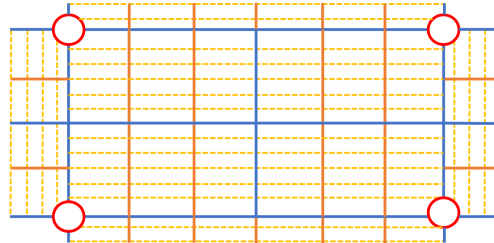


Figure 3.10: Typical deck layout (Main beams in blue, deck beams in orange and deck stringers in dotted yellow)

While the literature discussed in the previous section described that the column spacings of the main deck legs are typically 12x12 metres to 15x15 metres, the topsides from HSM Offshore Energy show a wider variety. The column spacings of the seven topsides vary from 13 to 23 metres. In most cases, the topsides are more rectangular than square, but this can be explained by the fact that the construction hall at HSM is longer than it is wide. The observed diameters of the columns varied from 30 inches to 42 inches, but the typical diameters were not found in the literature. The height of the columns showed the same range as the literature between the cellar, main and roofdeck, but when mezzanine decks were included, the height was often smaller, ranging from 3 to 5 metres.

For the main beams, profiles varying from 600 H-beams to 1200 mm high plate girders have been seen, which is a wider range than what is typically mentioned in the literature (that claims a range of 1000 to 1200 H-beams). Moreover, the length of the main beams in the topsides is different from what is mentioned in the literature, while the main columns have larger spacing, requiring longer main beams between them. The maximum span observed for a main beam is 23 metres.

The deck beams showed a wide variety of lengths on the different topsides, and no direct range could be found. The distance between the deck beams varied compared to what was found in the literature. The literature proclaimed a distance between the deck beams of 5 metres typical, but distances from 3 to 5 metres have been spotted in the seven topsides. The profile for a deck beam varied from 400 to 1000 H-beams and, in some situations, even a plate girder, typically when heavy equipment is located at that location.

As the deck stringers are located between the deck beams, their span varies from 3 to 5 metres. The distance between the deck stringers varies from 0.85 to 1.2 metres, comparable with the 1 metre from the literature, but the deck stringers had a wider range than the literature and varied from IPE180 to IPE240.

Different values were obtained for the length of cantilever beams as compared to those found in the literature. The length of cantilever beams assessed in the topsides ranged from 2 to 8 metres. It is important to note that to minimize the deflection of hanging deck parts, a circular tube tension member is often welded to the ends of longer cantilever beams. In such cases, these beams behave more like normal deck beams. The cross-sections varied from 300 H-beams to plate girders of 1200 mm .

The thickness of deck plating on the topsides ranged from 8 to 10 mm , which differs slightly from the literature that indicates 6 to 10 mm . HSM Offshore Energy prefers not to use 6 mm due to the defor-

mations that occur during welding. As a result, the minimum plate thickness HSM uses in offshore topsides is 8mm.

In addition, an attempt was made to compare different joints, but it was concluded that each joint differed too much. As columns and beams differ, the plate thickness, width, and size of the joint also differ. As a result, no generalized results for joints were assessed.

Despite the significant variations among all seven topsides, correlations were found for the deck layout and the profiles, lengths, and typical dimensions of its structural components. Table 3.2 presents generalized ranges of typical structural components within a topside based on the assessment made in this section and the literature discussed in the previous section.

Table 3.2: Generalized ranges of structural components from topside assessment and literature study

Component	Profile range (HSM)	Profile range (literature)	Length range (HSM)	Length range (literature)	Other
Main columns	Diameter: 30-42inch (0.76-1.07m)	Diameter: Not found	3-9m	6-9m	Spacing deck legs: Literature: 12-15m HSM: 13-23m
Main/primary beams	600 H-beam - 1200 plate girders	1000-1200 H-beams/plate girders	13-23m	12-15m	
Deck beams	400-1000 H-beams	800-1000 H-beams	-	-	spacing approx. 3-5m
Deck stringers	180-240 IPE	240-270 IPE / 240-280 HEA	3-5m	5m	spacing approx. 1m
Deck cantilevers	300 H-beams - 1200 plate girders	Not found	2-8m	6-7.5m	
Deck plating	8-10mm thickness	6-10mm	-	-	

From the weight reports of the topsides, the structural weight could be divided into four structural components: beams, columns and bracings, plating and nodes. By comparing the weight of the seven topsides, the weight percentage of each component can be obtained as shown in figure 3.11. The figure reveals that beams make up the majority of the weight percentage (approximately 34%), followed by columns and bracings (approximately 17%), deck plating (approximately 15%), and nodes (approximately 9%). The remaining 25% of the total steel weight is made up of other structural components. It's important to note that the weight of the nodes includes beams and columns as well because these nodes are constructed separately and then welded to the beams and columns later on. The average percentages are used to extend figure 1.2b introduced in chapter 1, and the extended Sankey diagram is shown in figure 3.12. From this diagram, it can be concluded that using high-strength steel for beams, columns, bracings, plating, and nodes will only affect about 17.9% of the total topside weight.

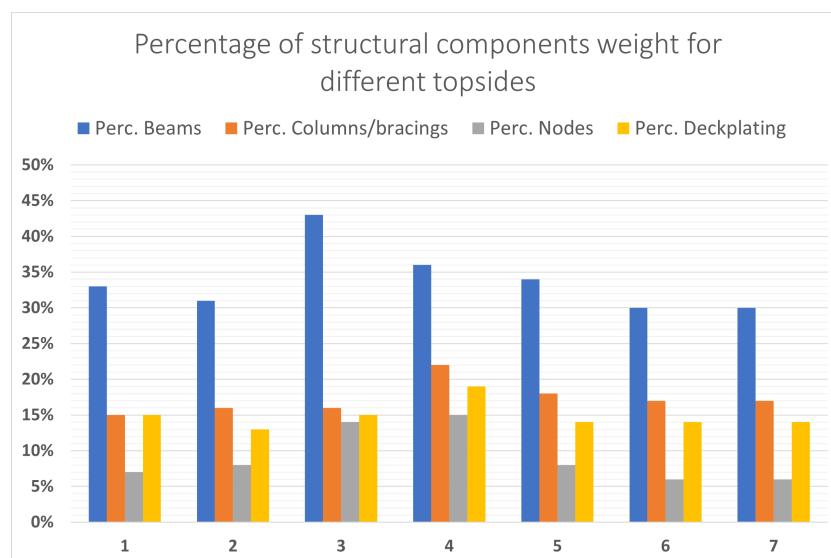


Figure 3.11: Weight percentage of different structural components for different topsides

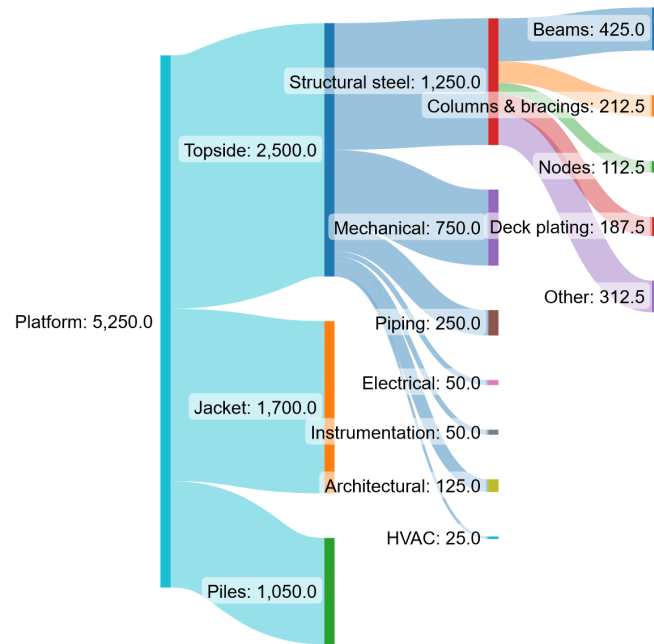


Figure 3.12: Extended Sankey diagram of weight [tonnes] based on Borkum Riffgrund

3.3. Conclusion regarding topside structural components

The previous sections have covered the structural design of topsides and evaluated various topsides for correlations. As this thesis aims to determine whether high-strength steel is generally feasible on topsides, it is challenging to include joints in this research. Joint sizes vary widely and are specific to the type of column or beam used. Moreover, research on the weight of structural components has shown that only 9% of the steel weight consists of joints, which also partly includes beams and columns. Using high-strength steel in beams and columns could thus automatically affect the joints. Therefore, this research will not assess the feasibility of high-strength steel for joints. Nevertheless, it is recommended to investigate the effect of smaller joints due to high-strength steel beams and columns, as smaller joints can cause fatigue issues but may also have potential benefits due to the smaller welds required.

Additionally, the deck plating and other structural components (except for beams, columns, and bracings) will not be further discussed. Thinner deck plating would only cause heavy deformations due to welding. Therefore, reducing plate thickness with high-strength steel will not be beneficial. The other structural components (except for beams, columns, and bracings) are often not specifically designed for their function. Most of the time, they are either bought ready-made, or their size is more critical than their weight. The components that are designed for their strength are very specific; therefore, none of these other structural components will be considered in this research.

The focus of this research is to examine the feasibility of using high-strength steel in beams, columns, and bracings. This will only impact approximately 12.1% of the total topside weight and 51% of the steel weight of a topside. It is suggested that utilizing high-strength steel will have greater benefits for smaller floor areas. The upcoming chapters will investigate the feasibility of using high-strength steel beams, columns, and bracings in the design of a topside and explore the potential economic advantages.

4

Feasibility of high-strength steel in topside beams, columns and bracings

This chapter will assess the feasibility of applying high-strength steel for beams, columns and bracings in topsides. The typical ranges of these components from table 3.2 will be used to determine the possibility of integrating high-strength steel in these structural components in topsides. Section 4.1 will discuss how the feasibility of high-strength steel beams is evaluated and will discuss multiple examples for different beam types. Section 4.2 assesses the feasibility of high-strength steel in circular hollow columns and bracings. Lastly, Section 4.3 will shortly summarize the conclusions obtained in this chapter. All calculations performed to assess members in this chapter are based on Eurocode 3 and some example calculations can be found in the appendices.

4.1. High-strength steel beams

This section evaluates the feasibility of using high-strength steel for the four different beams in a topside deck: deck stringers, deck beams, main beams and cantilever beams. As discussed in Chapter 2, hot-rolled high-strength beams are currently only available in S460, but this aspect is disregarded in the assessments in this paragraph to determine if S690 could be potentially advantageous. The first paragraph introduces the methodology used to evaluate the beams within a topside deck without knowing anything about the loads. The following paragraphs will subsequently discuss the four different types of beams and assess the feasibility of replacing them with high-strength steel.

4.1.1. Introduction to high-strength steel beams

The previous chapter discussed that preliminary topside designs are often created based on experience. Only after creating a deck layout and a simplified structural design will the loads be considered. However, it would be beneficial to assess the feasibility of using high-strength steel in this early design phase, even when the loadings are not yet precisely known. The lack of precise knowledge of the loads makes it complicated to determine whether a beam can be replaced with high-strength steel. To solve this problem, a method has been developed to evaluate the potential of high-strength steel in topside beams without knowing the exact loads. The method uses the fact that high-strength steel only benefits beams when deflection is not governing and looks for a beam's transition point from strength- to deflection-governing. Once this transition point, described in a certain beam length, is known, beams can be analyzed for their potential to use high-strength steel depending on their length. This way, preliminary designed decks can be easily evaluated for their potential for high-strength steel without knowing the exact loads.

If a beam is strength- or deflection governed depends on multiple variables such as the span of the beam, the cross-section modulus, the cross-section area moment of inertia, the material, the load and how the beam is supported. The different variables will be checked to see how significant their influence is for a beam to be strength- or deflection-governed.

As discussed in chapter 2, according to Eurocode standards, a static member that undergoes bending must be evaluated for both the ultimate limit state (ULS) and serviceability limit state (SLS). The ULS is checked based on the required cross-section resistance, while the SLS is assessed based on the maximum allowable deflection. In the simplest case, when the influence of the shear force is neglected, and a beam is assumed to be laterally restrained, these checks can be performed with equation 2.4 and 2.5. If both equations are less than 1, the limit states are satisfied, and the beam has enough resistance. The unity check with the highest value is the governing limit state, as that value is the closest to its limit of 1. Which of the limit states is governed can thus be calculated with equation 4.1. If equation 4.1 is higher than 1, the unity check for the ULS is higher than the unity check for the SLS; hence, the ULS is governing.

$$\frac{U.C.ULS}{U.C.SLS} = \frac{M_{Ed}/M_{c,Rd}}{\delta/\delta_{max}} > 1 \quad (4.1)$$

If now a simply-supported beam with cross-section class 1 is assumed, still laterally restrained and with no shear force influence, the maximum bending moment that occurs in the beam can be calculated with equation 4.2 and the maximum deflection of the beam can be calculated with equation 4.3. The design bending resistance can be calculated with equation 2.2, while the maximum allowable deflection equals $L/200$. When these four values are obtained, it can be assessed if the beam is strength- or deflection-governing by filling in these values in equation 4.1.

$$M_{Ed} = \frac{qL^2}{8} \quad (4.2)$$

$$\delta = \frac{5qL^4}{384EI} \quad (4.3)$$

Nevertheless, the Eurocodes state that different load factors should be used for the load for the ULS and SLS; it cannot be simply said that both loadings are equal. According to the Eurocode, a distinction between permanent loading and variable loading should be made. If only one permanent load (G) and one live load (Q) are considered to act on the beam, equations 4.4 and 4.5 can be used to calculate the corresponding factorized loads. It must be noted that the values can differ per country or project, but a factor of 1.35 for the permanent load and 1.5 for the variable load for the ULS are advised by the Eurocode. For the SLS for both the permanent and variable load, a factor of 1.0 is advised. When all factors would have been equal to 1.0, the load would cancel out when the unity check of the ULS and the unity check of the SLS are divided, but this is not the case when the correct factors are used. To assess a beam without knowing the load, a connection between the permanent and variable load should be constructed.

$$q_{ULS} = 1.35G + 1.5Q \quad (4.4)$$

$$q_{SLS} = 1.0G + 1.0Q \quad (4.5)$$

The variable load is usually defined by the regulations or is defined in the project's structural basis of design. For example, a variable floor load of $15kN/m^2$ is often used in storage areas on topsides. Based on Honfi [16], a load ratio can be introduced according to equation 4.6 to connect the unknown permanent load with the variable load. If the permanent load is extremely high, the load ratio would approach 0, and if the permanent load almost equals 0, the load ratio would approach 1. Let's for now consider a load ratio of 0.5; in that case, the permanent load equals the variable load and the permanent load can be calculated as a function of the load ratio with equation 4.7. The influence of the load ratio is analysed later on.

$$\lambda = \frac{Q}{G + Q} \quad (4.6)$$

$$G = \frac{Q}{\lambda} - Q \quad (4.7)$$

When a load ratio of 0.5 is assumed and equation 4.7 is substituted in equations 4.4 and 4.5, the loading can be defined as a function of the variable loading only. The loads can be substituted in equations 4.2

and 4.3, and the unity checks can be substituted in equation 4.1, then the final equation 4.8 is obtained. If this equation is higher than 1, the ultimate limit state will govern independently of the beam's applied load. The equation still depends on the cross-sectional modulus, area moment of inertia, span length and the material yield stress.

$$\frac{U.C.._{ULS}}{U.C.._{SLS}} = \frac{\left(\frac{M_{Ed}}{M_{c,Rd}}\right)}{\left(\frac{\delta}{\delta_{max}}\right)} = \frac{\left(\frac{2.85\gamma_{M0}QL^2}{8W_{el}f_y}\right)}{\left(\frac{3000QL^3}{384EI}\right)} = \frac{1094.4\gamma_{M0}EI}{24000W_{el}f_yL} \quad (4.8)$$

If an IPE240 made of S355 steel is selected, the cross-sectional modulus and the area moment of inertia are equal to 324cm^3 and 3892cm^4 , respectively. Figure 4.1 shows equation 4.8 as a function of the span of the beam. The blue horizontal line corresponds with the 1-value, the transition line where a beam goes from ULS governing to SLS governing. It can be seen that for this IPE240, the transition point is located at a beam span of 4.9 metres. If the beam is longer than 4.9 metres, deflection will be governing, and high-strength steel can never be beneficial for this situation. If the beam is shorter than 4.9 metres, high-strength steel could be beneficial, and it is worth investigating if the beam could be replaced with a smaller one to decrease the weight.

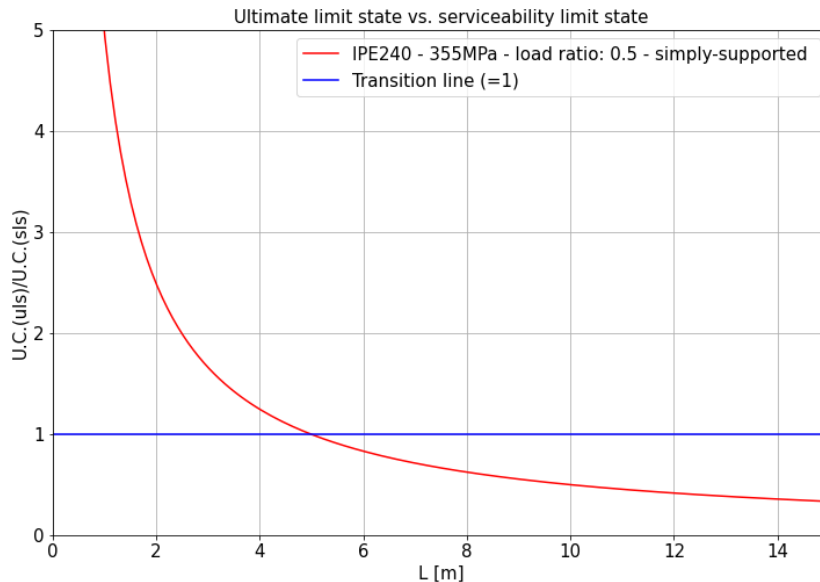


Figure 4.1: Ultimate limit state vs. serviceability limit state for an IPE240

Assumptions were made to construct figure 4.1, such as a simply-supported beam with a distributed load, the choice of an IPE240, S355 steel, and a load ratio of 0.5. These variables must be assessed for how they influence the transition point. The rest of this paragraph will analyse how much and how these variables influence the transition point.

The influence of the load ratio

First, the influence of the load ratio is assessed, while the assumption of connecting the variable load with the permanent load is very important for this method. The limits of the load ratio can be assessed as the load ratio can only vary between 0 and 1. First, the equation for the permanent load as a function of the load ratio (equation 4.7) is substituted into equations 4.4 and 4.5, which is shown in equations 4.9 and 4.10.

$$q_{uls} = 1.35 \left(\frac{Q}{\lambda} - Q \right) + 1.5Q = \frac{1.35Q}{\lambda} + 0.15Q \quad (4.9)$$

$$q_{sIs} = 1.0 \left(\frac{Q}{\lambda} - Q \right) + 1.0Q = \frac{Q}{\lambda} \quad (4.10)$$

If still a simply-supported IPE240 is assumed with a yield stress of 355MPa , all variables are constant values except for the permanent and variable loads (q_{uls}/q_{sls}). If these loads would be substituted into equation 4.1, the factor between these loads is the only variable, except for the length. This fraction can be simplified to equation 4.11. The limits of this fraction can be analysed to see how much this fraction can differ for when the permanent load is extremely high or extremely low.

$$\frac{q_{uls}}{q_{sls}} = \frac{\frac{1.35Q}{\lambda} + 0.15Q}{\frac{Q}{\lambda}} = 1.35 + 0.15\lambda \quad (4.11)$$

Equations 4.12 and 4.13 show that the fraction between the loads can vary between 1.35 and 1.5. When a load ratio of 0.5 is assumed, the value would equal 1.425. This means that when a load ratio of 0.5 is chosen, the ULS/SLS-ratio can only be 5.3% lower or higher when the permanent load is extremely high or low. This shows that the amount of load has a very low influence on the transition point of the beam.

$$\lim_{\lambda \rightarrow 0} \left(\frac{q_{uls}}{q_{sls}} \right) = \lim_{\lambda \rightarrow 0} (1.35 + 0.15\lambda) = 1.35 \quad (4.12)$$

$$\lim_{\lambda \rightarrow 1} \left(\frac{q_{uls}}{q_{sls}} \right) = \lim_{\lambda \rightarrow 1} (1.35 + 0.15\lambda) = 1.5 \quad (4.13)$$

Figure 4.2 shows the ULS/SLS-ratio for load ratios: 0.001, 0.5 and 1. This figure visualizes that the influence of the load is minimal on the transition point of the beam. As previously shown, an IPE240 with a load ratio of 0.5 has its transition point at 4.9 metres. If the permanent load is infinity high or approaching zero, the transition point only shifts with 30cm or 6.1%. This shift is assumed to be so insignificant that a load ratio of 0.5 can be assumed and that the transition point is independent of the load applied on a beam.

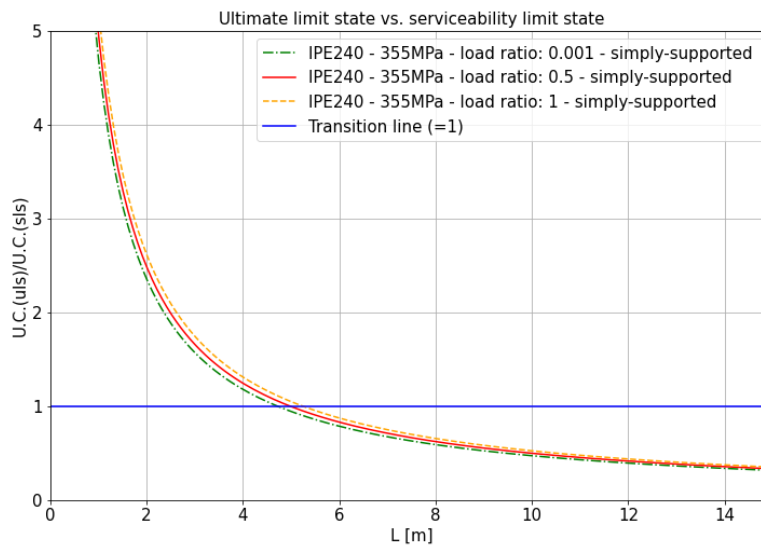


Figure 4.2: The influence of the load ratio on the ULS/SLS-ratio for an IPE240

The influence of the yield stress

High-strength steel increases the beam's strength; therefore, the beam's ultimate strength will increase, and the unity check of the ULS decreases for the same lengths compared with S355 steel. This all, while the deflection does not change because a higher yield stress does not result in an increased Young's modulus as discussed in chapter 2, which means that the SLS becomes governing for shorter beam spans.

Figure 4.3 visualizes the influence of the yield stress on the transition point of the beam's ULS/SLS-ratio. Where for S355 steel, the transition point is located at $4.92m$; for S460 and S690, this transition point shifts significantly to $3.83m$ and $2.52m$, respectively. For S690, this means that the transition point almost decreases with 50%. Therefore, the yield stress significantly affects the length where the transition point occurs.

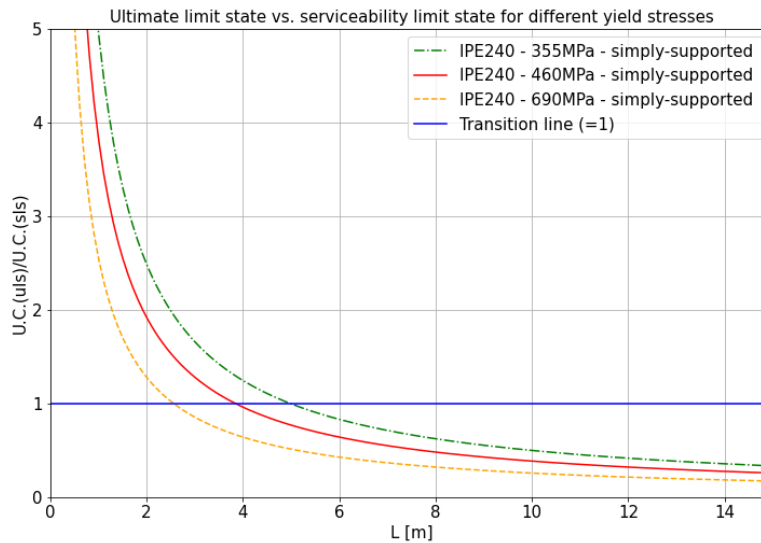


Figure 4.3: The influence of different yield stresses on the ULS/SLS-ratio for an IPE240

The influence of the cross-section

The cross-section also greatly influences the transition point of the ULS/SLS-ratio. Standard hot-rolled sections have a specific section modulus and area moment of inertia. When a higher beam is chosen, the area moment of inertia increases faster than the cross-section modulus. The section modulus increases slower with increasing beam height due to the definition of the cross-section modulus: $W = I/z$. The increase in the area moment of inertia has a very beneficial effect on the deflection resistance of a beam and results in a lower unity check for the SLS. While the unity check of the ULS also decreases but is less significant, the transition point will shift to the right if a bigger beam is chosen. This is presented in figure 4.4.

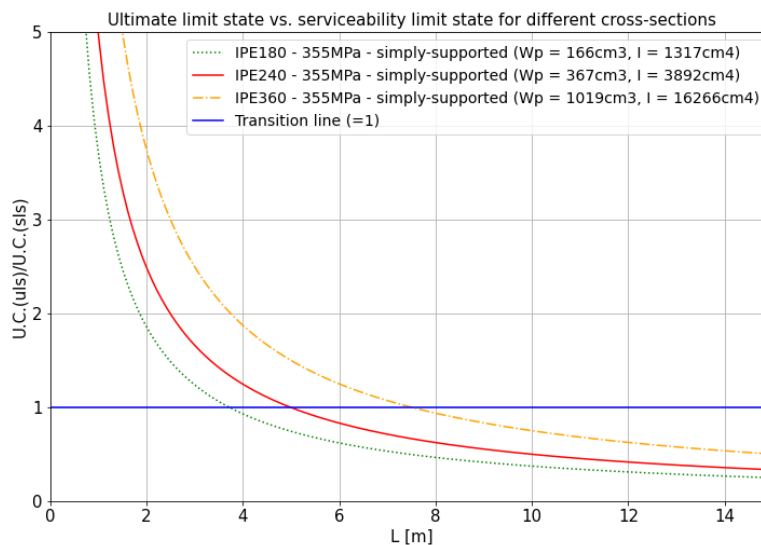


Figure 4.4: The influence of different IPE's on the ULS/SLS-ratio

Nevertheless, it must be noted that in this figure a plastic section modulus is used. When a beam has a cross-section classification of 3, the elastic section modulus must be used. The elastic modulus offers less resistance to the bending moment, and therefore, the lines would shift to the right, while a lower section modulus would result in an earlier strength-governing line. This indicates that the use of high-strength steel would be somewhat more beneficial for beams, which should be assessed with the elastic modulus.

The type of cross-section, I- or H-beam, also affects the transition point. Figure 4.5 visualizes the difference between the same-height IPE's and HEA's. The cross-section properties can explain this difference, as an IPE has thinner flanges compared to an H-beam. Therefore, the area moment of inertia is lower for an IPE, and the section modulus will, as a result, also be less. As the section modulus of an IPE is lower, the beam will, compared to an H-beam, be more susceptible to the ultimate strength. However, I-beams have a notable benefit in that the deflection resistance per weight is much higher. I-beams are, therefore, often used when low loads are applied, but long spans are required, while H-beams are often used to resist higher loads.

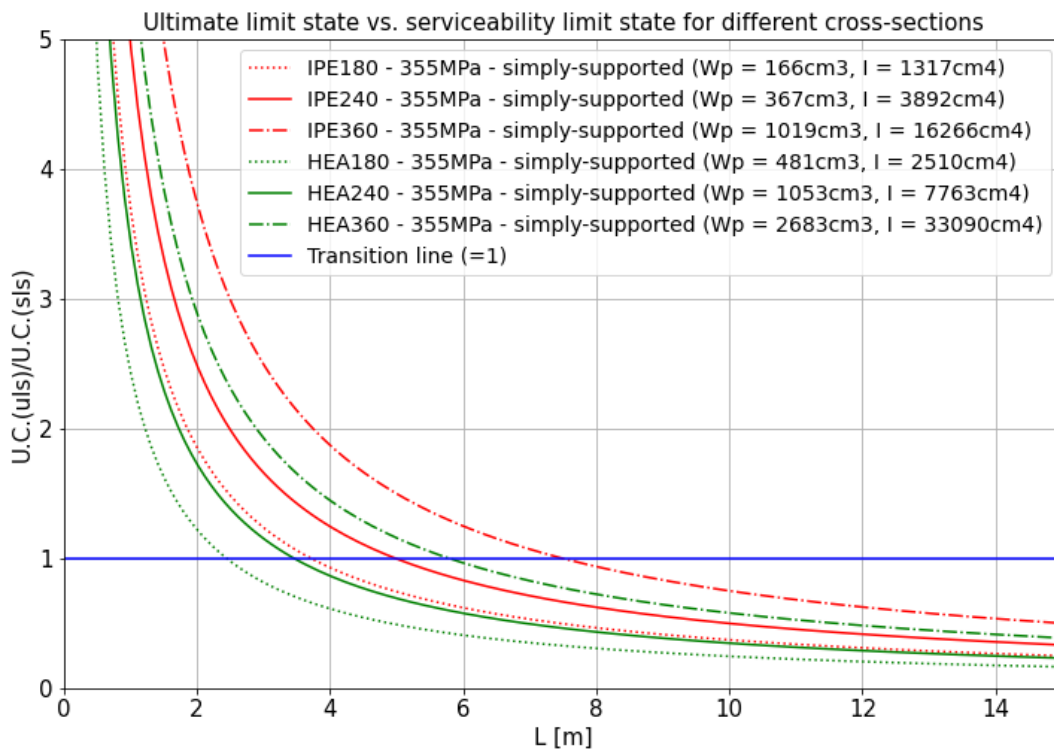


Figure 4.5: The influence of different type of cross-sections on the ULS/SLS-ratio

The influence of the support type

In the previous examples, a simply supported beam was assumed, but changing the maximum bending moment and deflection in the beam by changing the support type will significantly influence the transition point. Figure 4.6 shows the ULS/SLS-ratio for different support types in which the maximum bending moments and deflections are calculated as a function of the length of a beam with standard beam equations. The figure shows that a fixed assumption would result in a transition point at a three times longer length compared with a simply supported assumption. This effect is enormous; therefore, knowing how a particular beam can be modelled is of great importance. The desire to say something about at which length a beam becomes deflection governed requires having an equation in which the bending moment and deflection can be expressed as a function of the beam's length. In the following paragraphs, this aspect will extensively be discussed, and where necessary, a finite element model will be created to assess which assumption would best describe a particular beam.

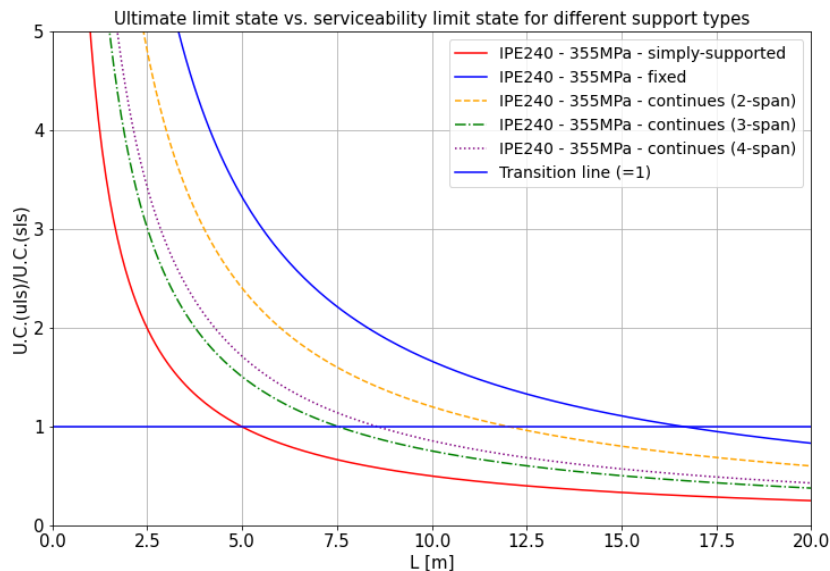


Figure 4.6: The influence of different type of supports on the ULS/SLS-ratio

The following paragraphs will show how the method introduced in this paragraph can be applied to review different beams. Each paragraph will apply this method, but some beams require additional checks, which will be discussed in the corresponding paragraph. From this paragraph, multiple conclusions can be made regarding the different variables affecting the use of high-strength steel. This paragraph concludes that the transition point of a beam to be strength- or deflection-governed is independent of the load on a beam. Of the parameters that affect the ULS/SLS-ratio, the assumed support type has by far the most considerable influence on the transition point; hence, extensive thought should be made about the support of a beam. The other parameters, area moment of inertia, section modulus and yield stress, also affect the transition point but are specific to a chosen beam. Therefore, different beams with a specific length can be compared with each other.

4.1.2. High-strength steel deck stringers

This paragraph will assess the feasibility of using high-strength steel in the deck stringer. According to the literature, summarized in table 3.2 of the previous chapter, deck stringers usually range from IPE240 to IPE270 or HEA240 to HEA280. After reviewing several topsides, it was found that only IPEs were used, which varied between IPE180 and IPE240. Therefore, this paragraph will first concentrate on the IPE ranges of 180 up to 270. An example from an existing topside will be used to determine if high-strength steel could be beneficial for these deck stringers. Later, the potential of high-strength steel for HEA deck stringers will be discussed using the same method as for IPEs since the literature suggests that HEAs can also be used, particularly for higher deck loads.

Figure 4.7 shows the ULS/SLS-ratio for all typical IPE deck stringers for a simply-support and fixed beam assumption. This figure uses a plastic section modulus, while standard IPEs have a cross-section class 1 for bending. Therefore, the Eurocodes allow a plastic analysis. This figure shows that for the 3 to 5-meter range (indicated with the red crosses), the fixed assumed deck stringers are heavily strength-governed. This indicates that high-strength steel could be beneficial for fixed deck stringers, but a fixed deck stringer support is normally not realistic. In reality, a deck stringer will be more designed as a simply-supported beam, while the connection can then be constructed easier and thus cheaper.

From figure 4.7, it can also be seen that for a simply-supported deck stringer, the strength-governing area does not cover the whole deck stringer range of 3 to 5 meters. This indicates that high-strength steel will not be beneficial for a simply-supported deck stringer or, in the best case, only for the biggest cross-sections when simply supported is assumed. However, deck stringers are normally welded to the deck beams, and a welded connection will always transfer somewhat of a moment, while a simply-supported beam assumes no moment transfer. Therefore, a deck stringer will always be different from

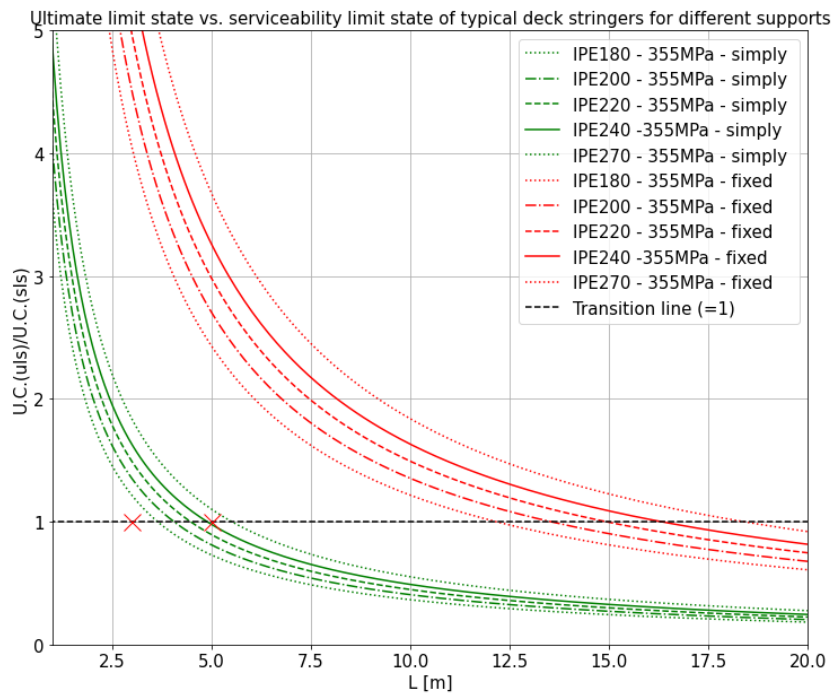


Figure 4.7: The ULS/SLS-ratio for all typical IPE deck stringers (different supports)

a simply-supported beam. Thus, the question arises before considering whether high-strength steel could be beneficial: *How to model a deck stringer?*

A typical example of an existing topside for the deck stringers is selected and shown in figure 4.8a. The selected deck consists of multiple IPE240 deck stringers with a span of 4.2m . These deck stringers have a sniped connection (shown in figure 4.8b) to the HEB600 deck beams with a length of 8.5m , and no equipment is located on this part of the deck. According to the project's Basis of Structural Design (BoSD), a variable load of $15\text{kN}/\text{m}^2$ should be used. The distance between the deck stringers is 0.85m ; hence, the deck stringers experience a variable load of $12.75\text{kN}/\text{m}$. From figure 4.7, it can be concluded that for the most conservative assumptions of a simply-supported beam, an IPE240 is strength governed up to a span length of 4.2 metres.

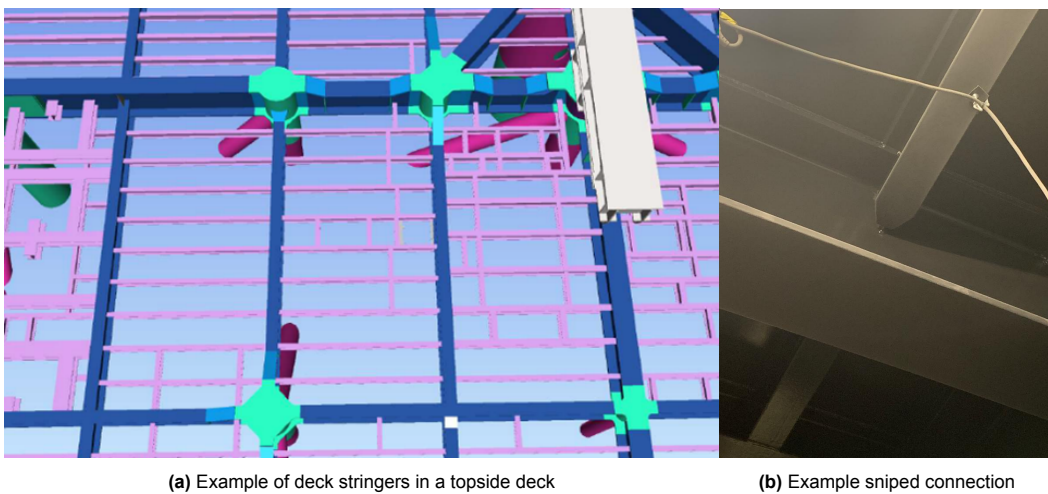


Figure 4.8: Example part of a deck for deck stringer assessment

It is nonetheless uncertain whether a sniped connection, illustrated in figure 4.8b, should be evaluated as simply supported. At the same time, the top flange and web of the deck stringer are welded to the deck beam, providing some rigidity to the joint. This connection could result in a bending moment in the joint, making a simply supported assumption too conservative. A simplified model of the example deck is constructed, as shown in figure 4.9, to analyse how these deck stringers will react with a finite element analysis. RFEM is selected for the FEM analysis because it offers a set with all the standard beams from the Eurocode, which can be easily implemented. Additionally, this program is also used at Enersea for the global assessment of topsides.

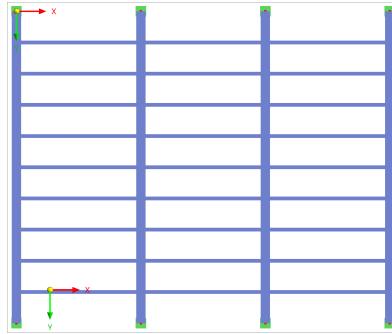


Figure 4.9: RFEM simplified model of example deck

As proved in the previous paragraph, the load does not contribute to the transition point of a beam to be feasible for using high-strength steel. Therefore, the load can freely be chosen when evaluating how the deck stringer joints will react. For this reason, a load ratio of 0.5 is assumed, and by equation 4.7, the permanent load is equal to the variable load. In RFEM, two load combinations are created to distinguish the calculations for the ULS and SLS according to equations 4.4 and 4.5, respectively. It is assumed that the deck loading is only applied to the deck stringers and that both the unfactored permanent and variable loads equal 15 kN/m . It is first assumed that there is no sniped connection and that the deck stringers are fully welded to the deck beams; therefore, no releases at the connection nodes are defined. A fixed nodal support is assumed and applied to the ends of the deck beams.

Figure 4.10 shows the moment diagram of the deck stringers, which is obtained when no sniped connection is assumed. The absolute maximum bending moment can be found at the joint with the deck beam and is equal to 65.98 kNm . The moment diagram shows that the connections on the end are definitely not rigid connections and that assuming fixed deck stringers is not an option for this situation. The diagram looks most comparable to the moment diagram of a continuous beam. When the standard moment equation for a three-span continuous beam at that beam's location is used ($M = 0.1ql^2$), a bending moment of 68.4 kNm is calculated, an overestimation of only 3.7%.

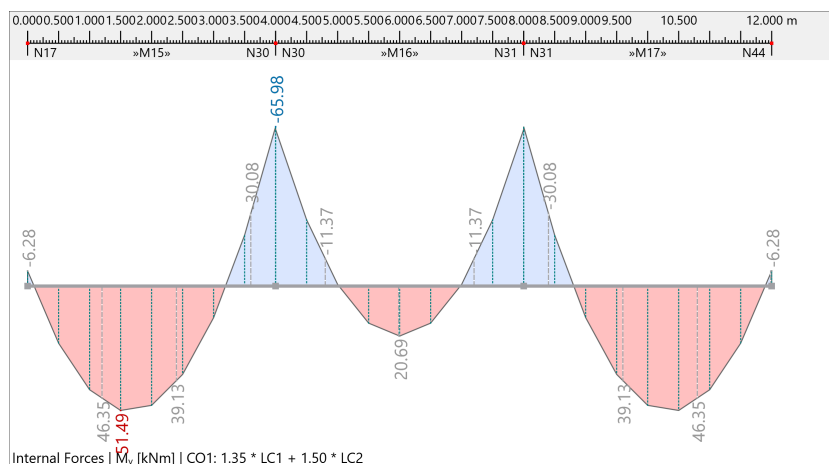


Figure 4.10: Moment diagram of middle deck stringers modelled in RFEM

When the maximum deflection is calculated from figure 4.11, a maximum deflection of 7.4mm can be found. When the maximum deflection for a continuous 3-span beam is calculated, a value of 6.5mm can be found, which underestimates the deflection with 12.2%. Assuming a continuous three-span for these deck stringers will thus result in overestimating the bending moment and underestimating the deflection and can, therefore, not be used to assess deck stringers exactly. Nevertheless, using the standard equations for a simply supported beam would overestimate the maximum bending moment at 66.1% and the deflection at 65.4%. Thus, choosing a simply supported assumption would lead to a very conservative but safer assumption, but continuous beam assumptions would lead to more accurate values but underestimates the deflection.

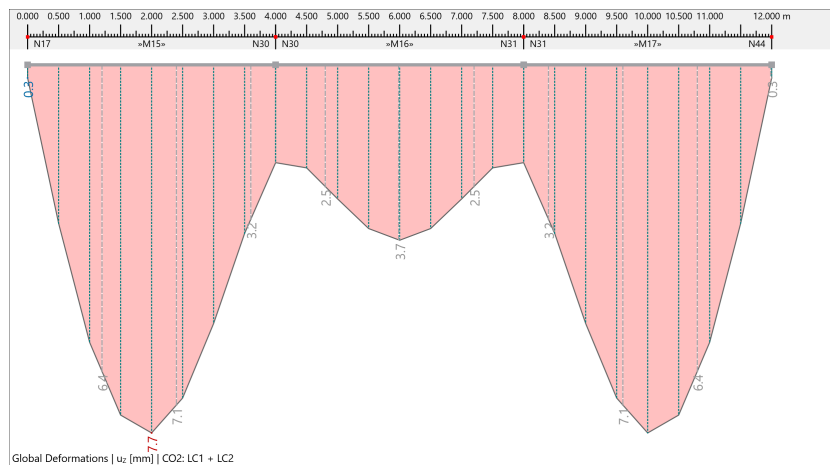


Figure 4.11: Deflection diagram of middle deck stringers modelled in RFEM

Nevertheless, the effect of a sniped connection should be checked to see if this changes the situation. The sniped connection is modelled in RFEM as a T-profile connected to the IPE240 on both sides, which is shown in figure 4.12. The T-profile matches the exact same sizes as the IPE240 except for the bottom flange. Typically a snipe has a length of 200mm according to HSM but the snipe length was checked for each 50mm . Table 4.1 shows for different lengths of a snipe connection the bending moments from the corresponding bending moment diagram and the deflections. Something that can be seen from the table is the decrease of the negative bending moment in the joint and an increase in the bending moment within the middle beam. This reduction indicates that the deck stringers are becoming somewhat more simply supported, although this effect is relatively low even for standard snipe connections of 200mm . In the table, it can be seen that assuming simply supported would still overestimate the sniped connection with 66.1% for the bending moment and 59% for the deflection. Using the continuous beam equations would overestimate the bending moment by 25.9%, while the deflection would be underestimated at 15.6%.

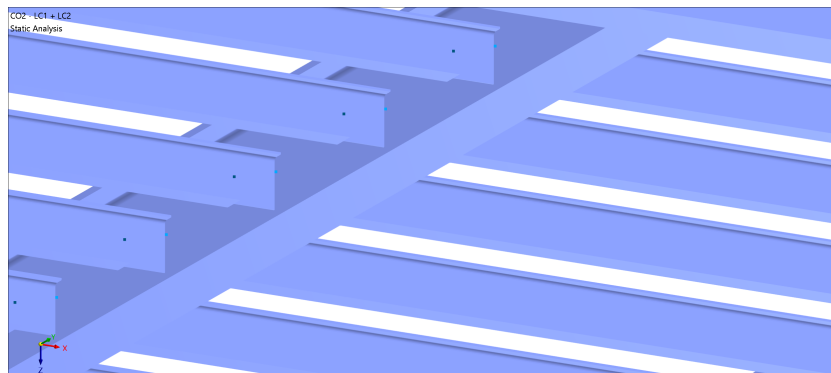
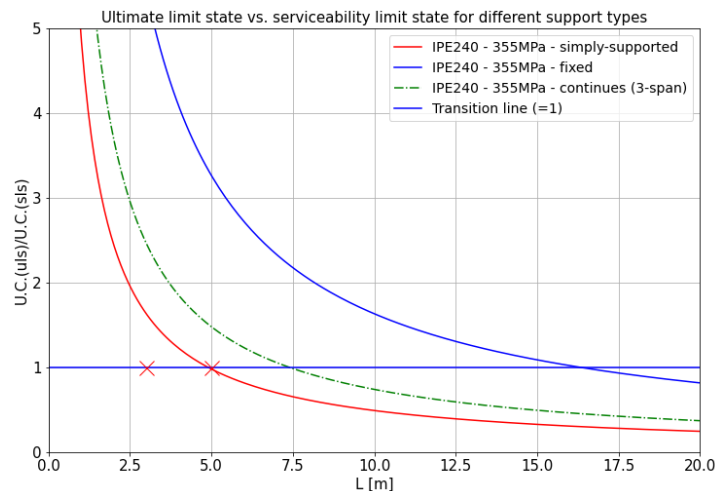


Figure 4.12: Sniped connections modelled as T-profile connected to the IPE240

Table 4.1: Effect of different snipe lengths on deck stringers

Snipe length [mm]	Mmax [kNm]	Mmin [kNm]	M (middle) [kNm]	Deflection left [mm]	Deflection middle [mm]
0	51.49	-65.98	20.69	7.4	2.7
50	50.35	-60.78	24.30	7.3	2.3
100	50.83	-58.16	26.26	7.5	2.6
150	51.21	-56.04	27.85	7.6	2.8
200	51.49	-54.33	29.14	7.7	3
Continuous 3-span beam assumption	54.72	68.4	17.1	6.5	-
Compared to snipe of 0mm	+6.3%	+3.7%	-17.4%	-12.2%	-
Compared to snipe of 200mm	+6.3%	+25.9%	-41.3	-15.6%	-
Simply supported assumption	85.5	-	-	12.24	-
Compared to snipe of 0mm	+66.1%			+65.4%	-
Compared to snipe of 200mm	+66.1%			+59.0%	-

Figure 4.13 shows the ULS/SLS-ratio of continuous 3-span IPE240 beam of 355MPa. It can be seen that when a continuous beam is assumed, the deck stringer range is entirely strength-governing, indicating that high-strength steel could possibly be beneficial for an IPE240. It can be concluded that the reality would be somewhere in between, and it heavily depends on the design of the joint. For the assessment of the feasibility of using high-strength steel in deck stringers, an example calculation will be made for both support assumptions. For the continuous beam, it is assumed that the deck stringers do not have sniped connections, which would increase the weld length but also increase the accuracy of the calculation. For a simply supported assumption, a sniped connection of 200mm is assumed. Appendix B shows all the calculations which have been made to assess the example deck stringer, and in this paragraph, the results will shortly be summarised with the assumption of a continuous beam. The simply supported beam assumption is assessed in the same way but only changing the standard equations.

**Figure 4.13:** Example of deck stringers in a lay-down area

In the BoSD of the topsides' project, it was found that for the example deck, the load for the ULS has to be calculated according to equation 4.14 and the load for the SLS according to 4.15. When the standard equations of the maximum bending moment and deflection for a continuous 3-span beam are substituted in equation 4.1, the ULS/SLS-ratio can be calculated. For the example deck, a ULS/SLS-ratio of 1.76 was found, which indicates that this deck stringer is strength-governed. To determine if

the IPE240 can be replaced with a smaller high-strength steel IPE, it is assumed that the IPE240 is designed for a unity check equal to 1, hence for the full capacity of the beam.

$$q_{uls} = 1.3G + 1.5Q \quad (4.14)$$

$$q_{sls} = 1.0G + 1.0Q \quad (4.15)$$

By substituting equation 2.2 and the equation for the maximum bending moment of a 3-span continuous beam into equation 2.4, equation 4.16 is obtained by assuming maximum capacity ($M_{Ed}/M_{c,Rd} = 1$). Equation 4.16 can be used to calculate the maximum load for which this beam is designed. The project's BoSD shows that $\gamma_{M0} = 1.16$ and that for the location of the deck stringer, a variable load (Q) of $12.75kN/m$ should be used. With this given, a maximum load of $63.6kN/m$ is obtained, and the design permanent load can be calculated by rewriting equation 4.14, resulting in a permanent load (G) of $34.2kN/m$.

$$q_{ULS(max)} = \frac{10\sigma_y W_p}{\gamma_{M0} L^2} \quad (4.16)$$

As this beam is designed for strength, it is now known that this beam is designed for a q_{uls} of $63.6kN/m$. When looking at whether this beam can be smaller when high-strength steel is used, it is assumed that the load of $63.6kN/m$ will stay the same when choosing a smaller beam size, hence neglecting the reduction of the self-weight of the beam. When equation 4.16 is again rewritten as equation 4.17, the minimum required plastic section modulus can be calculated for the different yield stresses. If S460 is used, a minimum plastic section modulus of $282.9cm^3$ is required for the beam to have sufficient bending resistance, while if S690 is used, only $188.6cm^3$ would be enough for the beam to resist the bending moment. Looking at different IPE cross-sections, an IPE 220 would be sufficient for S460 steel, while an IPE 200 would satisfy for S690 steel. However, as the required moment of inertia does not change when high-strength steel is used, this could restrict the use of high-strength steel, and therefore, the minimum required area moment of inertia must be calculated.

$$W_{p,minreq} = \frac{\gamma_{M0} q_{uls} L^2}{10\sigma_y} \quad (4.17)$$

The required minimum area moment of inertia can be calculated as the permanent load is determined. Equation 4.5 can be used to determine the load required for the deflection calculation, which equals $46.95kN/m$. By substituting the maximum deflection formula of a continuous beam and the deflection limit of $L/200$ into equation 2.5 and rewriting this equation, equation 4.18 is obtained to calculate the minimum required area moment of inertia, which is equal to $2285.8cm^4$. Looking at the list of IPE cross-sections again, an IPE220 is the lowest IPE possible to resist the deflection. Therefore, the area moment of inertia restricts the benefits of S690, and only an IPE220 of S460 steel could be used to reduce the cross-section.

$$I_{req} = \frac{1.38q_{sls}L^3}{E} \quad (4.18)$$

Nevertheless, only the bending moment resistance and the deflection check are now satisfied but the cross-section classification and whether the influence of the shear force should be considered is not yet included in the above calculations. When these are also performed, it can be concluded that the cross-section class remains a class 1 cross-section class for a standard IPE220 of S460 steel; hence, a plastic analysis may still be used. The shear force is calculated and is only 34.6% of the plastic shear resistance. For both calculations is referred to appendix B. It can be concluded that the above calculation satisfies the Eurocodes for a laterally restrained beam, and a high-strength IPE220 of S460 steel can be used in this example to reduce the overall weight. Compared to an IPE220 of S355 steel, an IPE240 of S460 steel has 14.7% less weight. When the prices of high-strength steel are used, a material cost reduction of 6% can be realised. Nonetheless, while it was chosen to assume a fully welded beam instead of a sniped connection to better approach a continuous beam assumption, the welding costs increased by 16.7%. This increase in welding costs resulted in a total cost reduction of only 1.83%.

When the calculations are performed for a simply supported beam, it is found that the deck stringer is still slightly strength-governing. However, a reduction of the cross-section by using a smaller beam is not possible, while the area moment of inertia restricts the use of a smaller beam. Therefore, no benefits can be found for this example when simply supported would be assumed.

The example in this paragraph shows that it can be beneficial to use high-strength steel for deck stringers when a continuous beam assumption is allowed. Especially when weight reduction is required, but using high-strength steel deck stringers will almost not reduce the total costs. Moreover, only S460 beams could reduce the weight and costs, while S690 had no benefits over S460 because of the area moment of inertia restriction. When assuming simply supported, no benefits can be found for this example, and as the reality lies between these two support types, it remains questionable if real benefits can be achieved with high-strength steel deck stringers.

According to the previous chapter, only a limited selection of IPEs is typically used in topsides for the deck stringers. Until now, this paragraph has described a method to assess whether a certain example deck stringer can be replaced by a smaller high-strength steel beam using either a simply- or a continuous support assumption. This can also be done for all typical deck stringer profiles by numerically computing the maximum load for the ultimate limit state for different lengths when assuming that a cross-section is loaded at full capacity. Once the minimum required section modulus and area moment of inertia are calculated, a suitable high-strength steel beam can be selected if there is enough capacity for a smaller cross-section. Tables 4.2 and 4.3 demonstrate the feasibility of high-strength steel for the typical IPEs used on topsides. Table 4.2 shows the possible replacement of beams when simply supported is assumed, and table 4.3 shows the possible replacement of beams when a continuous beam is assumed.

IPE	2m	3m	4m	5m	6m
180	-	-	-	-	-
200	-	-	-	-	-
220	200I	200I	-	-	-
240	220I	220I	-	-	-
270	-	-	-	-	-

Table 4.2: Possible replacement of beams with S460 (IPE) - simply supported and distributed load

IPE	2m	3m	4m	5m	6m
180	-	-	-	-	-
200	-	-	-	-	-
220	200I	200I	200I	-	-
240	220I	220I	220I	220I	-
270	-	-	-	-	-

Table 4.3: Possible replacement of beams with S460 (IPE) - 3-span continuous beam and distributed load

The data presented in the tables suggests that the use of high-strength steel in typical offshore topside IPEs for weight reduction can only be advantageous in specific situations. For the smallest cross-sections, such as an IPE180 or 200, the beams are immediately deflection-governing, which means that they cannot be replaced with a smaller cross-section, as the required minimum area moment of inertia restricts this. In both support cases, an IPE270 can also not be replaced with a smaller high-strength steel IPE, while the step to an IPE240 does not have sufficient resistance against bending when an IPE270 is loaded at its maximum capacity. Moreover, it can be observed that some benefits could be obtained for an IPE220 or IPE240, especially when a continuous beam is assumed. However, it has been previously concluded that a continuous beam best approximates the bending moment and deflection but still has a high level of uncertainty. To conclude, high-strength steel will only be feasible for IPE deck stringers in specific situations, and no significant advantages are expected. It is only recommended to consider the use of high-strength steel when weight reduction is crucial, and a conventional steel IPE220 or 240 is being used. The use of S690 steel is not beneficial in any of the deck stringer situations.

Previously, only IPEs were considered, but the same method can be applied to HEA deck stringers. HEA deck stringers are typically only used at HSM when higher deck loads are present, but they show benefits when replaced with high-strength steel within the range of deck stringer lengths. Tables 4.4 and 4.5 show the possible replacements for the typical HEA deck stringers. It is noticeable that a HEA240 cannot be replaced with a smaller cross-section, which is caused by the corresponding cross-section classification. When using conventional S355 steel, a HEA240 falls within cross-section class 2, but when S460 is used, the cross-section will fall in class 3, thus not allowing a plastic moment resistance check. The elastic section modulus of an HEA220 of S460 steel does not have enough resistance to

be used instead of a conventional S355 HEA240. HEA260 and HEA280 have more profitable cross-section classifications because they already fall within class 3 for conventional S355 steel and can, therefore, be replaced by a smaller profile, especially when a continuous beam assumption is considered. Consequently, it is concluded that if a deck would be designed with HEA deck stringers because of a higher deck load, it is recommended to consider using high-strength steel. In most cases, HEAs can be replaced with high-strength steel within the typical deck stringer length, except for HEA240s.

HEA	2m	3m	4m	5m
240	-	-	-	-
260	240A	240A	240A	-
280	260A	260A	260A	-

Table 4.4: Possible HEA S460 replacement - simply supported and distributed load

HEA	2m	3m	4m	5m	6m	7m	8m
240	-	-	-	-	-	-	-
260	240A	240A	240A	240A	240A	-	-
280	260A	260A	260A	260A	260A	260A	-

Table 4.5: Possible HEA S460 replacement - continuous beam (3-span) assumption

4.1.3. High-strength steel deck beams

The second type of beam considered in this research is the deck beam. These beams usually have a very wide range of length, somewhere from 5 to 15 metres, and have a cross-section made of a HEA or HEB beam with varying heights ranging from 400 to 1000mm. Deck beams are primarily responsible for supporting deck stringers and equipment. Unlike deck stringers, which mainly experience distributed loads, deck beams are subject to many point loads in equipment supports and at the connection points of deck stringers. Therefore, this paragraph will investigate the impact of point loads on the ULS/SLS-ratio and analyze the potential for high-strength steel in these typical deck beam ranges.

The graph displayed in Figure 4.14 demonstrates the ULS/SLS-ratio versus length for typical deck beams that are assumed to be either simply-supported or fixed. The beams that are assumed to be fixed (highlighted in red) shows a strength governing situation for the entire deck beam range (indicated by the red crosses). Yet, similar to deck stringers, these beams can't always be assumed to be fixed. If they are assumed to be simply-supported (highlighted in green), some beams are only partly strength-governing within the deck beam range. Again, the assumption of what kind of support significantly affects the ULS/SLS-ratio. Nonetheless, it is important to keep in mind that the graph in Figure 4.14 only shows the ULS/SLS-ratio for a distributed load. Since deck beams usually experience a lot of point loads, it is important to check the effect of point loads on the curve shift. The effect of point loads will be checked with the help of another case example and the detailed calculations are presented in Appendix C.

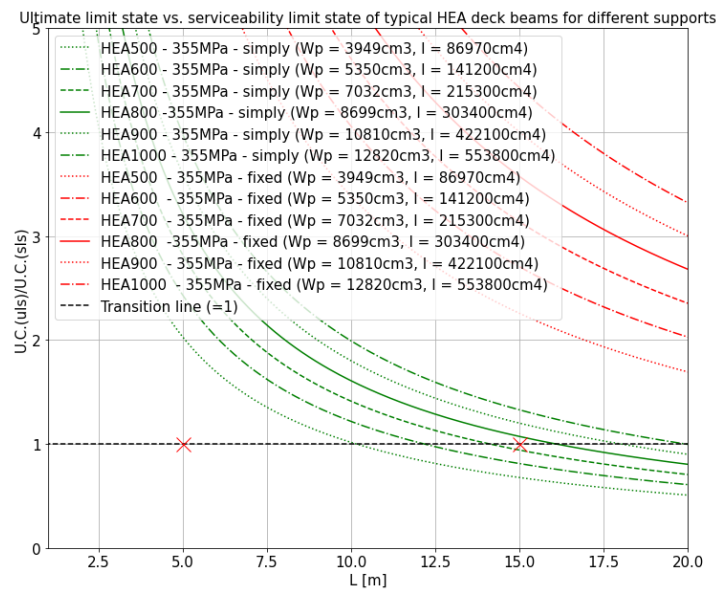


Figure 4.14: Different typical deck beams (different supports, distributed load)

Figure 4.15 shows the chosen example of the same platform deck as the deck stringer example. In this part of the deck, the only significant weights are the beams' weights and the two tanks with their equipment. The tanks are supported by a steel frame, which is, in turn, supported by the deck beam. In reality, these frames would also dissipate their weight on the deck stringers, but as the centre of gravity for the deck beams is exactly located above the deck beam, it is assumed that the deck beam will have to resist the total weight of the tanks. The deck beam has a length of 8.5 metres and has been chosen as a HEB600 by the designers. It is surrounded by other deck and main beams, with heights varying from 600 to 1000 and deck stringers in between. These deck stringers are again IPE240, but now they experience a lower variable load of $5\text{kN}/\text{m}^2$ instead of $15\text{kN}/\text{m}^2$, while it can now be assumed that these beams are located between equipment instead of a storage area. The deck stringers span 4.25 metres and are 0.85 metres apart. The deck beam is now fully welded to the adjacent beams.

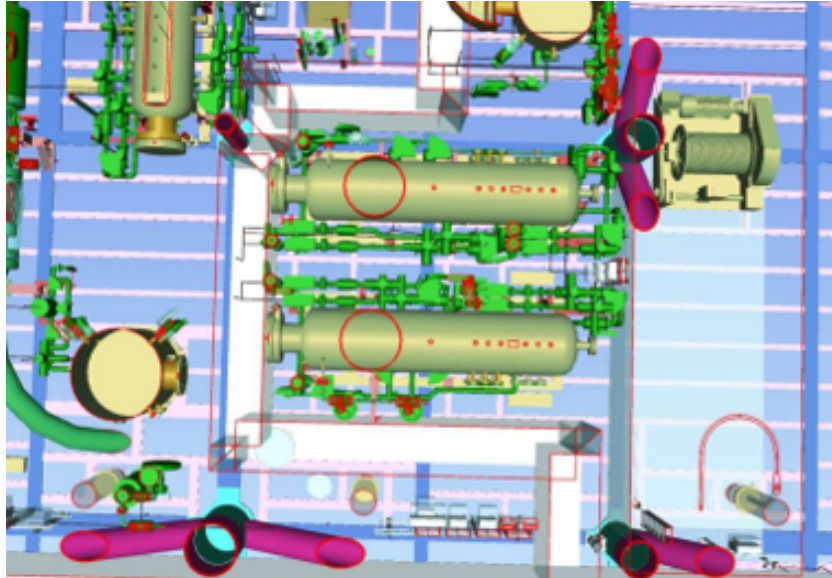


Figure 4.15: Example situation of a deck beam

Other than for the deck stringers, the example deck beam now experiences a combination of a point load by the deck beams and the equipment and a variable load in the form of its self-weight. While this research only considers small deflections, it is considered that superposition can be used and that the combination of point and variable loads can be plotted by adding the moment and deflection values. To investigate the effect of the added point load, figure 4.16 shows different support assumptions with a point load on the middle of the beam. For each support assumption, the point load varies from zero to infinity, and both situations are plotted. Interesting to see is that for the simply-supported and continuous beam situation, the ULS/SLS-ratio shifts to the right when a very high point load is added to the beam. While, for the fixed condition, the ULS/SLS-ratio shifts to the left for very high point loads. This is explainable, while the factors in the equations for fixed and simply supported are different. While two unity checks are divided by each other to obtain the ULS/SLS-ratio, this will be affected by the factors, and therefore, this difference can happen. This will partly be the case because of the difference in the maximum bending moment; for fixed beams this maximum can be found on the edges, while for simply supported beams this maximum moment is found in the middle of the beam. Hence, when a fixed assumption is made, it should be kept in mind that for heavy point loads, the ULS/SLS-factor decreases. Nevertheless, fixed connections are expensive to make, and it is most likely that these beams will not respond as a fixed assumption. From figure 4.16, it can be seen that a simply-supported beam with a distributed load could be used for conservative design, while this would always result in the lowest ULS/SLS-ratio.

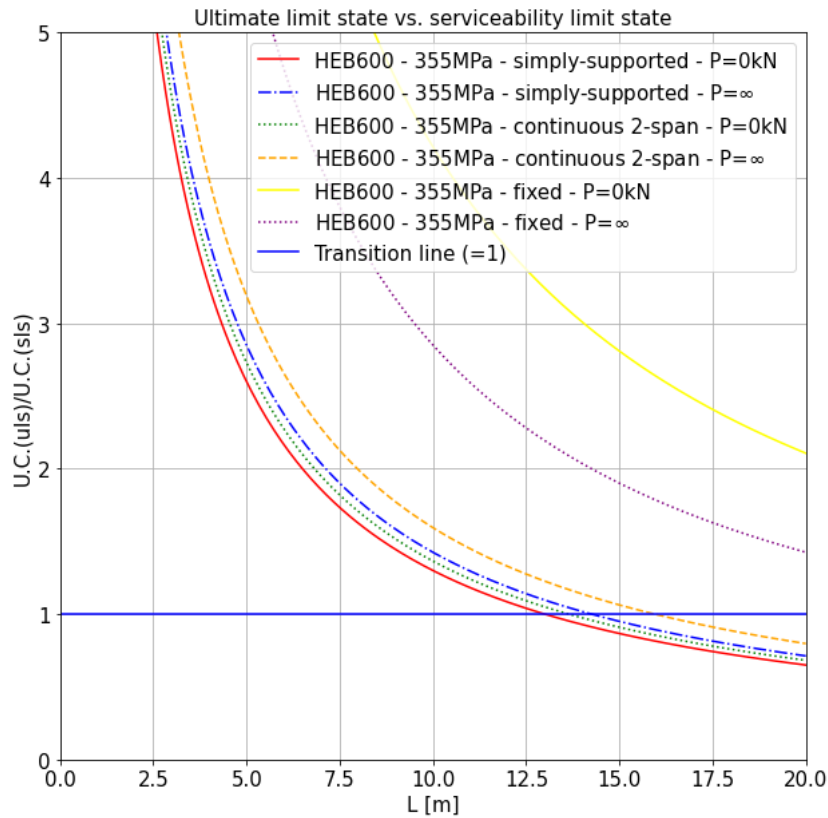


Figure 4.16: Effect of point loads on the ULS/SLS-ratio

The example is again modelled in RFEM, which is shown in figure 4.17. From this analysis, the maximum moment according to the ultimate limit state equals $1273.4kNm$ with a maximum shear force of $665.9kN$. The bending moment diagram is shown in figure 4.18. As a HEA600 has a cross-section classification 1, the plastic shear force resistance is calculated with equation 2.9. It can be concluded that the shear force interaction can be neglected while the maximum shear force is less than half the plastic shear force resistance ($2134kN$).

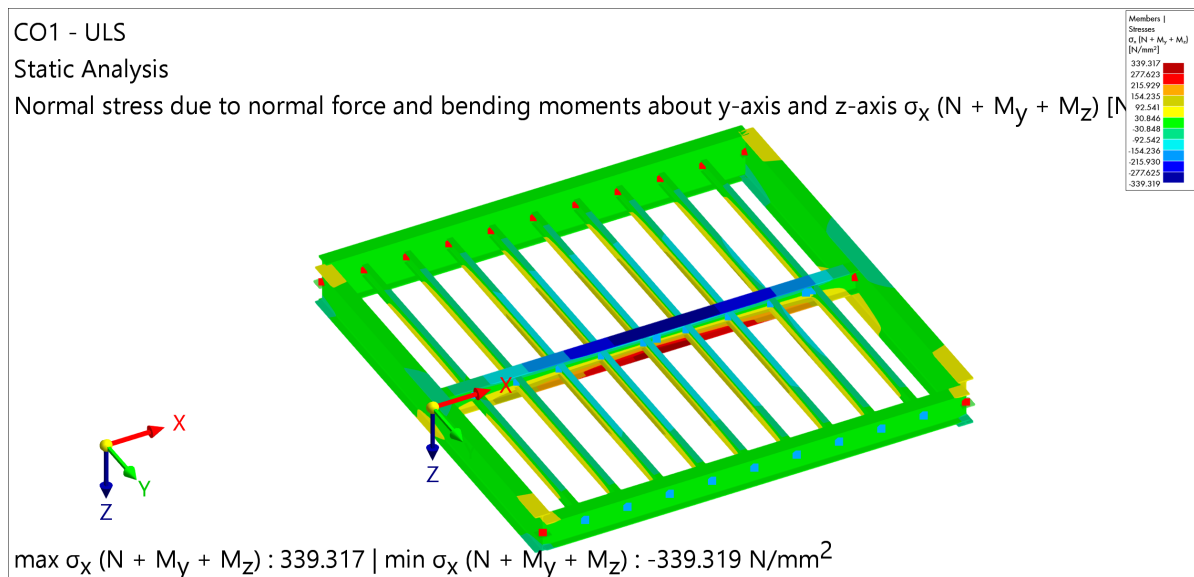


Figure 4.17: RFEM model of example deck beam

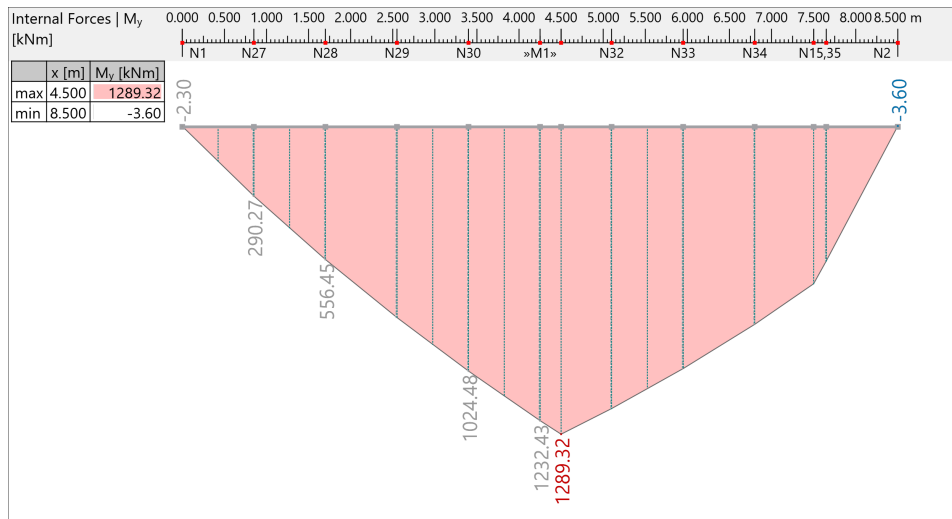


Figure 4.18: Moment diagram of deck beam modelled in RFEM

The maximum deflection is obtained with the serviceability load case and equals 21.7 mm . The whole deflection curve is shown in figure 4.19. The maximum bending moment and deflection can be used to obtain the ULS/SLS-ratio, using equation 4.1 and a value of 1.53 is obtained. This value is higher than 1, thus indicating that this beam is strength-governing. Strength-governing means possible benefits for HSS, hence a plastic analysis and cross-section 1 classification is assumed to check if HSS could be used. Afterwards, the cross-section classification is performed to validate this assumption. The bending moment is assumed to remain the same, and equation 2.2 is rewritten to obtain the minimum required section modulus. A minimum required section modulus of 3211 cm^3 and 2142 cm^3 for S460 and S690 are obtained, respectively. These required section modulus would lead to a HEA500 for S460 and a HEA400 for S690, but the deflection must still be checked.

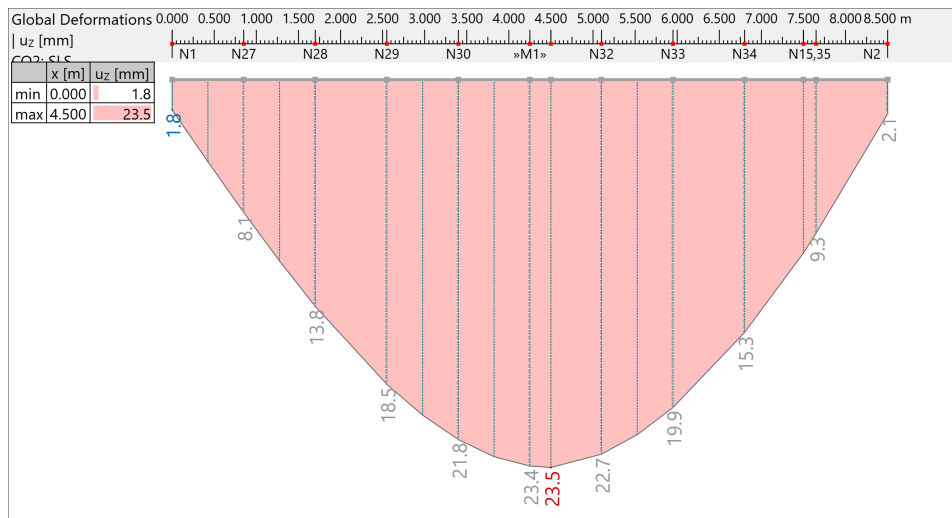


Figure 4.19: Deflection diagram of deck beam modelled in RFEM

For the deflection, an assumption regarding which type of support must be made. As previously discussed, the simply-supported assumption, with only a distributed load acting on it, is the most conservative one and could be used for a conservative approximation of the required area moment of inertia. If the equation for the deflection is set equal to the deflection found in RFEM, the distributed SLS load can be calculated, which equals 94.67 kN/m . Using the equation for the SLS unity check and filling in the calculated load gives the minimum required area moment of inertia, which is equal to 71980 cm^4 . This area moment of inertia would be satisfied by a HEA500 or higher, which concludes that S460 can

possibly lead to a cross-section reduction. At the same time, S690 would again not be beneficial to use as the deflection starts to be governing. The only thing remaining is to check if the cross-section is still class 1 and if shear force interaction should be included, but when both checks were performed, it was concluded that the beam is still class 1, and that shear force interaction can be neglected. Hence, the beam can be replaced with a smaller HEA500 of S460. A total weight reduction of 12.7% can be won by using S460, while the costs can be reduced by 6.6%.

This paragraph explained how using high-strength steel deck beams can result in significant weight reduction, even when assuming a conservative simply supported deck beam. However, other support assumptions are also possible in certain situations. For instance, if the deck beam is connected to other deck beams on both sides, the continuous beam assumption could be more accurate. Additionally, if the deck beam is connected to primary columns using very stiff connections, the fixed assumption would be more appropriate. Tables have been constructed for HEA and HEB beams for all three assumptions, with an example table for possible replacements for typical HEB deck beams when assuming simply supported provided in Table 4.6. Other tables for fixed and continuous for both HEA and HEB beams are shown in appendix D. The tables demonstrate that replacing deck beams with smaller cross-sections of high-strength steel is possible in many situations, even when simply supported deck beams are assumed.

Table 4.6: Possible replacement of beams with S460 (HEB) - simply supported and distributed load

HEB	5m	6m	7m	8m	9m	10m	11m	12m	13m	14m	15m
400	360B	360B	-	-	-	-	-	-	-	-	-
450	400B	400B	-	-	-	-	-	-	-	-	-
500	450B	450B	450B	-	-	-	-	-	-	-	-
550	500B	500B	500B	500B	-	-	-	-	-	-	-
600	550B	550B	550B	550B	550B	-	-	-	-	-	-
650	600B	600B	600B	600B	600B	600B	-	-	-	-	-
700	650B	650B	650B	650B	650B	650B	650B	-	-	-	-
800	700B	700B	700B	700B	700B	700B	700B	-	-	-	-
900	800B	800B	800B	800B	800B	800B	800B	800B	800B	-	-
1000	800B	900B	900B	900B	900B	900B	900B	900B	900B	900B	900B

4.1.4. High-strength steel main beams

In chapter 3, it has been concluded that main beams have a typical span of 12 to 15 metres. The typical range of standard hot-rolled main beams varies between HEB800 and HEB1000. However, main beams are often specially designed for load and deflection and built up from plating. These so-called plate girders often experience incredibly high loads, and it would be interesting if these could be replaced with high-strength steel. This paragraph will first discuss only standard hot-rolled main beams and then discuss whether using high-strength plate girders could be beneficial.

The first paragraph of this chapter explained that the area moment of inertia increases faster than the related section modulus, which results in a shift towards more strength-governing of the ULS/SLS-curves. As the main beams are usually the heaviest hot-rolled beams available or even more significant in the form of plate girders, they become dominantly strength-governing for very long spans. Figure 4.20 shows that all typical hot-rolled main beams are strength-governing within the typical main beam length range (indicated again with the red crosses). All the curves are plotted for a distributed load except for the blue and orange lines, which are plotted for a point load. It can be concluded that even in the longest, smallest scenario, a HEB800 of 15 metres, the beam is still strength-governed regardless of what type of support or load. Using the same approach as in the previous two paragraphs, the HEB800 could be replaced with a HEB700, causing a weight reduction of 8.2%.

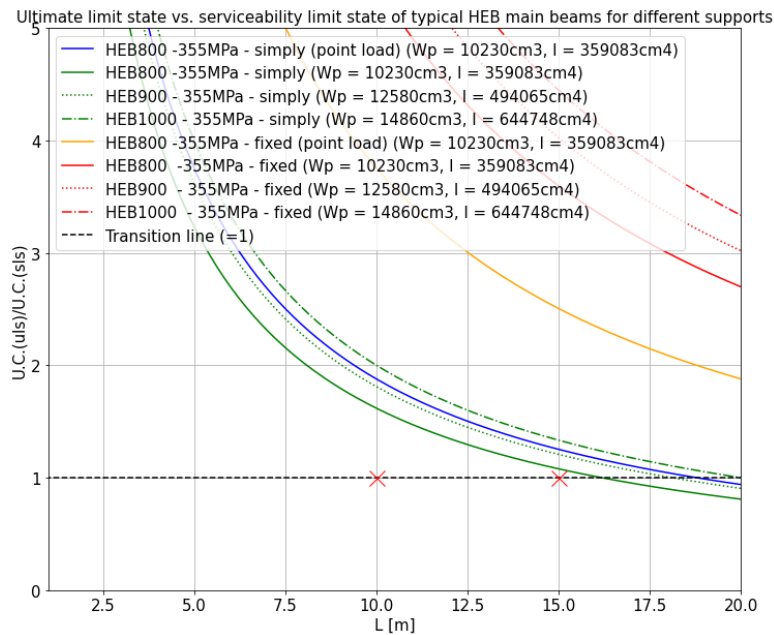


Figure 4.20: Different typical main beams (different supports, distributed load)

Nevertheless, the previously used method assumes a lateral restrained beam. The deck stringer could be assumed lateral restrained because of the welded deck plating on top of the beams, and the deck beams could be assumed lateral restrained while they have a deck stringer on both sides. However, the main beams are typically connected to other beams on only one side, allowing lateral-torsional buckling to occur. Hence, the lateral-torsional buckling reduction factor can not be neglected for the main beams. Therefore, the effect of this factor on applying high-strength steel should be investigated.

Figure 4.21 shows the decrease of the bending moment resistance over the length of a beam when the lateral-torsional reduction factor is included. It can be seen that if a beam is lateral unrestrained, the bending moment resistance of the beam decreases fast when the length increases.

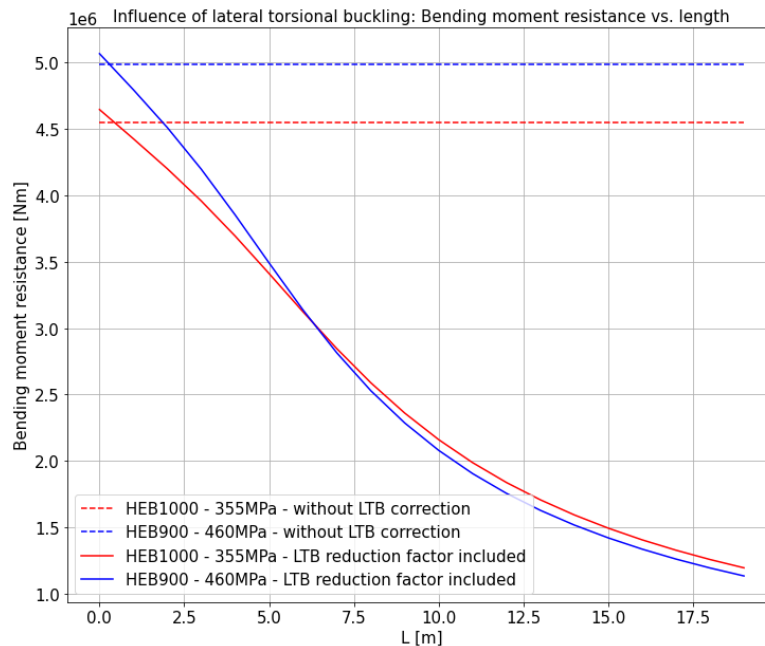


Figure 4.21: The effect of the lateral torsional buckling resistance

If the beams were lateral unrestrained, high-strength steel could not benefit HEB1000 main beams when the main beams are longer than approximately 7 metres. As typical main beams have a length of 12 to 15 metres, this would result in no benefits for main beams at all. However, in the previous example of figure 4.17, it is shown that the outer main beams are not entirely unrestrained but are partly restrained at only one side. If the middle beam is loaded, torsion shall occur on the outer beams. However, while all the beams interact, the outer main beams will experience some lateral-torsional resistance. The question arises: *Is the resistance against lateral-torsional buckling significant enough to assume a lateral restrained outer main beam?*

In some cases, the deck plating would also contribute to a higher lateral-torsional buckling resistance, but grating is also often used in the topside deck, which does not contribute to higher lateral-torsional resistance. Therefore, a deck part without deck plating will be assessed and an example deck is modelled in RFEM to answer this question. The layout is based on typical numbers from the previously performed topside analysis and is shown in figure 4.22. The deck is modelled as 15x12 with HEB1000 main beams on the edges and in the middle. The main beams are chosen as HEB600 at 1/4 and 3/4 of the width of the deck, and the deck stringers as IPE200. One massive piece of equipment, weighing 320 tonnes, is positioned on the deck. It is assumed that four supports transfer the equipment load onto the beams, equally dividing the mass of the equipment.

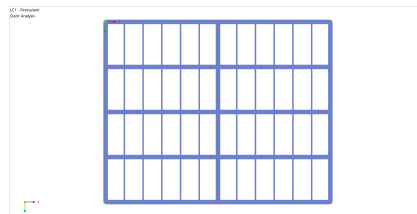


Figure 4.22: Example typical deck layout

Figure 4.23 shows an illustration of the stresses occurring on the deck when a heavy piece of equipment is put on it. The right beam of figure 4.22 is assessed for its bending moment, torsional moment and torsional rotations, which are shown in figure 4.24. The top diagram shows the bending moment through the beam with a maximum of 2020.75 kNm at approximately half the length. The middle diagram shows the torsional moment that occurred due to the deflection of the beams on which the equipment is located. The torsional moment only reaches 3.98 kNm at its maximum, a value of only 0.2% when compared with the bending moment. The bottom diagram shows the angular rotation around the beam's minor axis. The maximum rotation angle equals 11.7 mrad , which is equal to only 0.67° .

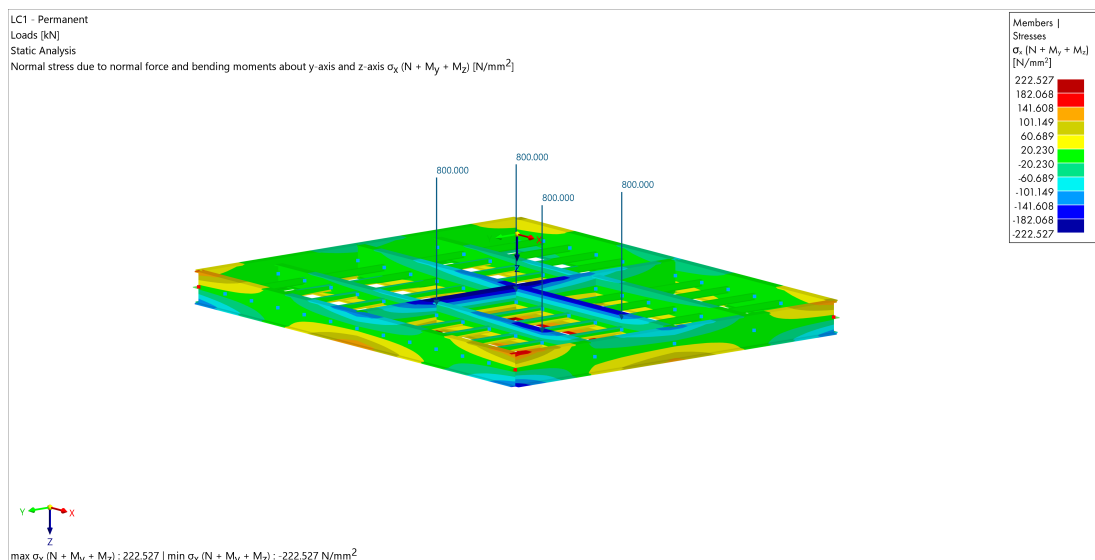


Figure 4.23: RFEM model of deck with heavy equipment

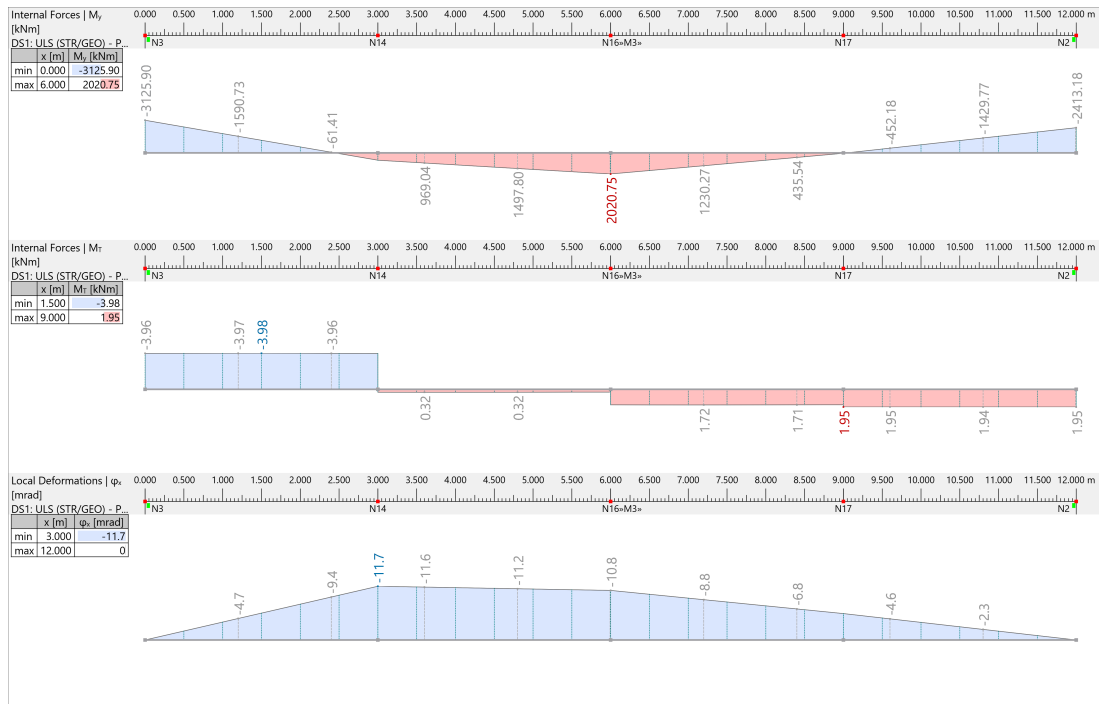


Figure 4.24: RFEM model of deck with heavy equipment

As the torsional moment and rotation are very small, it is thought that the interaction of the beams at one side of the main beam still makes the main beam lateral restrained. If the bending moment and lateral-torsional moment are used to calculate the occurring stresses, values for the longitudinal stress ($\sigma_{x,Ed} = M_{Ed}/W$), caused by bending, and the shear stress ($\tau_{Ed} = T_{Ed}/W_t$), caused by torsion, can be calculated. For the shear stresses, it is assumed that only the St Venant shear stress has a contribution and that the warping shear stress can be neglected. Moreover, an elastic calculation is assumed, and in that case, the ultimate resistance of a combination of both loads can be calculated with equation 4.19. When implementing both stresses ($\sigma_{x,Ed}=136\text{MPa}$ and $\tau_{Ed}=6\text{MPa}$) in the equation, a factor of 0.119 can be found, while if only the bending moment stress would be implemented, a value of 0.118 would be obtained. This difference is so small that it is expected that the occurrence of lateral-torsional buckling is very unlikely. Therefore it is assumed that the lateral-torsional buckling reduction can be neglected when looking at the feasibility of utilizing high-strength steel main beams in offshore topside decks.

$$\left(\frac{\sigma_{x,Ed}}{f_y/\gamma_{M0}}\right)^2 + 3\left(\frac{\tau_{Ed}}{f_y/\gamma_{M0}}\right)^2 \leq 1 \quad (4.19)$$

If lateral-torsional buckling is neglected, main beams can also be beneficially replaced with S460. As previously discussed, a HEB900 of S460 could replace the HEB1000 of S355. Looking at the costs, the welding costs would decrease by approximately 10%, while the material costs would increase by only 0.7%. The total cost reduction would then be equal to 4.65%. The weight reduction is equal to 7.2%. Hence, high-strength steel is still cheaper and makes the topside lighter if it is assumed that lateral-torsional buckling can be neglected. If, in other cases, it could not be neglected, extra measures such as torsional stiffness could be introduced. However, this automatically requires more welding, resulting in higher welding costs; Hence, it is probably not worth it. Stiffeners also introduce additional problems such as corrosion details, painting and engineering. If lateral-torsional buckling is possible for a beam, high-strength steel would not be beneficial or only for very short main beams.

Nevertheless, until now, only the hot-rolled standard main beams have been assessed. Usually, main beams experience incredibly high loads and are specifically designed to resist these loads in an optimal way. These beams are called plate girders and are manufactured from plate material. Plate girders require a different approach to assess if high-strength steel could benefit them. The STROBE research [6] performed some case studies with plate girders. The trick with plate girders is to keep the web of

S355 steel, while this thickness can not be reduced because of the resistance against deflection and only to change the flanges into higher strength steel. The Eurocodes allow the fabrication of these so-called hybrid girders, which could be used to reduce the weight. The first example STROBE researched was a primary IPE500 beam spanning 9 metres. The research replaced this beam with an S460 and an S690 hybrid plate girder, obtaining 24% and 38% in weight reduction and 11% and 24% of embodied carbon savings, respectively. However, as welding plate girders is much more expensive than buying a hot-rolled standard IPE500, the cost increased by 14% and 5%, respectively. This example shows that the weight of standard beams could be heavily reduced if hybrid plate girders were used; however, often, the cost is the governing factor, and in that case, it would be more beneficial to keep with the standard IPE500. Additionally, STROBE performed another case study comparing an S355 plate girder with a height of 1100mm with hybrid plate girders of S460 and S690 for a beam span of 15 metres. Weight savings of 21% and 41% were achieved, with embodied carbon savings of 19% and 36%, respectively. As the S355 plate girder also must be welded, the hybrid plate girders are now cheaper to fabricate, and cost reductions of 4% and 13% were achieved. The length and height of the example beam are very comparable with plate girders used in offshore topsides. As shown in the first paragraph of this chapter, the loading does not directly influence whether high-strength steel could be beneficial; therefore, these weights, embodied carbon and cost savings are also expected on offshore topsides. Therefore, it is concluded that hot-rolled main beams can be beneficially replaced with hot-rolled S460 beams and with hybrid plate girders when lateral-torsional buckling can be neglected; however, for the hybrid plate girders, this will not result in cost savings. Only when a plate girder must be higher than hot-rolled standard main beams, the S355 plate girders can be beneficially replaced with hybrid plate girders, resulting in weight, embodied carbon and cost savings.

4.1.5. High-strength steel cantilever beams

The final type of beam recognised in topside decks is the cantilever beam. Often, these beams enable the deck to extend out of the area between the main legs. These regions are usually not heavily loaded, and only the less heavy equipment is located in areas supported by cantilever beams. Where other beams have a limitation of $L/200$ for the deflection in the serviceability limit state, the deflection of cantilever beams is often not allowed to exceed $L/150$. Hence, cantilever beams are allowed to have more deflection. Figure 4.25 shows that typical HEB beams, often used for cantilever beams, quickly drop below the strength-governing range. However, cantilever beams can be pretty massive, and as an example, it can be seen in figure 4.25 that a HEB700 of more than 6 metres still has the potential to be replaced by a high-strength steel beam. Therefore, in many cases, the cantilever could be beneficially replaced with a smaller cross-section.

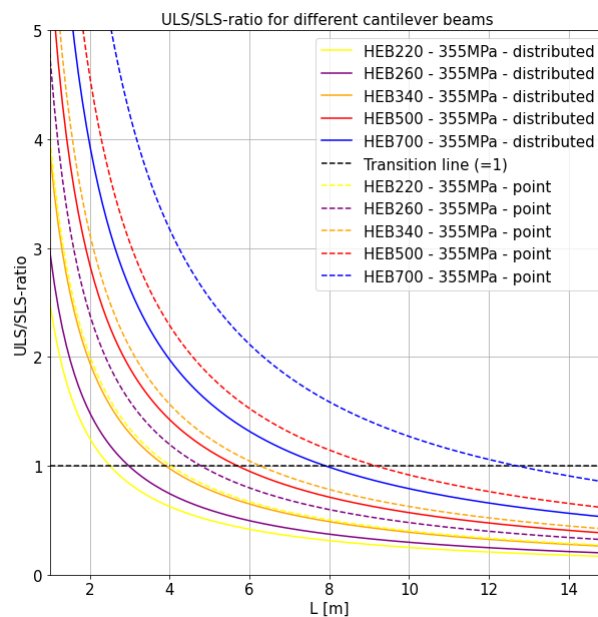


Figure 4.25: Different typical cantilever beams with different loadings

4.2. High-strength steel circular hollow columns & bracings

This section will evaluate columns for their feasibility of using high-strength steel. Columns are typically assessed in two ways: how they react in frames and as a local member. The sway deflections in frames can cause second-order effects, and require extra design attention. However, the topsides built at HSM have many bracings, so the frames react more as non-sway frames, and the second-order effects are neglected. Three checks for columns are necessary: axial compression force, buckling resistance, and the combination of a bending moment and an axial force. For columns in the topside, the vertical load is typically much higher than the horizontal loads, mainly consisting of the wind load. Thus, the last check is neglected as the axial forces are assumed to be much higher than the bending moments in the columns. Therefore, two checks remain for the assessment of columns: an axial force resistance check and a buckling resistance check. As steel columns are often relatively slender, the buckling resistance often governs the design of columns. Therefore, this check will be used to assess if columns can be replaced with high-strength steel. Bracings are typically in compression or tension, and tension will not form problems when going to higher-strength steels. However, making a column more slender can cause trouble. It is assumed that bracings are also only loaded by an axial force and can, therefore, be assessed in the same way as columns.

To determine the buckling resistance of a column, equation 2.13 can be used. If the design load is lower than the buckling resistance force of the member, the column can be considered safe. The buckling resistance force is calculated using equation 2.14, which is dependent on several factors, including the buckling reduction factor (χ), the area, yield stress, and the partial safety factor. The buckling reduction factor is, in turn, influenced by the non-dimensional slenderness of the column and the corresponding buckling curve defined by the Eurocodes. If high-strength steel is used, the yield stress will increase, but the cross-sectional area will decrease. As a result, the non-dimensional slenderness will increase, leading to a decrease in the benefits of using high-strength steel when a column becomes more slender. This controversy highlights the need for careful consideration of the trade-offs between material properties and design requirements when using high-strength steel for axially loaded columns.

According to HSM Offshore Energy, columns are typically available in two forms: hot-formed and cold-formed circular-hollow tubes. During the assessment of topsides, a maximum non-dimensional slenderness ratio of approximately 1.3 has been seen. Figure 4.26 shows the buckling resistance in N/m^2 of a column as a function of the non-dimensional slenderness for hot-formed columns using buckling curve a for S355 steel and using buckling curve a_0 for S460 and S690 corresponding the Eurocodes. It can be seen that at high slenderness, the buckling resistance of high-strength steel drastically drops, and as the cross-sectional area also drops for high-strength steel, it could be the case that high-strength steel will not show benefits at higher non-dimensional slenderness ratios. Nonetheless, the maximum concluded non-dimensional slenderness still shows that the columns are relatively stocky and that high-strength steel could potentially be beneficial in the most cases.

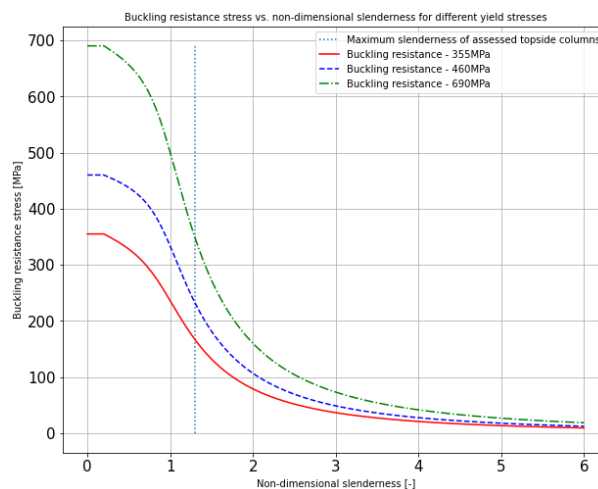


Figure 4.26: Buckling resistance [N/m^2] vs. non-dimensional slenderness for hot-formed tubulars

This drop of the buckling resistance over the slenderness drops faster when the less beneficial buckling curve c must be used for welded cold-formed columns. Figure 4.27 shows the buckling resistance for different steel versus the non-dimensional slenderness, and it can be seen that in all three cases, the buckling resistance quickly drops when the column becomes more slender. However, also here it can be seen that high-strength steel could potentially be beneficial when considering the non-dimensional slenderness ratio range of the assessed columns (0.1-1.3). Moreover, the literature showed that for high-strength steel cold-formed columns, the buckling curves a would be more appropriate, but these are not yet implemented in the regulations. When this would be allowed benefits for high-strength steel welded cold-formed columns will increase because of the more favorable buckling curves.

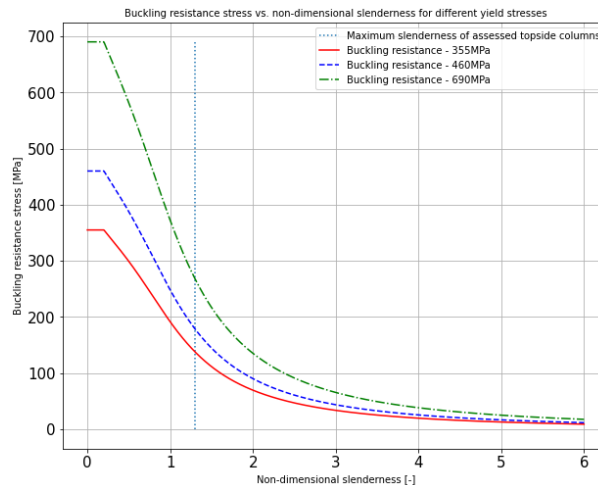


Figure 4.27: Buckling resistance [N/m^2] vs. non-dimensional slenderness for welded cold-formed tubulars

To evaluate the feasibility of high-strength steel for columns without any knowledge of the loads, it is necessary to match the buckling resistance of a high-strength steel column with that of an S355 column. Figure 4.28 is constructed to illustrate this. When the diameter and thickness of an S355 column are known, the buckling resistance in kN can be plotted against the column height, as shown by the red line. If the same graph is plotted for high-strength S460 steel, the member will have a higher buckling resistance, especially for shorter lengths, as shown by the blue line. As the length of the columns is already known, the line can be numerically pulled down until the high-strength steel columns matches the same resistance as the S355 steel column. This pulling down can be done numerically by decreasing the diameter or thickness of the column. The green line for S460 and the yellow line for S690 indicate the same buckling resistance can be achieved with smaller cross-sections. This approach would result in a weight reduction of 21% for S460 and 37% for S690. If the material costs are factored into this example, S460 would reduce costs by 14.7%, while S690 would reduce costs by 25.1%. Both the weight and cost calculations demonstrate that high-strength steel can be a beneficial choice for offshore topside columns.

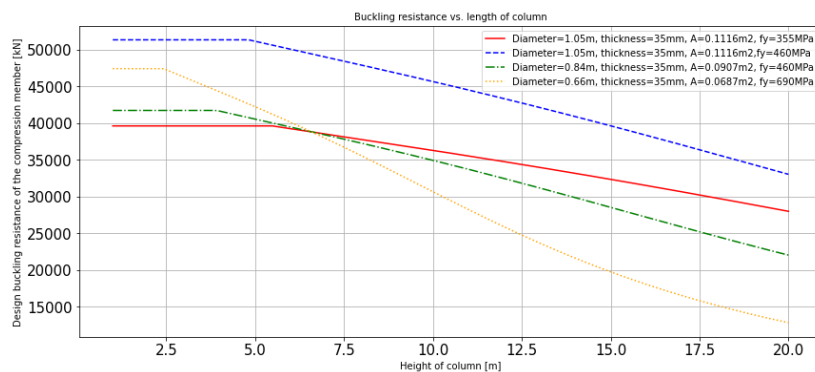


Figure 4.28: Example column of high-strength steel

Nevertheless, it's important to keep in mind that decreasing the cross-section will lead to different D/t ratios, which can cause manufacturing problems, especially for cold-formed columns. According to HSM, the minimum D/t ratio should be around 20. If the ratio is lower, the plate cannot be bent without damaging the material properties of the plates. For hot-rolled columns, the diameter and thickness are normally fabricated in standard steps. This is not included in the method described in this section, but there is a wide variety of hot-rolled columns available. Hence, it is assumed that this will not significantly change the results in practice.

In conclusion, high-strength steel can have advantages in both hot- and cold-formed columns. However, the level of those advantages mainly relies on how slender the column in a topside is and how much the diameter or thickness of a column can be reduced. Based on the maximum non-dimensional slenderness ratio observed, it can be concluded that the columns and bracings are most often stocky enough to be replaced with high-strength steel.

4.3. Conclusion of high-strength components in topsides

This chapter evaluated various structural components of a topside to determine their feasibility for using high-strength steel. The components that were assessed included beams, columns, and bracings. The assessment was based on examples, and conclusions in the form of typical lengths or slenderness were discussed.

It was concluded that the loading does not affect whether a beam is strength or deflection governing. Therefore, it is possible to determine the transition point from strength governing to deflection governing. If a beam is deflection governing, high-strength steel cannot be used. If a beam is strength-governing, it could be possible to use high-strength steel if enough resistance against deflection can be found for a smaller cross-section. The support type plays a crucial role in determining whether a beam is strength or deflection governing. A simply-supported beam results in a more deflection-governing situation, while a fixed support would result in a more strength-governing situation.

When it comes to using high-strength steel for small deck stringers in topsides, it is seldom beneficial. However, the stringers are sometimes strength-governing for specific cross-sections and short lengths. Using HEA beams instead of IPEs or applying a continuous beam assumption instead of a simply-supported beam can result in more benefits. For deck beams, using high-strength steel often leads to benefits, but it depends on the length. Assuming a distributed load would lead to the most conservative results for a simply-supported beam and a continuous beam, but assuming a point load would result in the most conservative situation for fixed beams. When looking at the main beams, in almost all typical cases, the main beams can be replaced with a smaller section of high-strength steel when lateral-torsional buckling can be neglected. Utilizing high-strength steel hybrid plate girders instead of S355 plate girders will result in high benefits in costs, weight and embodied carbon savings. Regarding the last type of beam, the cantilever beams, benefits were also found, but the extent of the benefits heavily depends on the cross-section and length. Overall, it can be said that in many cases, beams can be beneficially replaced with smaller high-strength steel beams.

When considering columns and bracings, it can be concluded that the maximum non-dimensional slenderness ratio often offers enough space to reduce the column dimensions with high-strength steel. However, it depends on the slenderness how much benefits can be achieved, and additional costs and embodied carbon savings still need to be assessed.

5

Methodology to assess the feasibility of high-strength steel in topsides

The previous chapter concluded that most of the beams, columns and bracings could be beneficially replaced with high-strength steel when making certain assumptions for the assessment. However, most of these conclusions were based on example calculations. This chapter will describe the screening tools constructed to assess the feasibility of using high-strength steel within an entire topside. The first two sections will explain how the beams and columns can be assessed. The methods described in these sections can be applied to multiple different steel structures and only require an inventory of all the steel beams and columns within an existing structure. Python is used to implement these methods for this research, but the methods are discussed such that they can be reproduced with other code languages or Excel. As the first two sections discuss screening tools which can be used when taking an existing topside as an example, the third section will shortly introduce how the constructed method can be used when making a preliminary design for a new topside.

5.1. Screening tool for beams in a deck

The method which is elaborated in this paragraph to assess the feasibility of using high-strength steel for beams within an existing deck is visualized in figure 5.1 and will be discussed below. The first step to assess the feasibility of using high-strength steel in beams of existing decks is to create an inventory of all primary and secondary beams within a deck along with their specifications such as beam type (plate girder or hot-rolled beam), cross-section dimensions (height, width, thickness, etc.), and length. For the method constructed in this research to work, both the bending moment and deflection should be calculated as a function of the length. In an ideal scenario, the support assumption that best approximates a particular beam should also be included in the inventory. However, this information is often not readily available. In such cases, the findings from the previous chapter can be used to assume certain support conditions for different types of beams. Where there is doubt about which support assumption to use, the most conservative one can be assumed. The list below shows which support types are assumed in this research, but it is important to note that the assumed support type can drastically affect the results.

- Deck stringer = simply-supported beam
- Deck beam = continuous beam
- Main beam = fixed beam
- Cantilever beam = cantilever beam

When the inventory is constructed, the plate girders and hot-rolled beams should be split from the list while they require two comparable but slightly different methods to assess the feasibility of high-strength steel. Let's start with the hot-rolled beams. These beams have standard dimensions defined by the Eurocodes or other standards, and come in different ranges, typically with heights up to 1000mm. The benefit of these beams is that they are rolled and therefore relatively cheap, since they don't need to be

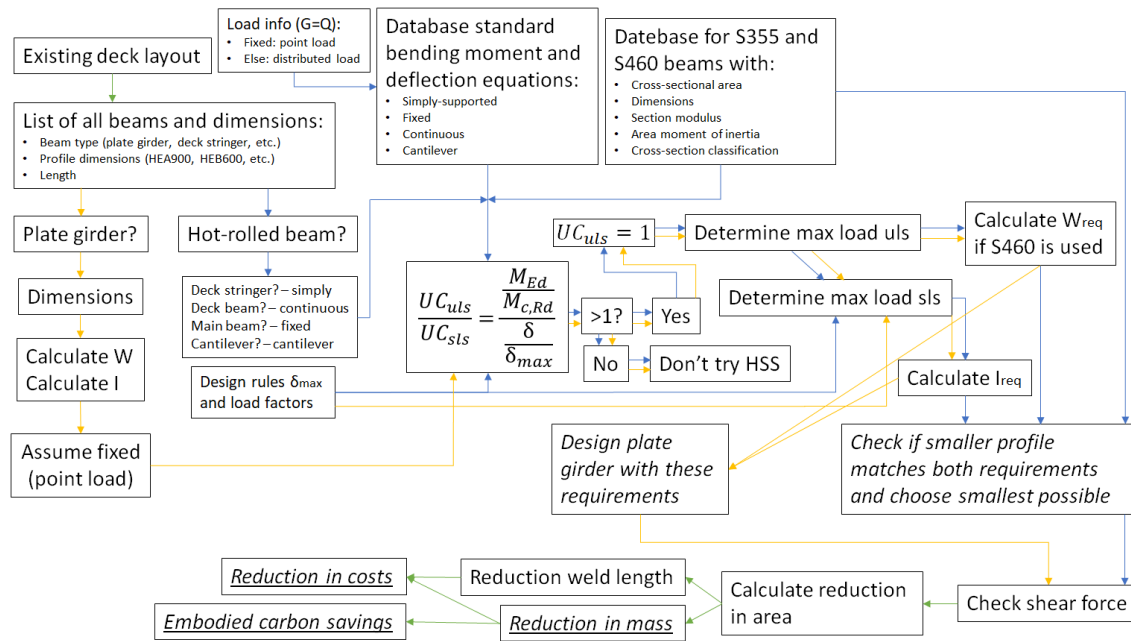


Figure 5.1: Visualization of the introduced methodology to assess the potential of high-strength steel beams in topside decks

welded from plates like the plate girders. However, their area moment of inertia and section modulus also change with the ranges due to the steps in height. The previous chapters concluded that the steps in area moment of inertia often restrict the use of S690 in beams and that S690 hot-rolled beams are not readily available on the global steel market. Hence, only S460 beams are being considered from this point on. It has been seen that if beams can be reduced with high-strength steel, it is usually only possible in steps of one cross-section smaller when it is assumed that the initial beam is loaded at its full capacity. Online sources [46] provide databases of all dimensions and cross-section classifications for S355 and S460 beams, which are directly implemented in the model.

A final database needs to be created that contains all the standard equations for the support assumptions discussed earlier. Multiple functions are created, which can be selected when a beam is considered a deck stringer, deck beam, main beam, or cantilever beam. The ULS/SLS-ratio can then be determined by obtaining the deflection limits and partial load factors from the basis of design of the considered topside. A load ratio based on the research of Honfi [16] and introduced in the previous chapter is used and always considered 0.5 to determine the ULS/SLS-ratio. This means that the variable and permanent load are always assumed to be equal when checking the ULS/SLS-ratio. In the previous chapter, it was concluded that the assumption of a point load is the most conservative for the fixed support assumption. On the other hand, the assumption of a distributed load is the most conservative of the other support assumptions. Therefore, this method only assumes a point load for fixed beams, while a distributed load is assumed in all other cases. When the ULS/SLS-ratio is lower than 1, high-strength steel will not be considered, while deflection will govern the design situation. If the ULS/SLS-ratio is higher than 1, the replacement of a beam with high-strength steel can be assessed.

If a beam is governed by its strength, it may be possible to replace it with high-strength steel. To assess this possibility, it is assumed that the original beam was designed for its maximum capacity, which is rarely the case in practice. However, since the loads are unknown, assuming a unity check equal to one is the most conservative approach. Given the known beam dimensions and yield stress, the maximum load for the ultimate limit state, including partial load factors, can be calculated. While the partial load factors are obtained from the basis of design, the maximum load in the serviceability limit state can be calculated without partial load factors. With the maximum load and partial load factors, the required section modulus for the beam can be calculated when the steel is changed from S355 to S460 steel. Using the maximum load of the serviceability limit state, without the partial load factors, the

required area moment of inertia can be calculated. Once these values are known, it can be checked if a smaller cross-section of S460 steel would still meet the minimum required area moment of inertia and section modulus by using the database of S460 beams. The shear force must still be checked if a smaller cross-section meets these requirements. When the shear force check is also satisfied, it can be concluded that a smaller beam made of S460 steel can replace the original beam.

When a beam can be replaced with a smaller beam of high-strength steel, the weight reduction, cost reduction, and embodied carbon savings can be assessed. First, with the smaller cross-section, the reduction of mass can easily be determined. This reduction in mass is connected to both the reduction in costs and embodied carbon savings. Two costs are included for the reduction in costs: the material costs and the welding costs. Other costs are assumed to be equal for both S355 and S460. It must be noted that the actual welding cost reduction is not viable to calculate, as the thickness of flanges, webs, etc., changes when smaller beams are used, and it is not viable to look at each weld individually. Hence, the reduction in weld length will be calculated, and it is assumed that the welding cost reduction is directly connected to this. Finally, the embodied carbon savings can be approximated. As limited information is found on the differences between high-strength steel and conventional steel in all life-cycle stages of an offshore topside, only the first three life-cycle modules are used (A1 to A3) based on STROBE [6], including material production, transport to workshop and manufacturing. This was tested, but it was concluded that in that case the embodied carbon savings are directly connected to the percentages of weight reduction. When more information about offshore transport and installation would be known, some difference is expected. Nevertheless, with the information which was found for this research, the embodied carbon savings are equal to the reduction in mass.

When it comes to plate girders, the method discussed earlier is mostly the same, with some minor changes in the approach. Typically, a plate girder is used as a main beam and, hence, is assumed to be always fixed in this method. Since plate girders are designed for specific dimensions, the initial area moment of inertia and section modulus must be calculated from the cross-section dimensions. Once this is done, the ULS/SLS-ratio can be calculated, and it can be determined whether high-strength steel can be assessed similarly to the hot-rolled sections. The maximum ultimate limit state and serviceability limit state loads can then be calculated, and the required area moment of inertia and new minimum required section modulus can be determined. After this stage, the most significant difference occurs, as a new plate girder must be designed since no standard section can be selected for this. When designing a new plate girder, the mass reduction, cost reduction, and embodied carbon savings can be calculated similarly to the hot-rolled section.

5.2. Screening tool for columns and bracings

The method constructed to assess the feasibility of high-strength steel for columns is totally different from the assessment of the beams. As it is assumed that the vertical load is much higher on offshore columns than the horizontal load and because of the many bracings included in offshore topsides, it is assumed that the frames of columns and bracings are stiff enough such that no second-order effects need to be considered. Figure 5.2 on the next page shows the method introduced to assess columns.

Just as with the beams, the first step is to construct an inventory of all the columns and bracings within a topside. This inventory should include the length, diameter, and thickness of each column or bracing. It is also important to differentiate between hot-rolled columns (seamless tubulars, TUS) and cold-formed columns (welded tubulars, TUW) since the Eurocodes require different buckling curves for each type. Additionally, S690 welded tubulars can be made from S690 plates by bending them to the correct radius, but S690 seamless tubulars are not yet available in large numbers. Therefore, this method will assess TUW columns for both S460 and S690 steel, while TUS columns will only be evaluated for S460.

The trick of this method is to introduce a factor β before the diameter. First, this factor β will be assumed to be equal to 1, and the area moment of inertia and cross-sectional area of the column will be calculated with the diameter, factor β and thickness. With the area moment of inertia, the Euler's critical load can be calculated, and together with the yield stress and cross-sectional area, the non-dimensional slenderness can be determined. Then, with the right corresponding buckling curve, the factor ϕ can

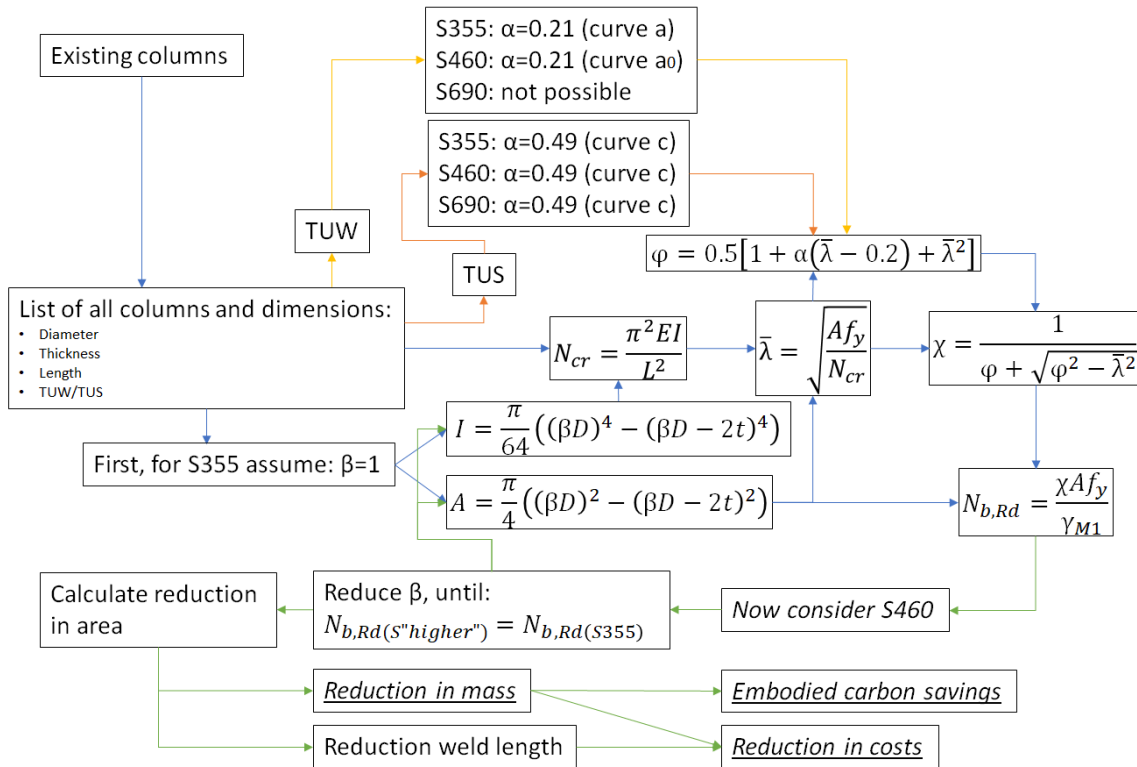


Figure 5.2: Visualization of the introduced methodology to assess the potential of high-strength steel columns and bracings

be determined for both a TUV or a TUS column and with this factor, the buckling reduction factor and buckling resistance load can be calculated. It is assumed that this buckling resistance load must remain the same when a smaller, higher-strength column is used. Therefore, the calculation is performed again, but now with reducing the factor β in small steps of 0.001. The calculation is run until the same buckling resistance load is found for higher-strength steel. Hence, the diameter of the column is reduced until the same buckling factor is concluded. With the reduced diameter, the new area of the column can be calculated, assuming that the thickness remains the same. With the new cross-sectional area for a column of high-strength steel, the mass reduction, cost reduction, and carbon savings can be calculated similarly to those for beams. Nevertheless, distinctions must be made between applying S460 steel for both TUV and TUS, or applying S460 only for the TUS and S690 for the TUV.

5.3. Methodology for preliminary design

The methods described in the previous two sections can easily be combined when the total mass reduction, cost reduction and carbon savings are added. In this way, the total effect of utilising high-strength steel on topsides can be assessed. The methods above can be extended with additional applications, design rules or components when more information is available by any engineer; in this way, the model can become more accurate in the future, resulting in an easy-to-use screening tool for the feasibility of high-strength steel within topsides.

Nevertheless, the previously discussed methods used an existing topside, but in many cases, it would be desired to say something about whether high-strength steel can be beneficial within an early design phase. One tool that engineers can use to determine the feasibility of high-strength steel beams is the length at which a beam becomes deflection governing. If an engineer draws a preliminary layout, the lengths can be checked with tables such as shown in figure 5.1 for IPE's. If the length is smaller than the lengths shown in the table, high-strength steel can possibly be beneficial, and it is interesting to check if a smaller high-strength steel cross-section could be used. Some more example tables are added in appendix D, but can also be constructed and calculated by setting the ULS/SLS-ratio equal to one and determining the corresponding length.

Table 5.1: Maximum length for IPEs (S355) to be strength-governing

IPE	Lmax [m] (Simply-supported - distributed load)	Lmax [m] (Fixed - point load)
180	3.65	8.47
200	4.06	9.43
220	4.48	10.4
240	4.90	11.36
270	5.52	12.81
300	6.13	14.23
330	6.75	15.66
360	7.36	17.09
400	8.16	18.94

For columns, it is advised to always check the feasibility of high-strength steel when horizontal forces and deflection are assumed to be negligible. Hence, when only small horizontal forces are expected or when sufficient bracings are present, benefits can be expected, and the method of section 5.2 can be used to assess the potential benefits.

6

Case study: feasibility of high-strength steel in topsides

This chapter will use the methodology constructed in the previous chapter to assess an entire topside for its feasibility of high-strength steel. The first section, section 6.1, will discuss the case topside and will give some basic information about the considered topside. Section 6.2 will elaborate on how all types of beams are assessed and will discuss the results. Section 6.3 will explain how the columns and bracings of the topside are assessed and will also discuss the results. Finally, section 6.4 will discuss the final results of the assessment of this case study.

6.1. Case introduction and assumptions

This case study examines the topside of an offshore gas production platform located in the southern North Sea. The entire platform was constructed by HSM Offshore Energy and weighs 7500 tonnes, including topside, jacket and piles. The topside accounts for 40% of this weight, weighing 3000 tonnes, and can be seen in figure 6.1.

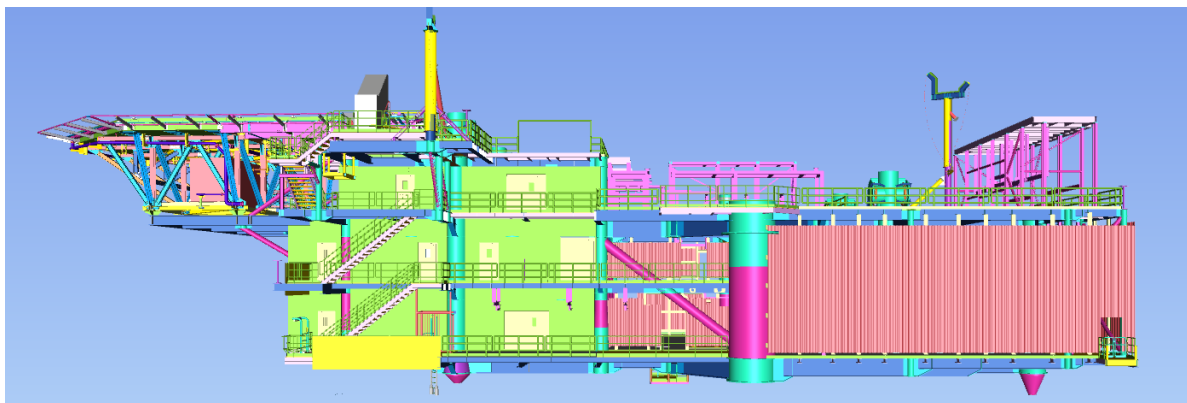


Figure 6.1: Considered topside for the case study

The goal of this case study is to evaluate the potential weight and cost savings that can be achieved by using high-strength steel beams, columns, and bracings instead of conventional steel ones. According to chapter 3, the weight of the steel scope accounts for 50% of the topside weight. For the case topside, this translates to a steel weight of around 1500 tonnes. Out of this total weight, the beam scope should weigh approximately 510 tonnes, while the column and bracing scope should weigh around 255 tonnes. The remaining 735 tonnes of steel consists of stairs, railings, joints, deck plating, wall sheets, pipe supports and other such steel components. Figure 6.2 depicts the topside without most of the steel components that are not considered. Note that the helideck is also not included in the figure; despite the helideck consisting of beams and columns, most of these are constructed with aluminium parts.

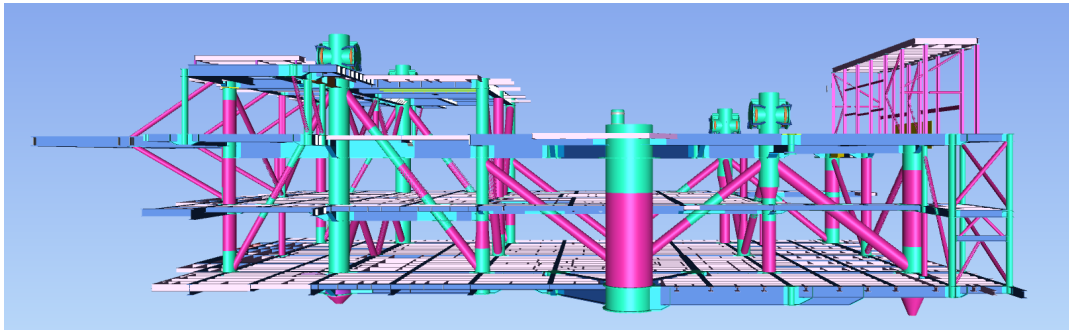


Figure 6.2: Steel scope of the considered topside

Of the steel shown in figure 6.2, some components are also excluded from this case study. Although the joints are still shown, they will not be considered for this research for reasons discussed in chapter 3. When decreasing the beams and columns, it is assumed that the joints decrease with the cross-sectional area reduction of the beams and columns. In reality, the plates of the joint could possibly also be reduced, leading to more economic and weight benefits, but this is not taken into account. Furthermore, only fully cylindrical columns and bracings are being assessed, while components such as cones and lifting cylindrical parts require different design calculations. Finally, plate girders are not considered for this case study. Although plate girders are much used in the considered topside, their design checks require a new design for each plate girder, which is not yet included in the models described in the previous chapter. Moreover, the research of STROBE has already proved that high-strength steel plate girders are beneficial for lengths typically seen on offshore topsides.

Part lists were generated for all the considered beams and columns using the traceability database of HSM Offshore Energy. These part lists contain information about lengths, diameters, thicknesses, cross-section types, and materials. The total weight of the considered beams is 359 tonnes, which is 29.6% lower than expected. This reduction can be explained by the exclusion of heavy plate girders, plate stiffeners, pipe supports, stairs beams, and other such components. The columns considered have a total weight of 143 tonnes, which is 44% lower than the total approximated column and bracing weight. This reduction can be explained by the exclusion of heavy column parts in the joints and lifting points. As a result, this case study can only affect 33.5% of the total topside steel weight and only 6.7% of the total platform weight.

This case study examines the potential benefits of using high-strength structural steel in the form of weight reduction, cost reduction, and embodied carbon savings. All three factors are linked to the reduction of cross-sectional area, which can be achieved by using high-strength steel. The mass reduction is proportional to the reduction of the area as the density and length of the components remain the same. Similarly, the embodied carbon savings are measured by the carbon equivalent per kg steel ($\text{kgCO}_2\text{e/kg}$), which is an almost identical value regardless of the material's yield strength during steel manufacturing, transport to shop, and fabrication of steel parts. However, no values of other stages, including offshore transport and installation, were found in the literature and it is challenging to make estimations about these stages. When assessing the embodied carbon savings, the percentage is proportional to the weight reduction. The cost reduction can be classified into two categories: material costs and welding costs. The reduction in material costs is directly related to the mass and type of material. The values described in Chapter 2 are used to estimate material costs. In contrast, estimating the reduction in welding costs is challenging as welding details vary in all components. A simplified estimation is made by calculating the circumference of each part and determining how much it is reduced when high-strength steel is used to determine the welding length reduction. For beams, welding cost reduction is equal to the welding length reduction because there is no significant difference in welding between S355 and S460 steel. For columns, the welding length decreases when using high-strength steel, but the welding speed of S690Q steel also decreases by approximately 30%, according to HSM. Table 6.1 shows an approximation of the costs per cubic meter of welding. For columns, it is assumed that V-welds with the plate thickness of a column are used to weld the columns. As discussed in the

previous chapter, the thickness of the column remains the same as other factors often limit the thickness, and the method used to assess columns, therefore, only decreases the diameter of the column. Comparing the welding costs per steel type gives an estimation of the welding cost reduction of the columns.

Table 6.1: Values used to estimate welding cost reduction for columns

Welding costs	S355/S460	S690
Welding speed	50 cc/h	35 cc/h
Assembly factor	2	2
Real speed	25 cc/h	17.5 cc/h
Salary	30 €/h	30 €/h
Overhead factor	3	3
Costs welder	90 €/h	90 €/h
Total welding costs	3.6 €/cc	5.14 €/cc

6.2. Case study: high-strength steel beams

All the standard HEA, HEB, and IPE beams are inventoried from the part lists with their corresponding length. The topside under consideration is composed of 2344 standard beams, excluding the plate girder beams. However, it is impossible to look at each beam individually and determine what type of support can be assumed. Hence, assumptions need to be made. To assess the most conservative situation, it is first assumed that all beams on the topside can be considered to be simply supported.

In order to evaluate all the beams, a numerical calculation, which is discussed in the previous chapter, of the ULS/SLS-ratio is performed for each beam. If this ratio is greater than 1, the maximum capacity is computed to determine if a smaller cross-section of high-strength steel can replace the cross-section of conventional steel. The results obtained are shown in Table 6.2, where the calculations are divided into different cross-sections encountered on the topside while assuming simply supported beams. It can be concluded that for all S355 H-beams higher than 240mm, a reduction in weight can be achieved. When all weight reductions are summed, a total weight reduction of 7.47% is achieved. This low percentage can partly be explained while of the 2344 beams, 1892 are deck stringers, contributing to 81% of the number of standard beams and 36% of the total weight. Unfortunately, in Chapter 4, it was already concluded that these deck stringers could not be replaced with smaller ones when simply supported would be considered. If a continuous beam assumption would only be applied for the deck stringers, the weight reduction would immediately increase to 11.24%, which is equal to 40 tonnes.

Table 6.2: Weight reductions caused by using S460 steel in topside beams (all beams assumed to be simply-supported)

Initial cross-section	Original weight S355M [kg]	Weight when replaced by smaller S460M cross-section [kg]	Weight reduction [%]	Welding length reduction [%]
HEA100	54	54	0.00%	0.00%
HEA180	156	156	0.00%	0.00%
HEA260	140	124	11.43%	7.87%
HEA300	21,603	19,286	10.73%	6.29%
HEA400	81,083	75,134	7.34%	3.42%
HEA600	82,389	77,069	6.46%	4.21%
HEA800	10,303	9,358	9.17%	7.24%
HEA1000	20,785	19,209	7.58%	6.32%
HEB160	165	165	0.00%	0.00%
HEB180	1,822	1,822	0.00%	0.00%
HEB200	451	451	0.00%	0.00%
HEB240	5,282	4,907	7.12%	6.60%
HEB300	3,615	3,189	11.76%	6.69%
IPE240	105,786	96,377	8.89%	6.79%
IPE270	21,662	21,662	0.00%	0.00%
IPE330	3,448	2,965	14.00%	7.70%
Total	358,743	331,928	7.47%	7.70%

The cost calculations took into account both the material costs and the estimated cost reduction due to welding. With regard to the material costs only, a 1.93% reduction was observed when all beams were assumed to be simply supported. This reduction can be explained by the fact that while the weight of the material decreases, the costs per kilogram slightly increase, resulting in only a small percentage reduction. On the other hand, the welding costs reduction is estimated by the reduction in weld length. The reduction in the weld length of all the beams combined resulted in a total weld reduction of 7.70%. It is difficult to determine the actual cost reduction by combining these percentages, as the welding costs depend on various welding details. However, welding is a labor-intensive and expensive fabrication process, and a reduction in weld length can result in significant cost savings. Therefore, the total cost reduction for beams will be higher than when only considering the material cost reduction. Would a continuous beam assumption be allowed for the deck stringers, the material cost reduction would increase to 6.34% and the reduction of welding cost would also further increase.

A secondary calculation was performed to determine if the results would vary significantly by implementing alternative support assumptions. For this calculation, each deck was manually assessed, and the connections marked with yellow in figure 6.3 were considered as simply supported beams, while the ones marked with red were assumed to be fixed connections. Despite this, Table 6.3 revealed that the results were almost identical and that the weight reduction only increases by 0.1%. This can be explained by the fact that the larger beams, which were typically marked as fixed beams, could already be replaced by a smaller cross-section for the simply supported assumption, resulting in no significant changes.

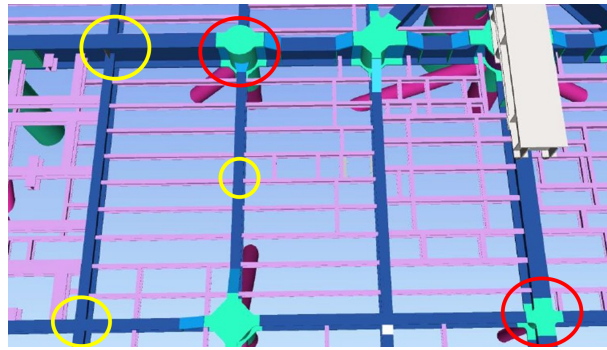


Figure 6.3: Type of assumed supports: simply supported: circled with yellow - fixed: circled with red

Table 6.3: Weight reductions caused by using S460 steel in topside beams (different support assumptions)

Initial cross-section	Original weight S355M [kg]	Weight when replaced by smaller S460M cross-section [kg]	Weight reduction [%]
HEA100	54	54	0.00%
HEA180	156	156	0.00%
HEA260	140	124	11.43%
HEA300	21,603	19,286	10.73%
HEA400	81,083	74,941	7.57%
HEA600	82,389	76,926	6.63%
HEA800	10,303	9,358	9.17%
HEA1000	20,785	19,209	7.58%
HEB160	165	165	0.00%
HEB180	1,822	1,822	0.00%
HEB200	451	451	0.00%
HEB240	5,282	4,907	7.12%
HEB300	3,615	3,189	11.76%
IPE240	105,786	96,377	8.89%
IPE270	21,662	21,662	0.00%
IPE330	3,448	2,965	14.00%
Total	358,743	331,593	7.57%

6.3. Case study: high-strength steel columns & bracings

The columns and bracings of the considered topside were assessed for their feasibility, as described in the previous chapter. For both the columns and the bracings, only axial compression was assumed and the effective length is assumed to be equal to the length of the columns. The buckling resistance force was first calculated for the same cross-section but with a higher yield strength, after which the cross-section was reduced until the same buckling resistance of an S355 member was found. Nevertheless, the topside contained two different columns and bracing types: hot-formed seamless tubular (TUS) and cold-formed welded tubular (TUW).

Both S460 and S690 steel plates can be used to make cold-formed welded tubulars. Table 6.4 shows the results of replacing all cold-formed (TUW) columns and bracings with either S460M or S690Q steel. The table compares the original material costs, welding costs, and the total weight of S355 columns and bracings with those of high-strength steel. The results show that high-strength steel can significantly reduce the weight of columns and bracings, especially when using S690 steel, which leads to a weight reduction of 42.14% and almost 30% in material cost reduction. Although the welding speed decreases for S690 steel, the welding cost reductions are almost equal to S460 steel, with a decrease of nearly 20%. This leads to significant overall cost reductions when applying S690. It is important to note that the D/t ratio was not checked, and if this ratio drops below approximately 20, the columns and bracings cannot be fabricated, while the material properties would be damaged. For S460 steel, both the preheating and D/t ratio would form less of a problem, and already stunning weight and material cost reductions of 20.91% and 16.85%, respectively, could be achieved. Additionally, the welding costs would even decrease by 20.68%.

Table 6.4: Weight and cost reduction for using S460M or S690Q for welded cold-formed tubular (axial loaded)

Welded cold-formed tubulars	S355M	S460M	S690Q
Material costs [€/t]	1350	1450	1620
Cold forming costs [€/t]	600	600	750
welded tubular costs [€/t]	1950	2050	2370
Total column & bracing mass [t]	101.83	80.54	58.92
Total column & bracing costs	€198,568.50	€165,107.00	€139,640.40
Weight reduction compared to S355M	-	-20.91%	-42.14%
Material cost reduction compared to S355M	-	-16.85%	-29.68%
Welding cost reduction compared to S355M	-	-20.68%	-18.08%

According to HSM, seamless columns and bracings are only widely available in S355 or S460 but not in S690. Therefore, S690 is not included in assessing seamless hot-formed columns and bracings. Table 6.5 shows the comparison between S355M and S460M hot-formed tubulars. Using high-strength steel for these columns results in a weight reduction of 18.02%, while material cost reductions of 6.54% can be achieved. Additionally, the welding cost reduction is again very high, at 18.69%, which could lead to significant total cost reductions.

Table 6.5: Weight and cost reduction for using S460M or S690Q for hot-formed tubulars (axial loaded)

Hot-formed tubulars	S355M	S460M
Tubular section costs [€/t]	3000	3420
Total column & bracing mass [t]	41.51	34.03
Total column & bracing costs	€124,530.00	€116,382.60
Weight reduction compared to S355M	-	-18.02%
Material cost reduction compared to S355M	-	-6.54%
Welding cost reduction compared to S355M	-	-18.69%

Finally, table 6.6 presents the weight, material costs and welding cost reductions when both types of columns and bracings are combined. For the S690 comparison, it is assumed that S460 hot-formed columns would be applied to achieve the highest possible benefits. In total, 20.07% of weight reductions could be achieved when only applying S460 for both types of columns and bracings, while a material cost reduction of 12.88% could be achieved and a welding cost reduction of 20.3%. When using S690 for cold-formed columns and bracings, and S460 for hot-formed columns and bracings, a weight reduction of 35.15% was achieved in combination with a material cost reduction of 20.76% and a welding cost reduction of 17.26%. As previously discussed, the carbon savings are assumed to be equal to the weight reduction. Thus, columns and bracings show high potential to be replaced with high-strength steel for weight reduction, cost reduction and carbon savings.

Table 6.6: Total weight and cost reduction for using S460M or S690Q for axial loaded columns and bracings

Columns & Bracings	S355M	S460M	S690Q
Mass TUW [t]	101.83	80.54	58.92
Costs TUW	€198,568.50	€165,107.00	€139,640.40
Mass TUS [t]	41.51	34.03	34.03
Costs TUS	€124,530.00	€116,382.60	€116,382.60
Total mass [t]	134.34	114.57	92.95
Total costs	€323,098.50	€281,489.60	€256,023.00
Weight reduction	-	-20.07%	-35.15%
Material cost reduction	-	-12.88%	-20.76%
Welding cost reduction	-	-20.30%	-17.26%

6.4. Conclusions of high-strength steel in a case topside

The case study performed in this chapter has considered a topside with a total steel weight of 1500 tonnes. Of these 1500 tonnes, 503 tonnes of steel beams, columns, and bracings were assessed. After performing the case study, it can be concluded that the weight, embodied carbon and costs can be reduced when high-strength steel is utilized for both the beams and the columns and bracings. If S460M is used for the beams and both types of columns, a total weight reduction of the considered components of 11% is realized. As embodied carbon savings are assumed proportional to the mass reduction, the same value was found for the embodied carbon savings. Material cost reductions of 7% can be achieved, while the total welding length can also be reduced by 7%. When this percentage of weight reduction is compared with the total steel weight of the topside, 3% of weight reduction can be found, while this leads to 1.56% of the total weight reduction of a topside.

In the case of using S690 for the cold-rolled columns and bracings and S460 for the beams and hot-rolled columns and bracings, a weight and embodied carbon savings of 15% were achieved when the beams and columns were combined. This weight reduction equals 68.54 tonnes, and for the entire steel weight, this amount equals 5% of the steel scope, while it equals 2% of the total topside weight. The total material costs, in this case, would be decreased by 10%, while the welding length would be reduced by 13%.

These results show that in all cases, weight reduction, cost reduction and embodied carbon savings are achievable when using high-strength steel. The achievable benefits are somewhat lower for beams, which can be explained by the deflection, which governs the weight reduction in many beams and the higher costs for S460 steel at the same time. For columns, the reductions are much higher. As this case study did not include all components of a topside, it is expected that high-strength steel could further decrease the weight, costs and embodied carbon. Furthermore, this case study did not include further benefits such as easier erection of parts, installation, transport, etc. Therefore, the overall potential of utilizing high-strength steel is even expected to be higher than concluded in this chapter.

7

Conclusions & recommendations

This chapter concludes the research that has been performed and described in the previous chapters. The conclusions found within this research are described in section 7.1. Furthermore, section 7.2 discusses the limitations of the constructed screening tools, which were used to derive the conclusions. Finally, section 7.3 provides some recommendations for the industry and section 7.4 gives recommendations for further research.

7.1. Conclusions

The popularity of high-strength steel in steel structure design has increased in recent decades as a way to reduce the climate footprint of steel structures. Still, it was unknown if benefits could be achieved for offshore topsides because of deflection and stability problems arising when using high-strength steel. This research aimed to answer the question: *is it feasible to use high-strength structural steel in offshore topsides, and how can the use of high-strength steel in topside design be optimised?* It was concluded that high-strength steel is feasible for topsides in almost all considered cases and can reduce weight, costs and embodied carbon. The design of topsides can be optimized by considering S460M steel for strength-governing beams and seamless tubular columns and using S690Q only for welded tubular columns. Two simple-to-use screening tools have been constructed for engineers to assess the feasibility of high-strength steel beams and columns in an early design phase. These screening tools can easily be expanded when more detailed information is available.

The research started with a study that was conducted to compare seven existing topsides with the literature, aiming to summarise their key figures, typical lengths, cross-section type, diameter, and thicknesses. It was concluded that, among all structural components in a topside, only the primary and secondary beams, columns, and bracings were attractive for initial research. This is mainly because other components contribute less to the overall structural weight and are often governed by factors other than strength.

The first screening tool for beams, uses the ULS/SLS-ratio to determine whether a beam is governed by deflection or strength. Using high-strength steel may be advantageous if the ULS/SLS-ratio is greater than 1. Further investigation could lead to weight and cost savings, as well as embodied carbon savings. Two key conclusions were drawn concerning the ULS/SLS-ratio. First, the ULS/SLS-ratio was found to be independent of the applied load on a beam, resulting in a transition length where the beam goes from strength- to deflection-governing, that was dependent only on the beam's dimensions, material, and support type. This makes it possible to assess existing or preliminary deck layouts for their feasibility to high-strength steel without knowing any load that acts on the deck. Second, the support type has a significant impact on this transition length. Therefore, the kind of support assumption that could be used for a specific beam must be known, even though the loads do not need to be known. This was carefully evaluated for all example beams.

After assessing typical beams like deck stringers, deck beams, main beams, and cantilever beams, it

was concluded that deck stringers could benefit from using high-strength steel only in certain cases or not at all. The other three beams showed that high-strength steel could replace a beam with a smaller one for most typical lengths and cross-sections, resulting in weight and cost reductions and embodied carbon savings. Nevertheless, the reductions are relatively small, especially the cost reductions, because the material costs increase despite the cross-section only becoming slightly smaller.

The second screening tool was constructed for columns and bracings, which were assessed by assuming axially loaded columns and numerically adjusting the cross-section of a column such that the buckling resistance of a high-strength steel column matches the buckling resistance of a conventional S355 steel column. The assessed slenderness ratio for typical topside columns proved relatively stocky, resulting in high-cost reductions, weight reductions and embodied carbon savings when using high-strength steel columns.

A study was conducted to assess the impact of using high-strength steel in primary and secondary beams, columns, and bracings in an entire integrated topside. The study found that the utilization of high-strength steel in these three components resulted in weight and cost reductions, as well as embodied carbon savings. However, the reduction in weight and cost is minimal for beams, as many beams cannot be replaced by high-strength steel because of the deflection limits. Columns and bracings contributed significantly to a topside's weight and cost reduction. Overall, the study found that replacing beams and columns with high-strength steel can only lead to a maximum weight reduction of 4.57% for the entire topside steel weight. Yet, for the considered components, the weight decreased by 15%, the material costs decreased by 10%, the welding length by 13%, and the embodied carbon savings by 15%.

Despite the modest reductions in the overall steel weight of the case topside, savings were achieved in terms of overall weight, costs, and embodied carbon. This was achieved by assessing only 33.5% of the steel weight of the case topside. Including all components in the assessment for high-strength steel can further increase these savings. Thus, high-strength steel can also play a part in reducing the carbon footprint of offshore platforms and will hopefully gain popularity in this industry as well. Moreover, the costs and weight would decrease simultaneously. Therefore, there is no need to wait to implement high-strength steel in offshore topsides.

7.2. Limitations

Two screening tools were developed for this research to assess the feasibility of using high-strength steel in the design of offshore topsides. Other engineers can use these screening tools to evaluate the feasibility of preliminary design scenarios, but the screening tools have some limitations.

Both screening methods assume full capacity, meaning the initial S355 beams and columns are believed to be loaded to their maximum ultimate capacity. In reality, designers usually incorporate some reserve capacity to ensure safety. When considering hot-rolled beams, if a beam was designed with some reserve capacity, a strength-governing beam experiences a lower design load. This lower load can result in less required minimum area moment of inertia and section modulus. Consequently, this can lead to smaller beams of high-strength steel compared to what was previously thought. This assumption has a lesser impact on plate girders and columns, as they are designed with variable dimensions instead of in steps of different heights like hot-rolled beams. Additionally, support assumptions are required for beams as equations are needed for the bending moment and deflection as a function of the beam length. Assuming simply-supported, continuous or fixed significantly affects the results, and careful thought should be given when considering a particular support type.

For columns, no horizontal forces are included, as it is assumed that the vertical forces are much higher. In reality, the structure should also be checked as to how it reacts in a frame. Moreover, usually, columns can have a higher thickness at the joints. For the constructed screening tools, only the column between the joints is considered with a constant thickness. The joint itself can probably also become smaller when applying high-strength steel, but at the joints, other considerations, such as punching shear, can govern the design of the column. Therefore, these short parts of the columns

are not assessed with this method. Nevertheless, if these column parts in the joint could decrease, the diamond plates within a joint could possibly also decrease, resulting in additional welding, costs and material reduction.

Another assumption made is that the loading and the cross-sectional area remain the same when changing a component to high-strength steel for both the beams and columns. When a component becomes lighter because of the application of high-strength steel, the loading would also decrease. For beams, the self-weight would decrease, while for columns, the vertical load would decrease because of the weight reduction of the beams and columns on top of the column. This effect is not included in the models and could lead to more benefits of using high-strength steel. Nevertheless, the self-weight is relatively low for beams compared to the deck loading. At the same time, the reduced vertical loading is likely more significant for columns, especially the columns at the bottom of the topside. Changing the cross-sectional area over the length of the beam could reduce the deflections, making a beam more strength-governing and could increase the potential of using high-strength steel. For columns, changing the diameter or thickness over length can also change the buckling characteristics of a column and could lead to more beneficial results.

The calculations performed did not take into consideration the effects of vibrations, dynamics, and fatigue on the structure. These are critical factors that can significantly impact the behaviour and performance of the structure over time. When the mass of a structure is reduced by applying high-strength steel, the vibrations, dynamics, and fatigue can become more severe and even start governing specific structural components. Therefore, it is imperative to consider these factors in the design as it could lead to fewer benefits of using high-strength steel.

Finally, there was limited information available to perform cost and embodied carbon calculations. For the cost analysis, only material and welding costs were taken into consideration. The material prices were obtained from a single steel manufacturer in September 2023. However, prices change frequently and it is possible that other manufacturers may offer more affordable materials, or that prices may decrease over time when demand increases. The welding costs were estimated by calculating the reduction in welding length, as detailed information about all welding details was not available. If welding details were included, different results could be obtained. Regarding embodied carbon savings, it was assumed that it was proportional to the mass. However, offshore transport and lifting operations should also be taken into account. It could be the case that the embodied carbon savings would increase for high-strength steel, but it is expected that the manufacturing of steel is the highest contributor. Therefore, less mass results in more embodied carbon savings.

7.3. Recommendations for the industry

The research conducted has produced some insightful conclusions that have led to two specific recommendations for the industry:

First, it is advised to consider high-strength steel in the earliest design stage. When drawing the preliminary deck layout, the feasibility of high-strength steel can already be assessed with the screening tools within this report. It is especially advised to start implementing S460M beams for beams that are strength-governing and for seamless tubular columns while using S690Q steel for cold-formed tubulars. Implementing this in the topside design will result in cost and weight reduction while reducing the climate footprint of a topside at the same time. Furthermore, it is advised to start implementing hybrid plate girders instead of S355 plate girders.

Secondly, it was challenging to find cost estimates for materials and welding in the literature and to better understand this, it is recommended that companies develop more sophisticated cost models that consider factors such as material properties, welding techniques, and other relevant parameters. By integrating these cost models into the screening tools, companies can more accurately estimate the cost savings associated with using high-strength steel. Ideally, these models should be able to calculate both material and welding costs as a function of the total weight and the material's yield stress.

7.4. Recommendations for further research

Additionally, to the recommendations for the industry, the research conducted has produced some insightful conclusions that have led to three recommendations for further research:

To ensure the structural integrity and safety of a topside, it is highly recommended to investigate the effects of high-strength steel on its joints. In order to achieve this, it is suggested that a detailed finite element analysis be performed on the joints. This analysis will provide answers to important questions, such as whether the thicknesses of diamond plates and columns can be reduced in the joint. Additionally, it can help determine what type of support conditions can be assumed in different situations. By conducting this analysis, a better understanding of the behaviour and performance of the joints made of high-strength steel can be gained. This can enable engineers to make more informed decisions regarding the topside's design and gives more insight into how to model the joints within the screening tools constructed.

The research study primarily concentrated on the construction phase of a topside. The study found that using high-strength steel in the construction phase of a topside could lead to cost savings and a reduction in embodied carbon. However, it is recommended that further research should be conducted to determine the effect of utilizing high-strength steel on the costs and embodied carbon savings within other stages of topside design. For instance, it would be interesting to examine the impact of weight reduction on offshore transport costs and carbon savings. If the weight of the topside could be reduced, this could potentially reduce the amount of fuel needed to transport it, thus lowering the carbon footprint. Additionally, it would be worthwhile to investigate the impact of weight reduction on lifting situations. If the topside is lighter, it may be easier and more cost-effective to lift it into place, which could also result in carbon savings. Therefore, further research in these areas could provide valuable insights into the potential benefits of using high-strength steel in topside design.

To optimize the performance of an offshore structure, it is essential to conduct a detailed analysis of the impact of weight reduction on various aspects, including vibrations, fatigue, and dynamics. This analysis can provide valuable insights into potential risks and challenges that may arise due to the changes in the structure's characteristics. Moreover, it is worth exploring how much the changes in the topside weight can impact the jacket design, as this can influence the offshore platform's overall costs and carbon savings. By conducting a comprehensive assessment of these factors, it is possible to develop an optimized design that can withstand the harsh offshore environment and operate efficiently over an extended period.

References

- [1] Terence Bell. *What are the different types of steel?* Jan. 2019. URL: <https://www.thoughtco.com/steel-grades-2340174>.
- [2] Qiang Yue et al. "Analysis of iron and steel production paths on the energy demand and carbon emission in China's iron and steel industry". In: *Environment, Development and Sustainability* (2022). ISSN: 15732975. DOI: 10.1007/s10668-022-02234-5.
- [3] European Union. *EU climate targets: how to decarbonise the steel industry*. 2022. URL: https://joint-research-centre.ec.europa.eu/jrc-news/eu-climate-targets-how-decarbonise-steel-industry-2022-06-15_en.
- [4] Mar. 2020. URL: <https://www.tatasteeleurope.com/construction/blogs-news/blogs/blog/high-strength-steel-in-construction>.
- [5] W Pors, A M Gresnigt, and Hans van Wortel. *VM125 - constructiestaalsoorten met Hoge Sterkte*. 2008. URL: <https://www.scribd.com/document/189824361/VM125-Constructiestaalsoorten-Met-Hoge-Sterkte>.
- [6] Michael Sansom and R. Mark Lawson. *WP 5: Life cycle assessment of comparative conventional strength and HSS designs*. May 2021. URL: <https://steel-sci.com/assets/downloads/reports/STROBE%20D5-1%20Weight,%20cost%20and%20carbon%20comparisons.pdf>.
- [7] Gert-Jan Smits. *Head of production HSM Offshore Energy*. Aug. 2023.
- [8] Hardy Mohrbacher. *Meeting modern engineering challenges*. Mar. 2020. URL: <https://www.imoa.info/molybdenum-media-centre/blog/blog-details.php?objectID=578&lang=en>.
- [9] Directorate-General for Research et al. *Optimal use of high strength steel grades within Bridge (OPTIBRI)*. 2019. URL: <https://op.europa.eu/en/publication-detail/-/publication/d8bd0ac1-4479-11e9-a8ed-01aa75ed71a1/language-en/format-PDF/source-281206476>.
- [10] Sérgio Nascimento, José J. Oliveira Pedro, and André Biscaya. "Flange-induced buckling of plate girders of high strength steel". In: *Thin-Walled Structures* 159 (2021), p. 106974. DOI: 10.1016/j.tws.2020.106974.
- [11] Y. Kurobane et al. *CIDECT 9: Design guide for structural hollow section column connections*. TÜV-Verlag, 2004.
- [12] Hoang Van Long et al. "Field of application of high strength steel circular tubes for steel and composite columns from an economic point of view". In: *Journal of Constructional Steel Research* 67.6 (2011), pp. 1001–1021. DOI: 10.1016/j.jcsr.2011.01.008.
- [13] Han Fang, Tak-Ming Chan, and Ben Young. *Structural performance of cold-formed high strength steel tubular columns*. Oct. 2018. URL: <https://www.sciencedirect.com/science/article/pii/S0141029618320327?via%3Dihub>.
- [14] Xiaoyi Lan et al. *The continuous strength method for the design of high strength steel tubular sections in compression*. Feb. 2018. URL: <https://www.sciencedirect.com/science/article/pii/S0141029617324057?via%3Dihub>.
- [15] Subrata Kumar Chakrabarti. *Handbook of Offshore Engineering*. Elsevier, 2005.
- [16] Dániel Honfi. "Design for Serviceability - A probabilistic approach". PhD thesis. Jan. 2014, p. 244. ISBN: 9789197954372. DOI: 10.13140/RG.2.1.4732.1361.
- [17] Chrysanthos Maraveas, Zacharias C. Fasoulakis, and Konstantinos Daniel Tsavdaridis. "Mechanical properties of high and very high steel at elevated temperatures and after cooling down". In: *Fire Science Reviews* 6.1 (2017). DOI: 10.1186/s40038-017-0017-6.

- [18] N.T. Switzner et al. *Influence of line pipe steel microstructure on NDE yield strength predictive capabilities*. Feb. 2020.
- [19] Falko Schröter and Ronny Willms. "Welding and fatigue in high performance steel". In: (2006).
- [20] Nancy Baddoo and Anqi Chen. *High Strength Steel Design and execution guide*. Steel Construction Institute, 2020.
- [21] Gerhard Sedlacek and Christian Müller. *High strength steels in steel construction*. 1995. URL: https://niobium.tech/-/media/niobiumtech/attachments-biblioteca-tecnica/nt_high-strength-steels-in-steel-construction.pdf.
- [22] Ana M. Girão Coelho, Frans S.K. Bijlaard, and Henk Kolstein. "Experimental behaviour of high-strength steel web shear panels". In: *Engineering Structures* 31.7 (2009), pp. 1543–1555. ISSN: 0141-0296. DOI: <https://doi.org/10.1016/j.engstruct.2009.02.023>. URL: <https://www.sciencedirect.com/science/article/pii/S014102960900087X>.
- [23] J. Wang et al. "Flexural behaviour of hot-finished high strength steel square and rectangular hollow sections". In: *Journal of Constructional Steel Research* 121 (2016), pp. 97–109. ISSN: 0143-974X. DOI: <https://doi.org/10.1016/j.jcsr.2016.01.017>. URL: <https://www.sciencedirect.com/science/article/pii/S0143974X16300177>.
- [24] Vol. EN10025-4_2019. 2019.
- [25] Vol. EN10025-3_2019. 2019.
- [26] European Commission et al. *Modern plastic design for steel structures*. Publications Office, 2010. DOI: [doi/10.2777/91747](https://doi.org/10.2777/91747).
- [27] Anders Sumuelsson and Falko Schröter. *Production processes, mechanical and chemical properties ... - dillinger*. n.d. URL: https://www.dillinger.de/imperia/md/content/dillinger/publikationen/stahlbau/technischeliteratur/dh_production_processes.pdf.
- [28] Helen Bartsch et al. "Experimental and numerical investigations on the rotation capacity of high strength steel beams". In: *ce/papers* 4.2–4 (2021), pp. 1630–1636. DOI: 10.1002/cepa.1466.
- [29] Helen Bartsch et al. "On the plastic design of high strength steel beams". In: *Steel Construction* 14.4 (2021), pp. 222–235. DOI: 10.1002/stco.202100017.
- [30] Trayana Tankova et al. "Lateral-torsional buckling of high strength steel beams: Experimental resistance". In: *Thin-Walled Structures* 164 (2021), p. 107913. DOI: 10.1016/j.tws.2021.107913.
- [31] Iván Negrin, Moacir Kripka, and Víctor Yepes. "Design optimization of welded steel plate girders configured as a hybrid structure". In: *Journal of Constructional Steel Research* 211 (2023), p. 108131. DOI: 10.1016/j.jcsr.2023.108131.
- [32] Trayana Tankova, Luís Simões da Silva, and Filipe Rodrigues. "Stability design of high strength steel beams". In: *ce/papers* 4.2–4 (2021), pp. 1624–1629. DOI: 10.1002/cepa.1465.
- [33] Jia-Lin Ma, Tak-Ming Chan, and Ben Young. "Cold-formed high strength steel tubular beam-columns". In: *Engineering Structures* 230 (2021), p. 111618. DOI: 10.1016/j.engstruct.2020.111618.
- [34] Fatemeh Javidan et al. "Application of high strength and ultra-high strength steel tubes in long hybrid compressive members: Experimental and Numerical Investigation". In: *Thin-Walled Structures* 102 (2016), pp. 273–285. DOI: 10.1016/j.tws.2016.02.002.
- [35] Joshua Omajene, Jukka Martikainen, and Paul Kah. "Weldability Of Thermo-Mechanically Rolled Steels Used In Oil And Gas Offshore Structures". In: *The International Journal Of Engineering And Science (IJES)* 3.5 (May 2014), pp. 62–69.
- [36] Louise Davis. *Highlighting the advantages of TMCP steel plates for the construction of storage tanks*. July 2017. URL: <https://www.engineerlive.com/content/thermomechanical-tank-technology>.
- [37] Richard Stroetmann. "Eurosteel 2011". In: *Eurosteel 2011: 6th european conference on steel and composite structures: Research, design, construction: August 31, September 2, 2011, Budapest, Hungary*. ECCS, 2011.

- [38] Jeroen Bodt. *Welding consultant at HSM Offshore Energy*. Dec. 2023.
- [39] Abílio M.P. de Jesus et al. "A comparison of the fatigue behavior between S355 and S690 Steel grades". In: *Journal of Constructional Steel Research* 79 (2012), pp. 140–150. DOI: 10.1016/j.jcsr.2012.07.021.
- [40] D. V. Reddy and Swamidas A S J. *Essentials of offshore structures: Framed and gravity platforms*. CRC Press, Taylor & Francis Group, 2014.
- [41] Meenu Krishnan. *What are different steel sections used for construction?* Feb. 2023. URL: <https://www.eigenplus.com/what-are-different-steel-sections-used-for-construction/>.
- [42] Feb. 2020. URL: <https://www.offshore-technology.com/projects/britannia/>.
- [43] ESDEP European Steel Design Education Program. *Lecture Series, Offshore Structures, Lecture 15A: Structural systems: Offshore*. 1993. URL: <http://fgg-web.fgg.uni-lj.si/~pmoze/ESDEP/master/wg15a/toc.htm>.
- [44] A.J.T Buijsse. "Platform removal in the North Sea: Concept design of a single lift vessel". PhD thesis. Eindhoven University of Technology, 2005, p. 4.
- [45] Jaco Lemmerzaal. *Director HSM Offshore Energy*. Aug. 2023.
- [46] EurocodeApplied team. *Table of properties for IPE, hea, Heb, hem, UB, UC, UBP profiles - eurocode 3*. 2005. URL: <https://eurocodeapplied.com/design/en1993/ipe-hea-heb-hem-design-properties>.
- [47] Los Angeles Public Library. URL: <https://tessa2.lapl.org/digital/collection/photos/id/101274>.
- [48] Bruce Wells. *Offshore drilling history*. Apr. 2023. URL: <https://aoghs.org/offshore-history/offshore-oil-history/>.
- [49] J.H Vugts. *Handbook of bottom founded offshore structures*. Vol. 1. Eburon, 2013.
- [50] Clyde W. Burleson. *Deep Challenge!: The true epic story of our quest for energy beneath the sea: A trade book*. Gulf, 1999.
- [51] Yoana Cholteeva. *Deepwater exploration: What it takes to drill really really deep*. Apr. 2020. URL: <https://www.offshore-technology.com/features/deepwater-exploration-what-it-takes-to-drill-really-really-deep/>.
- [52] Sean van Elden et al. "Offshore oil and gas platforms as novel ecosystems: A global perspective". In: *Frontiers in Marine Science* 6 (2019). DOI: 10.3389/fmars.2019.00548.
- [53] July 2023. URL: <https://www.rmt.org.uk/news/rmt-marks-35th-anniversary-of-the-piper-alpha-disaster/>.
- [54] UN. *The Paris Agreement*. URL: <https://unfccc.int/process-and-meetings/the-paris-agreement>.
- [55] unfccc. *COP27 Reaches Breakthrough Agreement on New "Loss and Damage" Fund for Vulnerable Countries*. 2022. URL: <https://unfccc.int/news/cop27-reaches-breakthrough-agreement-on-new-loss-and-damage-fund-for-vulnerable-countries> (visited on 12/24/2020).
- [56] Ministerie van Algemene Zaken. *Nederland Maakt ambitie wind op Zee Bekend: 70 gigawatt in 2050*. Sept. 2022. URL: <https://www.rijksoverheid.nl/actueel/nieuws/2022/09/16/nederland-maakt-ambitie-wind-op-zee-bekend-70-gigawatt-in-2050>.
- [57] S. Robak and R.M. Raczowski. "Substations for offshore wind farms: a review from the perspective of the needs of the Polish wind energy sector". In: *Bulletin of the Polish Academy of Sciences Technical Sciences* 66.No 4 (2018), pp. 517–528. URL: <http://journals.pan.pl/Content/108424/PDF/17-00902-kolor.pdf>.
- [58] H. Díaz and C. Guedes Soares. "Review of the current status, technology and future trends of offshore wind farms". In: *Ocean Engineering* 209 (2020), p. 107381. DOI: 10.1016/j.oceaneng.2020.107381.

- [59] Mike Schuler. *World's deepest offshore wind turbine foundation installed in Scotland*. Apr. 2023. URL: <https://gcaptain.com/worlds-deepest-offshore-wind-turbine-foundation-installed-in-scotland/#:~:text=Scotland%E2%80%99s%20largest%20offshore%20wind%20farm,off%20the%20coast%20of%20Angus..>
- [60] Chiemela Victor Amaechi et al. "Review on fixed and floating offshore structures. part I: Types of platforms with some applications". In: *Journal of Marine Science and Engineering* 10.8 (Aug. 2022), p. 1074. DOI: 10.3390/jmse10081074.
- [61] Steve A Will. *Compliant towers: The next generation | offshore*. July 1999. URL: <https://www.offshore-mag.com/business-briefs/equipment-engineering/article/16757589/compliant-towers-the-next-generation>.
- [62] Huixing Meng, Leïla Kloul, and Antoine Rauzy. "Production availability analysis of floating production storage and offloading (FPSO) systems". In: *Applied Ocean Research* 74 (2018), pp. 117–126. DOI: 10.1016/j.apor.2018.02.026.
- [63] J N Sørensen, G C Larsen, and A Cazin-Bourguignon. "Production and cost assessment of offshore wind power in the North Sea". In: *Journal of Physics: Conference Series* 1934.1 (May 2021), p. 012019. DOI: 10.1088/1742-6596/1934/1/012019.
- [64] Maria Clara Martins et al. "Offshore energy structures in the North Sea: Past, present and future". In: *Marine Policy* 152 (Mar. 2023), p. 105629. DOI: 10.1016/j.marpol.2023.105629.

A

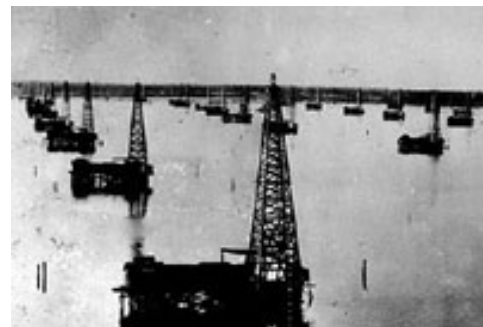
Additional information about the offshore industry

This appendix will describe some additional background information about offshore engineering and consists of two sections. The first section, section A.1, briefly discusses the fascinating history of the offshore industry and its future perspective. The second section, section A.2, describes the different types of offshore platforms, discusses their presence in the world's seas and oceans and explains why this research only focuses on the southern North Sea.

A.1. Short history and future perspective of the offshore industry



(a) Piers into the ocean at Summerland in 1901 [47]



(b) Platforms on Lake Caddo in 1911 [48]

Figure A.1: Offshore piers and on-lake platforms

The offshore industry is categorized as a relatively new industry. Offshore exploration started at the end of the 19th century when the demand for oil and gas rose. In different locations worldwide, such as California and the Caspian Sea, companies started building wooden piers into the oceans and seas to support wooden derricks [15]. An example of these piers in Summerland, California, is shown in figure A.1a. At the same time, oil was produced in multiple inland lakes, initially in North America, for example, Lake Caddo, shown in figure A.1b. Soon, other countries, such as Lake Maracaibo in Venezuela, followed these methods. In these lakes, simple wooden platforms on initial wooden piles were constructed to support all drilling equipment. However, in Lake Maracaibo, a teredo worm worked up the piles from the inside, and after a few months, the platform collapsed, leading to new material usage on Lake Maracaibo, such as concrete piles from 1927 and steel piles from 1934 onwards [49].

The real start of the offshore age coincides with the construction of a wooden offshore platform with steel piles by Kerr-McGee in 1947, shown in figure A.2. The wooden platform only supported the drilling derrick, and a floating vessel supported the other equipment [50]. In the following decades, the offshore oil and gas industries expanded and grew rapidly, and many companies invested in new offshore projects

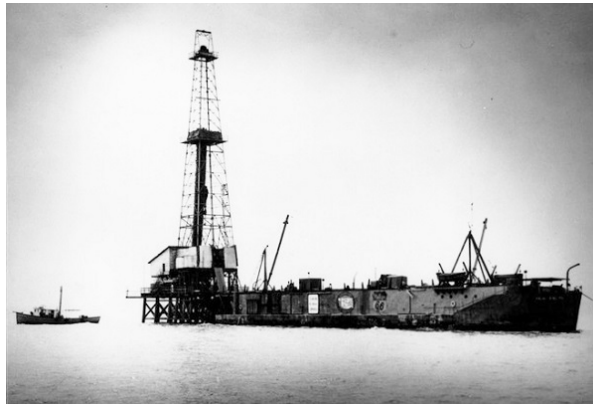


Figure A.2: Kerr-McGee's Kermac Rig No.16 is considered to be the world's first offshore platform, located 10 miles from the shore [48].

and research and development. At first, the pioneering offshore developments were focused around the Gulf of Mexico, but when the Groningen gas field in the Netherlands was discovered in 1959, European countries also developed an interest in the offshore industry. However, the North Sea differs considerably from the Gulf of Mexico in weather conditions and water depths; therefore, the North Sea quickly became another powerhouse for new offshore developments [49].

The first bottom-founded offshore structures were comparable with the Kerr-McGee structure but were optimized. The steel piles were replaced with a framed steel structure, giving rise to the jacket-type structures; this is still the most installed offshore structure type today [49]. As companies tried to expand their drilling to deeper waters each year, bottom-founded structures became very expensive to construct. Alternatives for the jackets, such as the guyed tower, the compliant tower and gravity-based structures, arose, but as the water depth kept increasing, floating offshore structures were designed, with the first being a converted semi-submersible on the Argyle field in the North Sea in 1975 [15]. Nowadays, water depths of around 3500m can be reached [51], emphasizing the huge developments this industry has experienced in the last century. There are now more than 12,000 offshore structures globally installed [52], but this number is rapidly rising.



Figure A.3: The world's biggest oil disaster: Piper Alpha [53]

The offshore industry is constantly changing. Some severe accidents in the 20th century, such as the Piper Alpha disaster on the 6th of July 1988 (figure A.3), costing the lives of 167 men [53], triggered the world to be very careful with offshore structures. Rules and standards were created worldwide, and nowadays, all offshore structures must be designed according to the proper standards [15]. Moreover, while the public eye is heavily focussing on the problem of climate change, the offshore industry needs to adapt in the future. In 2015, The Paris Agreement was signed by 196 countries with the primary goal to hold [54] "the increase in the global average temperature to well below 2°C above pre-industrial

levels” and pursue efforts ”to limit the temperature increase to 1.5°C above pre-industrial levels.” More recently, in November 2022, the world nations again agreed that global warming should be limited to 1.5°C, which would require a reduction of greenhouse gas emissions of 45% within eight years only [55]. This triggers a massive energy transition from the conventional oil and gas industry to the renewable energy industry, such as the wind industry. In the Netherlands alone, 75% of the country’s energy should be produced by wind farms within seven years, with most of this energy produced by offshore wind turbines [56]; a huge undertaking in which multiple offshore companies are already actively participating.

Just as with oil at the beginning of the 20th century, offshore companies started pioneering wind energy in shallow waters at the end of the 20th century. The world’s first offshore wind farm, Vindeby, was built in 1991 in Denmark in waters with a depth of only 4 metres. During this first stage in the wind energy industry, offshore substations were not yet required, while the wind turbines were directly connected to an onshore installation [57]. However, the wind industry has been rapidly growing for the past two decades, from a total installed capacity of 0.06GW at the beginning of the century to 36GW at the beginning of 2020, a total rise of 412%. The industry is expected to grow to a 154 GW installed capacity in 2030 [58]. As with oil, companies are looking to expand their wind industry to deeper waters, and nowadays, the maximum reached water depth is 58.6 metres [59]. This water depth expansion often results in longer distances from shore, introducing the need for an offshore substation from which the electricity can be transported to shore. An offshore substation is comparable with an oil or gas platform, except for the equipment. While water depths are not yet deep enough to make floating offshore platforms economically attractive, the Kerr McGee concept of a bottom-founded platform is still an essential part of the offshore industry 80 years later. Moreover, as new industries such as offshore hydrogen, tidal and wave energy are rising in shallow waters, bottom-founded offshore platforms are expected to remain a crucial working horse in the industry. Therefore, it remains of great importance to improve these structures by, for example, reducing the carbon dioxide emissions and weight. High-strength steel could play an essential role in this optimization.

A.2. Type of offshore platforms and North Sea perspective

An offshore platform usually consists of a substructure and a superstructure. The superstructure, or topside, is designed for the specific function of the platform, while the substructure’s goal is to withstand all environmental loads and give carrying capacity for the superstructure. Because the design of the substructure heavily depends on the water-depth, bathymetry and location, classification of offshore platforms is typically performed by looking at the substructure type.

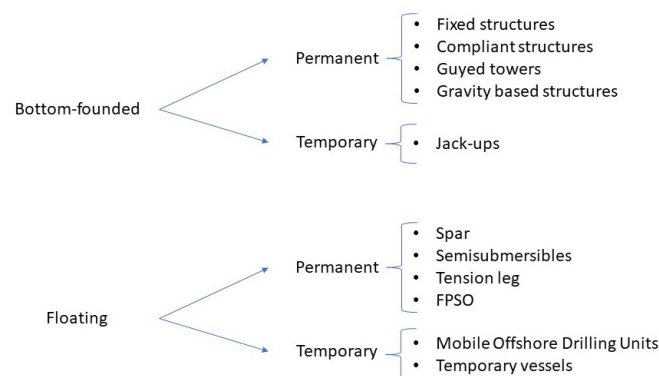


Figure A.4: Classification of offshore structures

There are multiple ways to categorize different offshore structures. First, structures can be distinguished by the way they resist direct actions. Secondly, structures can be distinguished by the duration of their stay at one location and finally between the types of foundations [49]. Figure A.4 shows how offshore structures can be classified. A structure can be considered bottom-founded when the actions acting on the structures are entirely or predominantly transferred into the seabed. However, floating structures transfer actions through buoyancy or (partly) mooring lines. Furthermore, the structure can be assigned

a permanent or temporary structure. Permanent structures are often platforms which stay their entire lifetime at one location to perform a process. This process can be oil or gas related or, for example, be an offshore substation. However, some floating platforms can be considered permanent but can be moved during certain events, e.g., a floating platform when an iceberg is nearing or when a well has dried out. Temporary structures are structures which are only at location for a certain amount of time, for example, a drilling jack-up. Finally, offshore structures can be divided into different structure types. Most of the permanent structure types are shown in figure A.5 and these structures will shortly be explained in more detail. Temporary structures will not be discussed, while this research focuses on permanent platform types.

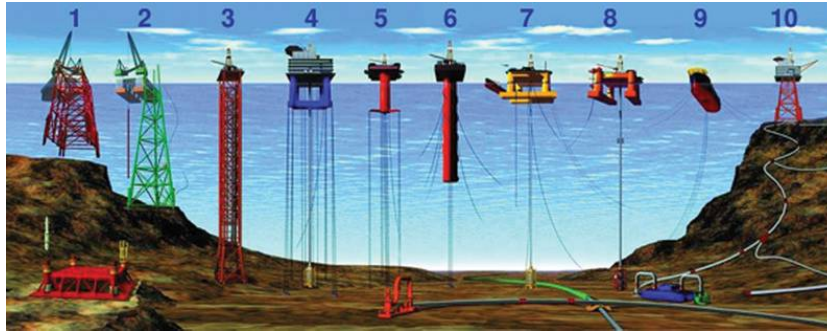


Figure A.5: Fixed structures (1,2,10), compliant tower (3), TLP (4,5), SPAR (6), Semisubmersible (7,8), FPSO (9)

Fixed structures are the most commonly used structures in the offshore industry [15]. These structures consist of jacket-type structures (most dominantly used), monotowers and free-standing and braced caissons. However, there are only a few actual monotower platforms and the caisson structures are only used in very shallow waters [49]. Therefore, in this report, fixed structures will, by definition, refer to jacket structures. Jacket structures consist mainly of tubular members, which are connected in frames. Usually, a jacket consists of four to eight legs placed at an angle to improve its stability performance. Piles are hammered into the seabed to fix the structure to the seabed. Actions acting on the structure are transferred through the piles into the seabed. Jackets can handle huge topside weights and are designed to stand still in the water. A huge disadvantage is the increased weight when water depth increases and the need for heavy installation ships [60]. Therefore, jacket structures are only economically feasible in water depths ranging between 10 to around 400 metres [49].

Compliant towers are slender towers which are fixed to the seabed. However, these structures are allowed to deflect when actions are acting on the structures. These structures will absorb the energy through the movement, and therefore they can be installed in much deeper waters ranging from 450m to 900m [61]. Because they can move, they can be built lighter than fixed structures. However, the installation of these structures is complicated because of the length of these structures. Guyed towers are compliant structures that also use anchor lines to ensure the stability of the structure. Compliant structures are mostly all installed in the Gulf of Mexico [60].

Gravity-based structures are fixed offshore structures that are only kept in place by their weight [15]. Usually, these types of structures are built with concrete. For transportation, vacuum spaces or caissons are included in the structure to provide the structure with enough buoyancy to float. While no piles and anchor lines are required, these platforms are quickly installed. However, building these structures takes a long time and requires sufficient soil conditions [60].

Single Point Anchor Reservoir (SPAR) are floating offshore structures designed for an optimal natural period outside of the wave spectrum. The platform consists of a cylindrical buoy with a topside on top. The buoy can be giant but will not reach the seabed. The platform is kept in place by anchoring lines. SPAR-type platforms are one of the most often used structures out on the ocean [60]. The advantages of these structures are the best possible stability properties, low maintenance costs and

the ease of fabricating these platforms. The disadvantages are the installation and the lack of storage capacity.

Semisubmersible are floating offshore structures with multiple legs interconnected underwater with horizontal buoyant members. The advantage of semisubmersibles is that they are highly mobile and have good stability properties. However, they have high maintenance costs, limited topside-weight-capacity, and the risers must be designed for fatigue [60].

Tension Leg Platform (TLP) are vertically moored platforms which are also compliant to move, but only in the horizontal direction. The structures have good deep water capability and relatively low maintenance costs. Disadvantages are high initial costs and the sensitivity for fatigue [60].

Floating Production Storage and Offloading (FPSO) are floating offshore structures which look like a ship, with a turret mooring system installed at its bow. The advantages of these structures are the provided storage onboard, the low costs and the mobility to relocate. However, these structures are limited to smaller oil fields and often involve high maintenance costs. When the seas are very rough, these structures have poor stability properties [62].

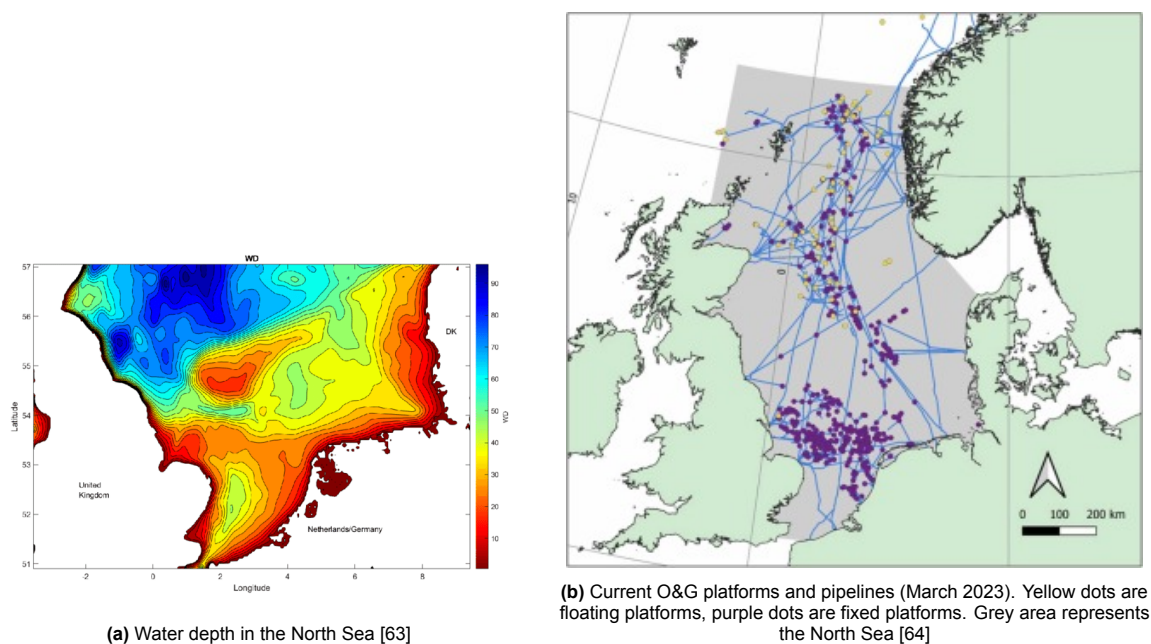


Figure A.6: Waterdepth of southern North Sea vs. bottom-founded and floating platform distribution in the North Sea

All the structures described above have advantages and disadvantages, and water depth is often one of the first properties determining if a specific structure is suitable. In March 2023, 95% of the offshore structures in the North Sea are fixed structures [64]. That means that only 5% of the structures operating in the North Sea are floating structures. The explanation can be found in the bathymetry of the north sea shown in figure A.6a. The North Sea generally has a mean water depth of 95 metres, but figure A.6a shows that the southern North Sea, along the coasts of the UK, the Netherlands and Denmark, only has a mean water depth of 20 to 25 metres. Figure A.6b shows that most offshore platforms are located in this part of the North Sea and that these structures are all fixed. Floating offshore structures operate only north of the North Sea near Norway, with much higher water depth. The transition towards renewable energies is not yet operating in these waters, while the costs and difficulties increase in deeper waters. Therefore, this report only considered bottom-founded offshore structures, while it is expected that most platforms in the near future will be built in these shallow waters. However, while gravity-based structures and compliant towers are also bottom-founded, these structures are not considered because gravity-based structures mainly consist of concrete, and compliant towers are not built in the North Sea. Hence only fixed jacket-type platforms were considered in this report.

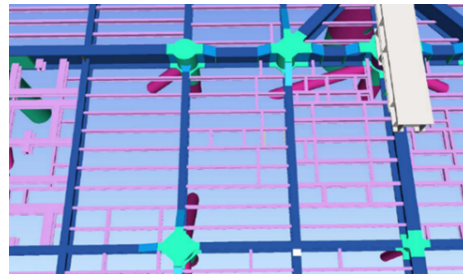
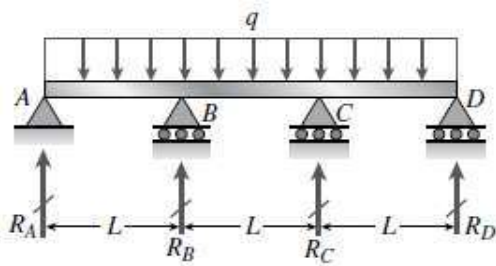
B

Deck stringer calculations

1. Example deck stringers

Appendix B

1.1 Situation: three span continuous beam (laterally restrained) - no snipe



Example includes:		Example info:	
Cross-section classification		Deck beams:	HEB600
Verification of moment resistance		Deck stringers:	IPE240
Verification of shear resistance		Length deck stringers:	4.2 m

1.2 Section properties for initial IPE240 beam

Depth of section	h =	240 mm
Width of flange	b =	120 mm
Flange thickness	tf =	9.8 mm
Web thickness	tw =	6.2 mm
Web height	hw =	220.4 mm
Weld thickness	aw =	6 mm
Plastic section modulus	Wp =	366.6 cm ³
Area moment of inertia	Iyy =	3892 cm ⁴
Cross-section class = 1		

1.3 Other properties

Initial yield stress	fy =	3.55E+08 Pa
Material resistance	γM0 =	1.16 (based on BoSD)
Young's modulus	E =	2.10E+11 Pa
Cost S355 beam		1.175 €/kg
Cost S460 beam		1.275 €/kg
Welding speed	v =	50 cc/h
Assembly factor	Fa =	2
Real welding speed	v/Fa =	25 cc/h
Welder salary	Ws =	30 €/h
Overhead factor	Fo =	3
Real welder cost	Ws*Fo =	90 €/h
Welding volume (k6)		30 cc/m
Variable load	Q =	12.75 kN/m (based on BoSD)

1.4 Determine costs IPE240

Beam has no sniped connection		
Cost IPE240 of 4.2m	$1.175 \times 4.2 \times 31.3 =$	€154.5 (IPE240: 31.3 kg/m)
Length flange weld	1x	120 mm
Length web weld		230.2 mm
Length of HEB600 flange weld		142.3 mm
Total weld length		492.5 mm
Total weld cost = weld length x welding volume x (real welder cost/real welding speed)		
Total weld cost =		52.19 €
Total costs IPE240 =		207.69 €

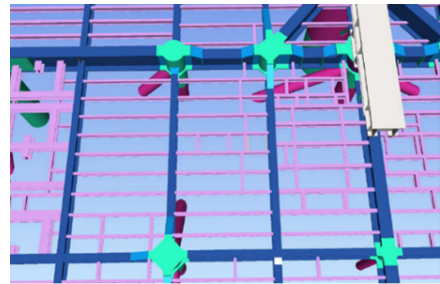
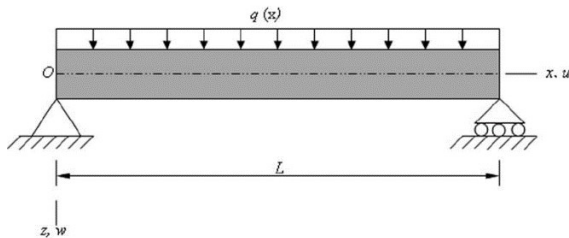
1.5 Equations for three span continues beam			
$M_{max} = 0.1q_{uls}L^2$	$\delta_{max} = \frac{0.0069q_{sls}L^4}{EI}$	$V_{max} = 0.6q_{uls}L$	
1.6 Determine ULS/SLS-ratio			
G = Q (as $\lambda = 0.5$ is assumed)			
$q_{uls} = 1.3G + 1.5Q$	(based on BoSD)		
$q_{sls} = G + Q$	(based on BoSD)		
$U.C.(ULS) = \frac{M_{Ed}}{M_{c,Rd}} = \frac{\gamma_{M0}q_{uls}L^2}{10\sigma_yW_p}$	$U.C.(SLS) = \frac{\delta}{\delta_{max}} = \frac{1.38q_{sls}L^3}{EI}$		
$\frac{U.C._{ULS}}{U.C._{SLS}} = \frac{2.8\gamma_{M0}EI}{27.6\sigma_yW_pL} = \frac{2.8 \times 1.16 \times 210E^9 \times 3892E^{-8}}{27.6 \times 355E^6 \times 366.6E^{-6} \times 4.2} = 1.76$	(strength governing)		
1.7 Calculate maximum possible permanent load			
Strength governing			
Load is unknown, so it is assumed that beam is designed for it's maximum resistance:			
$\frac{M_{Ed}}{M_{c,Rd}} = 1$			
$q_{ULS(max)} = \frac{10\sigma_yW_p}{\gamma_{M0}L^2} = \frac{10 \times 355E^6 \times 366.6E^{-6}}{1.16 \times 4.2^2} = 63.6 \text{ kN/m}$			
$G = \frac{q_{uls} - 1.5Q}{1.3} = \frac{63.6 - 1.5 \times 12.75}{1.3} = 34.2 \text{ kN/m}$			
1.8 Determine minimum possible Wp for HSS and minimum Iyy			
$U.C.(ULS) = \frac{M_{Ed}}{M_{c,Rd}} = \frac{\gamma_{M0}q_{uls}L^2}{10\sigma_yW_p} = 1$			
S460: $W_{p,req} = \frac{\gamma_{M0}q_{uls}L^2}{10\sigma_y} = \frac{1.16 \times 63.6E^3 \times 4.2^2}{10 \times 460E^6} = 282.9 \text{ cm}^3$			
S690: $W_{p,req} = \frac{\gamma_{M0}q_{uls}L^2}{10\sigma_y} = \frac{1.16 \times 63.6E^3 \times 4.2^2}{10 \times 690E^6} = 188.6 \text{ cm}^3$			
Required I does not change from S355 situation:			
$q_{sls} = G + Q = 34.2 + 12.75 = 46.95 \text{ kN/m}$			
$I_{req} = \frac{1.38q_{sls}L^3}{E} = \frac{1.38 \times 46.95E^3 \times 4.2^3}{210E^9} = 2285.8 \text{ cm}^4$			
When HSS would be used, an IPE220 could be used.			
The required section modulus for S690 would be enough for IPE200, but this is restricted by the required area moment of inertia			
1.9 Cost calculation for IPE220 (S460)			
Beam has no sniped connection			
Cost IPE220 of 4.2m	$1.275 \times 4.2 \times 26.7 = \text{€}142.98$		(IPE220: 26.7 kg/m)
Length flange weld	2x	110 mm	
Length web weld		201.6 mm	
Length of HEB600 flange weld		142.3 mm	
Total weld length		563.9 mm	

Total weld cost = weld length x welding volume x (real welder cost/real welding speed)					
Total weld cost =				60.9 €	
Total costs IPE240 =				203.88 €	
1.10 Check cross-section classification					
Standard IPE220 of S460 is still class 1 :					
https://eurocodeapplied.com/design/en1993/ipe-hea-heb-hem-design-properties					
1.11 Check if shear force influence can be neglected as assumed					
$V_{max} = 0.6q_{uls}L = 160.3 \text{ kN}$					
$A_v = 2024 \text{ mm}^2$					
$V_{pl,Rd} = \frac{A_v \left(\frac{f_y}{\sqrt{3}} \right)}{\gamma_{M0}} = 463.4 \text{ kN}$					
$V_{Ed} < 0.5V_{pl,Rd}$					
The design shear force is smaller than 0.5 the plastic shear resistance, no correction required					
1.12 Conclusion					
Deck stringers can be replaced with high-strength steel in a beneficial manner.					
Weight percentage reduced:		14.70%			
Material cost percentage reduced:		7.46%			
Welding cost percentage reduced:		-16.69%			
Total cost reduction:		1.83%			

2. Example deck stringers

Appendix B

2.1 Situation: simply supported beam - snipe connection



Example includes:		Example info:	
Cross-section classification		Deck beams:	HEB600
Verification of moment resistance		Deck stringers:	IPE240
Verification of shear resistance		Length deck stringers:	4.2 m

2.2 Section properties for initial IPE240 beam

Depth of section	h =	240 mm
Width of flange	b =	120 mm
Flange thickness	tf =	9.8 mm
Web thickness	tw =	6.2 mm
Web height	hw =	220.4 mm
Weld thickness	aw =	6 mm
Plastic section modulus	Wp =	366.6 cm ³
Area moment of inertia	Iyy =	3892 cm ⁴
Cross-section class = 1		

2.3 Other properties

Initial yield stress	fy =	3.55E+08 Pa
Material resistance	γM0 =	1.16 (based on BoSD)
Young's modulus	E =	2.10E+11 Pa
Cost S355 beam		1.175 €/kg
Cost S460 beam		1.275 €/kg
Welding speed	v =	50 cc/h
Assembly factor	Fa =	2
Real welding speed	v/Fa =	25 cc/h
Welder salary	Ws =	30 €/h
Overhead factor	Fo =	3
Real welder cost	Ws*Fo =	90 €/h
Welding volume (k6)		30 cc/m
Variable load	Q =	12.75 kN/m (based on BoSD)

2.4 Determine costs IPE240

Beam has a sniped connection (only top flange and web are welded to HEB600)			
Cost IPE240 of 4.2m		$1.175 \times 4.2 \times 31.3 = \text{€}154.5$	(IPE240: 31.3 kg/m)
Length flange weld		120 mm	
Length web weld		230.2 mm	
Length of HEB600 flange weld		142.3 mm	
Total weld length		492.5 mm	
Total weld cost = weld length x welding volume x (real welder cost/real welding speed)			
Total weld cost =		53.2 €	
Total costs IPE240 =		207.8 €	

2.5 Equations for simply supported beam			
$M_{max} = \frac{q_{uls}L^2}{8}$	$\delta_{max} = \frac{5q_{sls}L^4}{384EI}$	$V_{max} = 0.5q_{uls}L$	
2.6 Determine ULS/SLS-ratio			
G = Q (as $\lambda = 0.5$ is assumed)			
$q_{uls} = 1.3G + 1.5Q$	(based on BoSD)		
$q_{sls} = G + Q$	(based on BoSD)		
$U.C.(ULS) = \frac{M_{Ed}}{M_{c,Rd}} = \frac{\gamma_{M0}q_{uls}L^2}{8\sigma_yW_p}$	$U.C.(SLS) = \frac{\delta}{\delta_{max}} = \frac{1000q_{sls}L^3}{384EI}$		
$\frac{U.C._{ULS}}{U.C._{SLS}} = \frac{2.8\gamma_{M0}384EI}{16000\sigma_yW_pL} = \frac{2.8 \times 1.16 \times 384 \times 210E^9 \times 3892E^{-8}}{16000 \times 355E^6 \times 366.6E^{-6} \times 4.2} = 1.17$ (strength governing)			
2.7 Calculate maximum possible permanent load			
Strength governing			
Load is unknown, so it is assumed that beam is designed for it's maximum resistance:			
$\frac{M_{Ed}}{M_{c,Rd}} = 1$			
$q_{ULS(max)} = \frac{8\sigma_yW_p}{\gamma_{M0}L^2} = \frac{8 \times 355E^6 \times 366.6E^{-6}}{1.16 \times 4.2^2} = 50.8 \text{ kN/m}$			
$G = \frac{q_{uls} - 1.5Q}{1.3} = \frac{50.8 - 1.5 \times 12.75}{1.3} = 24.4 \text{ kN/m}$			
2.8 Determine minimum possible Wp for HSS and minimum Iyy			
$U.C.(ULS) = \frac{M_{Ed}}{M_{c,Rd}} = \frac{\gamma_{M0}q_{uls}L^2}{8\sigma_yW_p} = 1$			
S460:	$W_{p,req} = \frac{\gamma_{M0}q_{uls}L^2}{8\sigma_y} = \frac{1.16 \times 50.8E^3 \times 4.2^2}{8 \times 460E^6} = 282.47 \text{ cm}^3$		
S690:	$W_{p,req} = \frac{\gamma_{M0}q_{uls}L^2}{8\sigma_y} = \frac{1.16 \times 50.8E^3 \times 4.2^2}{8 \times 690E^6} = 188.3 \text{ cm}^3$		
Required I does not change from S355 situation:			
$q_{sls} = G + Q = 24.4 + 12.75 = 37.15 \text{ kN/m}$			
$I_{req} = \frac{1000q_{sls}L^3}{384E} = \frac{1000 \times 37.15E^3 \times 4.2^3}{384 \times 210E^9} = 3413.2 \text{ cm}^4$			
When HSS would be used, the area moment of inertia restricts the use of smaller IPE's			
A smaller high-strength IPE cannot be used			

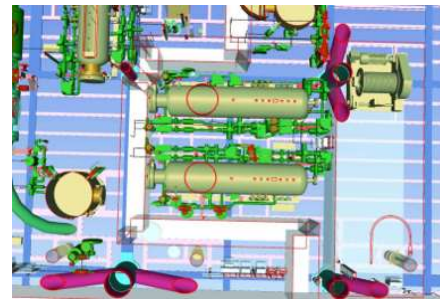
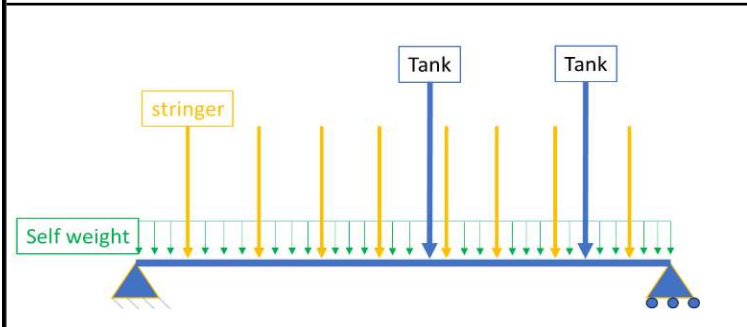
C

Deck beam calculations

2. Example deck beams

Appendix 2

2.1 Situation: combination of loads (laterally restrained)



<u>Example includes:</u>		<u>Example info:</u>	
Cross-section classification		Deck beam:	HEA600
Verification of moment resistance		Deck stringers:	IPE240
Verification of shear resistance		Length deck beam:	8.5 m

2.2 Section properties for initial HEA600 beam

Depth of section		h =	590 mm
Width of flange		b =	300 mm
Flange thickness		tf =	25 mm
Web thickness		tw =	13 mm
Web height		hw =	550 mm
Plastic section modulus		Wp =	5350 cm ³
Area moment of inertia		Iyy =	141200 cm ⁴
Cross-section class = 1			

2.3 Other properties

Initial yield stress		fy =	3.55E+08 Pa
Material resistance		γM0 =	1.16 (based on BoSD)
Young's modulus		E =	2.10E+11 Pa
Cost S355 beam			1.175 €/kg
Cost S460 beam			1.275 €/kg
Welding speed		v =	50 cc/h
Assembly factor		Fa =	2
Real welding speed		v/Fa =	25 cc/h
Welder salary		Ws =	30 €/h
Overhead factor		Fo =	3
Real welder cost		Ws*Fo =	90 €/h
Welding volume (H7)			49 cc/m
Welding volume (H13)			169 cc/m
Welding volume (K25)			347 cc/m
Tank weight		P =	265 kN

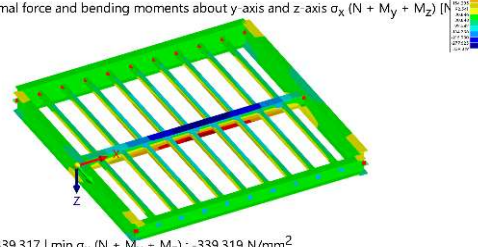
2.4 Determine costs HEA600

Beam has a full connection (flanges and web are welded to HEB1000)			
Cost HEA600 of 8.5m		$1.175 \times 8.5 \times 181 = \text{€}1807.74$	(HEA600: 181 kg/m)
Length flange weld (K25)		300 mm	
Length flange weld (H13)		300 mm	
Length web weld (H7)		540 mm	
Length of HEB1000 flange weld (H7)		140.5 mm	

Cost H7 weld =				120 €		
Cost H13 weld =				185.52 €		
Cost K25 weld =				374.76 €		
Total weld cost =				680.28 €		
Total costs HEB600 =				2488.02 €		

2.5 FEA is used to find maximum moment, deflection and shear force

CO1 - ULS
Static Analysis
Normal stress due to normal force and bending moments about y-axis and z-axis $\sigma_x (N + M_y + M_z)$



max $\sigma_x (N + M_y + M_z)$: 339.317 | min $\sigma_x (N + M_y + M_z)$: -339.317 N/mm²

Mmax =	1273.5 kNm
Deflection =	21.7 mm
Vmax =	665.9 kN

2.6 Determine ULS/SLS-ratio

$$U.C.(ULS) = \frac{M_{Ed}}{M_{c,Rd}} = \frac{\gamma_{M0} 1273.5E3}{\sigma_y W_p} = 0.78$$

$$U.C.(SLS) = \frac{\delta}{\delta_{max}} = \frac{200\delta}{L} = 0.51$$

$$\frac{U.C.ULS}{U.C.SLS} = 1.53 \quad (\text{strength governing})$$

2.7 Determine minimum possible Wp for HSS

Strength governing

Load is unknown, so it is assumed that beam is designed for it's maximum resistance:

$$\frac{M_{Ed}}{M_{c,Rd}} = 1, \quad M_{Ed} \text{ remains the same}$$

$$W_{req} = \frac{M_{Ed} \gamma_{M0}}{\sigma_y} = \frac{1273.5E3 \times 1.16}{460E6} = 3211 \text{ cm}^3 \quad (S460) \quad \boxed{\text{HEA500} \quad 3949 \text{ cm}^3}$$

$$W_{req} = \frac{M_{Ed} \gamma_{M0}}{\sigma_y} = \frac{1273.5E3 \times 1.16}{690E6} = 2141 \text{ cm}^3 \quad (S690) \quad \boxed{\text{HEA400} \quad 2311 \text{ cm}^3}$$

However, deflection should still be checked before conclusions can be made

2.8 Determine minimum possible Iyy

Required I does not change from S355 situation

However, we do not know which support, hence we assume simply (most conservative)

$$\delta = \frac{5q_{sls}l^4}{384EI} \quad \text{Deflection} = \quad 21.7 \text{ mm}$$

Rewrite to calculate qsls

$$q_{sls} = \quad 94.67 \text{ kN/m}$$

$$I_{req} = \frac{2.6q_{sls}L^3}{E} = \frac{2.6 \times 94.67E^3 \times 8.5^3}{210E^9} = 71980 \text{ cm}^4 \quad \boxed{\text{HEA500} \quad 86970 \text{ cm}^3}$$

When HSS would be used, a HEA500 (S460) could be used.

S690 will not lead to more benefits while deflection becomes dominant below HEA500

2.9 Cost calculation for HEA500 (S460)			
Beam has a full connection (flanges and web are welded to HEB1000)			
Cost HEA500 of 8.5m (S460)	$1.275 \times 8.5 \times 158 =$	€1712.33	(HEA500: 158 kg/m)
K-weld can be lower because flange is now 23mm instead of 25mm, new welding volume = 302 cc/m			
Length flange weld (K23)		300 mm	
Length flange weld (H13)		300 mm	
Length web weld (H7)		444 mm	
Length of HEB1000 flange weld (H7)		140.5 mm	
Cost H7 weld =		103.12 €	
Cost H13 weld =		182.52 €	
Cost K23 weld =		326.16 €	
Total weld cost =		611.79 €	
Total costs HEB600 =		2324.12 €	
2.10 Check cross-section classification			
Standard HEA500 of S460 is still class 1 :			
https://eurocodeapplied.com/design/en1993/ipe-hea-heb-hem-design-properties			
2.11 Check if shear force influence can be neglected as assumed			
$V_{max} = 665.9 \text{ kN}$			
$A_v = 7472 \text{ mm}^2$			
$V_{pl,Rd} = \frac{A_v \left(\frac{f_y}{\sqrt{3}} \right)}{\gamma_{M0}} = 1711 \text{ kN}$			
$V_{max} < 0.5V_{pl,Rd}$			
The design shear force is smaller than 0.5 the plastic shear resistance, no correction required			
2.12 Conclusion			
Deck beam can be replaced with high-strength steel in a beneficial manner.			
Weight percentage reduced:		12.70%	
Material cost percentage reduced:		5.30%	
Welding cost percentage reduced:		10%	
Total cost reduction:		6.59%	

D

Extra tables

Table D.1: Possible replacement of beams with S460 (HEB) - simply supported and distributed load

HEB	2m	3m	4m	5m	6m	7m	8m	9m	10m	11m	12m	13m	14m	15m
200	-	-	-	-	-	-	-	-	-	-	-	-	-	-
220	200B	200B	-	-	-	-	-	-	-	-	-	-	-	-
240	220B	220B	-	-	-	-	-	-	-	-	-	-	-	-
260	240B	240B	240B	-	-	-	-	-	-	-	-	-	-	-
280	260B	260B	260B	-	-	-	-	-	-	-	-	-	-	-
300	280B	280B	280B	-	-	-	-	-	-	-	-	-	-	-
320	300B	300B	300B	300B	-	-	-	-	-	-	-	-	-	-
340	300B	300B	300B	320B	-	-	-	-	-	-	-	-	-	-
360	320B	320B	320B	320B	340B	-	-	-	-	-	-	-	-	-
400	360B	360B	360B	360B	360B	-	-	-	-	-	-	-	-	-
450	400B	400B	400B	400B	400B	-	-	-	-	-	-	-	-	-
500	450B	450B	450B	450B	450B	450B	-	-	-	-	-	-	-	-
550	500B	500B	500B	500B	500B	500B	500B	-	-	-	-	-	-	-
600	550B	550B	550B	550B	550B	550B	550B	550B	-	-	-	-	-	-
650	600B	600B	600B	600B	600B	600B	600B	600B	600B	600B	-	-	-	-
700	650B	650B	650B	650B	650B	650B	650B	650B	650B	650B	-	-	-	-
800	700B	700B	700B	700B	700B	700B	700B	700B	700B	700B	-	-	-	-
900	800B	800B	800B	800B	800B	800B	800B	800B	800B	800B	800B	800B	-	-
1000	900B	900B	900B	900B	900B	900B	900B	900B	900B	900B	900B	900B	900B	900B

Table D.2: Possible replacement of beams with S460 (HEB) - fixed assumption (point load)

HEB	6m	7m	8m	9m	10m	11m	12m	13m	14m	15m	16m	17m	18m	19m	20m
200	-	-	-	-	-	-	-	-	-	-	-	-	-	-	-
220	200B	200B	-	-	-	-	-	-	-	-	-	-	-	-	-
240	220B	220B	220B	-	-	-	-	-	-	-	-	-	-	-	-
260	240B	240B	240B	240B	-	-	-	-	-	-	-	-	-	-	-
280	260B	260B	260B	260B	260B	-	-	-	-	-	-	-	-	-	-
300	280B	280B	280B	280B	280B	280B	-	-	-	-	-	-	-	-	-
320	300B	300B	300B	300B	300B	300B	300B	-	-	-	-	-	-	-	-
340	300B	300B	300B	300B	300B	300B	320B	320B	-	-	-	-	-	-	-
360	320B	320B	320B	320B	320B	320B	320B	340B	340B	-	-	-	-	-	-
400	360B	360B	360B	360B	360B	360B	360B	360B	360B	-	-	-	-	-	-
450	400B	400B	500A	400B	400B	400B	400B	400B	400B	400B	-	-	-	-	-
500	450B	450B	450B	450B	450B	450B	450B	450B	450B	450B	450B	450B	-	-	-
550	500B	500B	500B	500B	500B	500B	500B	500B	500B	500B	500B	500B	500B	500B	500B
600	550B	550B	550B	550B	550B	550B	550B	550B	550B	550B	550B	550B	550B	550B	550B
650	600B	600B	600B	600B	600B	600B	600B	600B	600B	600B	600B	600B	600B	600B	600B
700	650B	650B	650B	650B	650B	650B	650B	650B	650B	650B	650B	650B	650B	650B	650B
800	700B	700B	700B	700B	700B	700B	700B	700B	700B	700B	700B	700B	700B	700B	700B
900	800B	800B	800B	800B	800B	800B	800B	800B	800B	800B	800B	800B	800B	800B	800B
1000	900B	900B	900B	900B	900B	900B	900B	900B	900B	900B	900B	900B	900B	900B	900B

Table D.6: Possible replacement of beams with S460 (IPE)

IPE	2m	3m	4m	5m	6m	7m	8m	9m
160	-	-	-	-	-	-	-	-
180	-	-	-	-	-	-	-	-
200	-	-	-	-	-	-	-	-
220	200I	200I	-	-	-	-	-	-
240	220I	220I	-	-	-	-	-	-
270	-	-	-	-	-	-	-	-
300	-	-	-	-	-	-	-	-
330	300I	300I	300I	-	-	-	-	-
360	330I	330I	330I	330I	-	-	-	-
400	360I	360I	360I	360I	-	-	-	-
450	-	-	-	-	-	-	-	-
500	450I	450I	450I	450I	450I	450I	-	-
550	500I	500I	500I	500I	500I	500I	-	-
600	550I	550I	550I	550I	550I	550I	550I	-

Table D.7: Possible replacement of beams with S460 (IPE) - continuous beam (3-span) assumption

IPE	2m	3m	4m	5m	6m	7m	8m	9m	10m	11m	12m	13m
160	-	-	-	-	-	-	-	-	-	-	-	-
180	-	-	-	-	-	-	-	-	-	-	-	-
200	-	-	-	-	-	-	-	-	-	-	-	-
220	200I	200I	200I	-	-	-	-	-	-	-	-	-
240	220I	220I	220I	220I	-	-	-	-	-	-	-	-
270	-	-	-	-	-	-	-	-	-	-	-	-
300	-	-	-	-	-	-	-	-	-	-	-	-
330	300I	300I	300I	300I	300I	300I	-	-	-	-	-	-
360	330I	330I	330I	330I	330I	330I	330I	-	-	-	-	-
400	360I	360I	360I	360I	360I	360I	360I	-	-	-	-	-
450	-	-	-	-	-	-	-	-	-	-	-	-
500	450I	450I	450I	450I	450I	450I	450I	450I	450I	-	-	-
550	500I	500I	500I	500I	500I	500I	500I	500I	500I	500I	500I	-
600	550I	550I	550I	550I	550I	550I	550I	550I	550I	550I	550I	550I

Table D.8: Maximum length for HEBs to be strength governing.

HEB	Lmax [m] (Simply-supported - distributed load)	Lmax [m] (Fixed - point load)
180	3.67	8.52
200	4.09	9.49
220	4.51	10.24
240	4.93	11.45
260	5.36	12.45
280	5.79	13.45
300	6.21	14.41
320	6.61	15.35
340	7.02	16.3
360	7.42	17.23
400	8.23	19.10
450	9.25	21.48
500	10.26	23.83
550	11.16	25.92
600	12.28	28.5
650	13.27	30.8
700	14.23	33.02
800	16.19	37.57
900	18.11	42.04
1000	20.01	46.45

Table D.9: Maximum length for HEAs to be strength governing.

HEA	L_{max} [m] (Simply-supported - distributed load)	L_{max} [m] (Fixed - point load)
180	3.56	8.27
200	3.96	9.20
220	4.39	10.19
240	4.81	11.16
260	5.76	13.37
280	6.22	14.45
300	6.68	15.51
320	6.49	15.08
340	6.90	16.02
360	7.31	16.96
400	8.11	18.83
450	9.14	21.21
500	10.16	23.58
550	11.16	25.92
600	12.17	28.25
650	13.17	30.56
700	14.12	32.77
800	16.08	37.34
900	18.01	41.80
1000	19.92	46.24